

# Interannual variability of lithogenic particle fluxes in the subtropical North Atlantic

## Dissertation

zur

Erlangung des akademischen Grades  
doctor rerum naturalium (Dr. rer. nat.)  
der Mathematisch-Naturwissenschaftlichen Fakultät  
der Universität Rostock

vorgelegt von

**Juliane Brust**

geb. am 08.01.1980 in Greifswald

Rostock, den 29.06.2011



## **Gutachter**

Prof. Dr. Detlef E. Schulz-Bull  
Sektion Meereschemie  
Leibniz-Institut für Ostseeforschung Warnemünde

PD Dr. habil. Joanna Waniek  
Sektion Meereschemie  
Leibniz-Institut für Ostseeforschung Warnemünde

Prof. Dr. Michal Kucera  
Fachbereich Geowissenschaften  
Eberhard Karls Universität Tübingen

Prof. Dr. Dr. h.c. Gerold Wefer  
MARUM - Zentrum für Marine Umweltwissenschaften  
Universität Bremen

**Datum der öffentlichen Verteidigung:** 24.10.2011



# Table of contents

<b>Abstract</b>	<b>I</b>
<b>Zusammenfassung</b>	<b>III</b>
<b>Preface</b>	<b>VI</b>
<b>1 Introduction</b>	<b>1</b>
1.1 Global scientific framework . . . . .	1
1.2 Scientific question . . . . .	5
<b>2 Study sites, methods and additional data</b>	<b>9</b>
2.1 Study sites . . . . .	9
2.2 Methods . . . . .	11
2.3 Additional data . . . . .	14
<b>3 Atmospheric dust contribution to deep-sea particle fluxes in the subtropical Northeast Atlantic</b>	
<i>Brust, J., and J. J. Waniek, published 2010 in Deep-Sea Research I 57,</i> <i>988–998</i>	<b>15</b>
3.1 Abstract . . . . .	15
3.2 Introduction . . . . .	16
3.3 Material and Methods . . . . .	18
Study area . . . . .	18
Sediment trap material . . . . .	18
SEM–EDX analysis . . . . .	19
Repeatability . . . . .	21
3.4 Results & Discussion . . . . .	21
Lithogenic fluxes from February 2002 to March 2005 . . . . .	21



Grain size distribution of particles . . . . .	25
Mineralogy and origin of the lithogenic particles . . . . .	27
Link between biogenic and lithogenic flux . . . . .	33
3.5 Conclusions . . . . .	38
3.6 Acknowledgements . . . . .	38
<b>4 Descending particles: from the atmosphere to the deep ocean – A time series study in the subtropical NE Atlantic</b>	
<i>Brust, J., D. E. Schulz-Bull, T. Leipe, V. Chavagnac, and J. J. Waniek, published 2011 in Geophysical Research Letters</i>	<b>39</b>
4.1 Abstract . . . . .	39
4.2 Introduction . . . . .	39
4.3 Sampling material and methods . . . . .	40
4.4 Results and discussion . . . . .	41
4.5 Acknowledgments . . . . .	48
4.6 Auxiliary material . . . . .	48
Study area . . . . .	48
Material and methods . . . . .	49
Satellite and GOCART data . . . . .	51
<b>5 Barite and North African dust in 3200 m deep sediment trap material southeast of Bermuda</b>	
<i>Brust et al., manuscript, to be submitted to Deep-Sea Research I</i>	<b>53</b>
5.1 Introduction . . . . .	53
5.2 Material and Methods . . . . .	56
Sediment trap material and SEM–EDX analysis . . . . .	56
Catchment area . . . . .	58
Satellite data . . . . .	60
5.3 Results and Discussion . . . . .	60
Particle flux and biogenic fluxes . . . . .	60
Lithogenic composition, aerosol contribution and sources . . . . .	64
5.4 Conclusions and summary . . . . .	74
<b>6 General conclusions and future perspectives</b>	<b>76</b>

References	81
List of figures	97
List of tables	99
List of Abbreviations	100
Specific contribution to the manuscripts	101
Acknowledgements	102
Eidesstattliche Erklärung	103

## Abstract

Desert dust from North Africa regularly spreads out over the tropical and subtropical North Atlantic Ocean. These dust outbreaks are seasonally controlled by main wind fields, which are confined by the Intertropical Convergence Zone. The transport of dust over the Atlantic Ocean occurs within the trade winds and the Saharan Air Layer. Thereby dust deposition in open ocean regions plays an important role in delivering nutrients to the ocean surface and controls lithogenic particle flux in the deep sea. Within this study the contribution of lithogenic particles to deep-sea particle fluxes and its mineralogical composition is investigated at two different mooring sites within the oligotrophic subtropical North Atlantic Ocean. The investigations put forth the question for the variability of North African sources and for a possible fertilization effect of dust on surface ocean productivity.

The analysis is based on a three year sediment trap time series (2002–2005) of a deep-sea mooring site situated in the eastern part of the subtropical North Atlantic Ocean (Kiel 276, 33°N, 22°W, 2000 m deep sediment trap) and a one year lasting sediment trap time series (1998–1999) of a site located in the western part of the subtropical North Atlantic Ocean (BATS-IOW, 31.76°N, 64.07°W, 3200 m deep sediment trap).

The determination of major lithogenic and biogenic particles within sediment trap samples is based on an automated particle analysis carried out with a SEM-EDX (Scanning Electron Microscope coupled with an Energy Dispersive X-ray system). Sediment trap data were compared with satellite and modeled aerosol data and with satellite derived chlorophyll-a data. Data from literature were used for comparing typical mineralogical and chemical compositions of North African soils and aerosols with obtained clay mineral and chemical compositions of investigated sediment trap samples.

The mineralogical composition of lithogenic sediment trap material at the eastern subtropical North Atlantic mooring site revealed that North African dust

sources vary rather interannually than seasonally between 2002 and 2005. During the year mineralogical compositions of sediment trap samples seem to be less variable. Despite this observation, the comparison of lithogenic flux and satellite and modeled aerosol optical depth data pointed to a time lag of one and a half months between dust occurrence over the catchment area of the trap and measured lithogenic flux at 2000 m water depth. Hence, dust deposition is reflected by deep-sea lithogenic particle flux at this site of the Atlantic Ocean.

A response of ocean surface biological productivity to eolian nutrient input is most likely visible during summer months, when nutrients in the euphotic zone are depleted causing low surface biological productivity and low particle flux at depth. North African dust outbreaks reached the sampling site Kiel 276 mostly during winter/spring. Only summer 2004 is characterized by multiple dust outbreaks that occur also over the sampling site. Following one of these outbreaks biogenic particle flux at depth is elevated in August 2004. This enhanced biogenic flux during summer is interpreted as a response of ocean surface primary production to nutrient input by dust. An effect, which is obscured by satellite chlorophyll-a data due to the presence of a deep-chlorophyll-a maximum at this site.

Based on chemistry and mineralogy of sediment trap material North African dust was also detected at BATS-IOW. Lithogenic particles found at this site originate from northwestern North African source regions. Although distinct North African sources could be detected, lithogenic mineral compositions at both, the eastern and western sampling sites point to a mixture of source regions or lateral influx of lithogenic particles.

To make statements concerning the long-term variability of North African dust sources and strength of dust transport to the subtropical North Atlantic, there is a need for longer lasting sediment trap time series together with overlapping long-term satellite observations.

## Zusammenfassung

Mineralstaub aus Nordafrika wird regelmäßig über den tropischen und subtropischen Nordatlantik transportiert. Diese Staubaussbrüche sind an die vorherrschenden Windsysteme geknüpft, welche wiederum durch die Lage der Innertropische Konvergenzzone gesteuert werden. Der Staubtransport findet hauptsächlich mit den Passatwinden und in der 'Saharan Air Layer' statt. Die Staubaablagerung im offenen Ozean bestimmt den lithogenen Partikeltransport im tiefen Ozean und spielt eine besondere Rolle als Nährstoffquelle für das Phytoplankton in der euphotischen Zone. Die vorliegende Studie untersucht den lithogenen Partikeltransport und seine mineralogische Zusammensetzung an zwei Verankerungspositionen im oligotrophen subtropischen Nordatlantik. Dabei zielen die Untersuchungen auf die Beantwortung der Frage nach den Liefergebieten des eingetragenen Staubes aus Nordafrika und auf einen möglichen Düngeeffekt, den der Staub auf die biologische Produktivität im Oberflächenwasser haben könnte, ab.

Hierzu wurde eine dreijährige Sinkstofffallenserie (2002–2005) einer Tiefseeverankerung im östlichen Teil des subtropischen Nordatlantiks (Kiel 276, 33°N, 22°W, 2000 m tiefe Sinkstofffalle) und eine einjährige Sinkstofffallenserie (1998–1999) im westlichen Teil des subtropischen Nordatlantiks (BATS-IOW, 31.76°N, 64.07°W, 3200 m tiefe Sinkstofffalle) untersucht.

Die Bestimmung der lithogenen und biogenen Partikelzusammensetzung des Sinkstofffallenmaterials basiert auf Ergebnissen der automatischen Partikelanalyse mit der REM-EDX-Analytik (Rasterelektronenmikroskopie mit gekoppelter Energiedispersive Röntgenspektroskopie). Diese Daten wurden mit vom Satelliten abgeleiteten und modellierten Aerosol-optischen Dichten sowie mit Satelliten-Chlorophyll-a-Konzentrationen des Oberflächenwassers verglichen. Weiterhin wurden Literaturdaten herangezogen, um die mineralogische und chemische Zusammensetzung der Fallenproben mit der Zusammensetzung von Boden- und Aerosolproben potentieller nordafrikanischer Liefergebiete zu vergleichen.

Die Mineralogische Zusammensetzung der lithogenen Fraktion im Sinkstofffallenmaterial des östlichen subtropischen Nordatlantiks zeigte, dass im Beobachtungszeitraum von 2002 bis 2005 keine saisonale, sondern eine zwischenjährliche Variabilität der nordafrikanischen Liefergebiete existiert. Innerhalb eines Jahres war die mineralogische Zusammensetzung der Proben sehr ähnlich und durch wenig Variabilität charakterisiert. Obwohl dies der Fall war, so konnte der Vergleich der lithogenen Flüsse mit den Aerosol-optischen Dichten zeigen, dass es nur einen anderthalb monatigen Versatz zwischen atmosphärischer Staubverteilung über dem Einzugsgebiet der Falle und dem gemessenen lithogenen Fluss in 2000 m Tiefe gab. Daraus lässt sich Schlussfolgern, dass sich Staubablagerungen an dieser Position des Atlantischen Ozeans in der Tiefe wiederfinden lassen und die Variabilität der Staubablagerungen durch den lithogenen Fluss reflektiert wird.

Bezüglich eines möglichen Düngeeffektes durch Staubeinträge lässt sich festhalten, dass diese vorzugsweise in den Sommermonaten beobachtet werden können. Im Sommer sind Nährstoffe in der euphotischen Zone in geringen Konzentrationen vorhanden, was eine geringe biologische Produktivität in der ozeanischen Deckschicht und einen geringen biogenen Partikelfluss in der Tiefe verursacht. Staubaussbrüche aus Nordafrika erreichten die Probenahmestation Kiel 276 hauptsächlich in den Winter- und Frühjahrsmonaten. Im Sommer 2004 konnten mehrere Staubbahnen über der Verankerungsposition beobachtet werden. Folgend auf einen dieser Staubaussbrüche wurde im August 2004 ein erhöhter biogener Partikelfluss in 2000 m Tiefe gemessen. Dieser erhöhte Partikelfluss scheint auf eine erhöhte biologische Produktivität im Oberflächenwasser zurückzugehen, welche wahrscheinlich durch den äolischen Eintrag von Nährstoffen ausgelöst wurde. Die Chlorophyll-a-Konzentrationen des Satelliten spiegeln diesen Effekt jedoch nicht wider. Eine Ursache dafür könnte die Ausprägung eines Tiefenchlorophyllmaximums (120 m) an dieser Position im Atlantik sein, welches vom Satelliten nicht erkannt wird.

Basierend auf der mineralogischen und chemischen Zusammensetzung des Sinkstofffallenmaterials konnte auch an der westlichen Probenahmestation BATS-IOW, Staub aus Nordafrika nachgewiesen werden. Die an dieser Position untersuchten lithogenen Partikel stammen aus nordwestlichen Liefergebieten Nordafrikas. Obwohl für die lithogene Fraktion beider Untersuchungsstationen im östlichen und westlichen Teil des subtropischen Nordatlantiks, diskrete Liefergebiete in Nordafrika

bestimmt werden konnten, so deutet die mineralogische Zusammensetzung des lithogenen Materials auf eine Vermischung von Partikeln unterschiedlicher Herkunft bzw. auf den durch Strömung bedingten lateralen Eintrag lithogener Partikel hin.

Um die Variabilität der nordafrikanischen Liefergebiete des Staubes und Änderungen in Ausprägung und Stärke der Staubaussbrüche auf längeren Zeitskalen beobachten zu können, sind länger Zeitserien der Sinkstofffallenbeprobung und zeitlich parallel laufende Satellitenbeobachtungen notwendig.

## Preface

The present work "*Interannual variability of lithogenic particle fluxes in the subtropical North Atlantic*" has been accomplished in the framework of the project "*Zwischenjährliche Variabilität lithogener Partikelflüsse in der Subtropenfront des Nordostatlantiks*" funded by the Deutsche Forschungsgemeinschaft (DFG).

"*Lithogenic*" particles encompass minerals or particles that are derived from crustal or continental rocks. The word itself derives from *lithos* (Greek), which means 'rock' or 'stone' and from *genesis* (Latin, from Greek), which stands for 'origin'. The lithogenic particle flux in open ocean regions like the open subtropical North Atlantic Ocean is mainly controlled by eolian dust input [e.g. *Kuss and Kremling*, 1999a; *Ratmeyer et al.*, 1999a,b; *Neuer et al.*, 2004].

Particle fluxes of this study are measured by means of deep-moored sediment traps at two different sites within the subtropical region of the North Atlantic. The lithogenic fraction is analyzed regarding its mineralogical composition, its provenance and impact on oceans biology. The results of these analyses are presented in this doctoral thesis, which is principally based on three manuscripts. Two of them have been already published in peer-reviewed international scientific journals (*Deep-Sea Research I*, Chapter 3 and *Geophysical Research Letters*, Chapter 4). Chapter 5 contains a manuscript in draft form. The references of all manuscripts were compiled to one reference list at the end of this thesis. Nevertheless, content-wise repetitions of text parts as for instance study site or methods and material were ineluctable.

The thesis starts with an introduction (**Chapter 1**), which gives an insight into the global scientific framework of this study and presents an outline of main scientific questions of the presented work.

On behalf of completeness the description of the study area, sampling methods and methodology occurs in **Chapter 2**, but is deliberately kept brief to avoid repetitions.



In **Chapter 3**, *Brust and Waniek* [2010] analyses the contribution and provenance of lithogenic material delivered to the subtropical Northeast Atlantic and the interannual variability of dust input and its sources. Mineral and specifically clay mineral assemblages in sediment trap samples point to different source regions of dust in North Africa.

In **Chapter 4**, *Brust et al.* [2011] outline the connection between atmospheric dust occurrence and the whole lithogenic flux, based on satellite-derived and modeled aerosol data and sediment trap data. Furthermore, the link between dust input and biological response is discussed in this chapter.

**Chapter 5**, *Brust et al.* [in prep.] focuses on a one year sediment trap time series in the western part of the subtropical North Atlantic. Chemical and mineralogical investigations of sediment trap material indicate North African sources of lithogenic minerals and particles also at this site of the North Atlantic. The presence of barite at this site is linked to ocean surface biology. The sediment trap data are shown in comparison with satellite data.

The main findings of the thesis, open questions and future perspectives are outlined in **Chapter 6**.

# 1 Introduction

## 1.1 Global scientific framework

The climate on Earth varies through time and its recent trend is subject of the 'Global Change' debate nowadays. Linked to past climate changes is the carbon dioxide (CO<sub>2</sub>) content of Earth's atmosphere. Since the 'Industrial Revolution' in the 19<sup>th</sup> century the atmospheric content of the 'green house' gas CO<sub>2</sub> is continuously increasing. The rise of atmospheric CO<sub>2</sub> concentrations was detected in atmospheric gas bubbles of ice cores [*Neftel et al.*, 1985; *Siegenthaler et al.*, 2005] and by continuous direct atmospheric measurements since 1959 [e.g. *Keeling et al.*, 1976; *Thoning et al.*, 1989]. Parallel to the CO<sub>2</sub> increase, a global rise in mean temperatures is observed [*Jones et al.*, 1986, 1999]. Therefore, changes in atmospheric CO<sub>2</sub> content also seem to be connected to past climatic changes. It is hypothesized, that during glacial periods not orbital forcing (Milankovich cycle) alone determined the onset of cold periods in Earth's history. Rather, a decline in CO<sub>2</sub> concentrations have led to global cooling [*Sigman and Boyle*, 2000]. Measurements of ice cores showed that CO<sub>2</sub> concentrations were lower during glacial periods than today [*Sigman and Boyle*, 2000]. The reason for this CO<sub>2</sub> drop down could be an enhanced oceanic productivity associated with increased carbon fixation and triggered by a stronger supply of nutrients such as iron, which reached the oceans by dust [*Martin*, 1990; *Sigman and Boyle*, 2000]. John Martin's quotation "Give me a half tanker of iron, and I will give you an ice age." in the late 1980ies have led scientists to discuss this hypothesis with regard to anthropogenic induced CO<sub>2</sub> and global temperature increase and to test this iron fertilization hypothesis in the field. First ocean fertilization experiments (OFE) have been carried out in the 1990ies and are still of interest in deciphering the response of oceans biology to additional iron input today. Specifically, High Nutrient Low Chlorophyll (HNLC) regions, which are the eastern equatorial Pacific Ocean, the subarctic North Pa-

cific Ocean, and the Southern Ocean, were selected for fertilization experiments [de Baar *et al.*, 2005]. These regions are characterized by relatively high concentrations of the essential macronutrients nitrogen and phosphorous but by low productivity. This fact and the absence of large deserts, which could supply iron bearing dust to these ocean regions, finally led to the assumption that another micronutrient 'iron' is one of the limiting factors for biologic productivity. 'Global Warming' together with anthropogenic land use (overexploitation of arable land, overgrazing, deforestation) leads to droughts and spread of desert areas.

Some climate models predict an increase of dust production due to desertification. Increasing dust production would mean, that also more iron could reach large ocean areas and fuel biological production. The feedbacks in the aerosol cycle are rather complex. Aerosols do not only influence biogeochemical processes of land [Swap *et al.*, 1992; Okin *et al.*, 2004; Bristow *et al.*, 2010] and ocean [Duce *et al.*, 1991; Baker *et al.*, 2006; Jickells *et al.*, 2005] ecosystems, but also impact Earth's radiation budget via absorption and reflection of sunlight and cloud physics and chemistry [e.g. Tegen *et al.*, 1997; Kaufman *et al.*, 2002, 2005; Martin *et al.*, 2003; Andreae *et al.*, 2005; IPCC, 2007]. Jickells *et al.* [2005] outlined the complex interactions between continents, atmosphere and ocean, that are mediated by dust (Figure 1.1). Dust production from land surfaces is controlled by the availability of dust in semi-arid and arid regions characterized by low or lacking vegetation cover [Okin and Gillette, 2006]. From there dust is transported with the main wind fields and can travel long distances [e.g. Carlson and Prospero, 1972; Prospero and Carlson, 1972; Prospero, 1981; Perry *et al.*, 1997], whereby the mean grain size decreases rapidly during transport due to gravitational settling of coarser grains [e.g. Jaenicke, 1980; Westphal *et al.*, 1987]. It has been shown that eolian dust comprises a major fraction of marine deep sea clays. Pelagic sediments reflect the distribution of major wind fields and sources from adjacent continents [Griffin *et al.*, 1968; Windom, 1976; Rea *et al.*, 1985; Rea, 1994] and the downcore variations of eolian dust content and composition of sediment records has been put into the framework of past atmospheric circulation patterns and climate [Rea, 1994]. On global scale, huge amounts of dust are mobilized and deposited annually, which are in the range of teratons per year [Jickells *et al.*, 2005].

The Sahara desert is the largest dust productive area of the world and thus

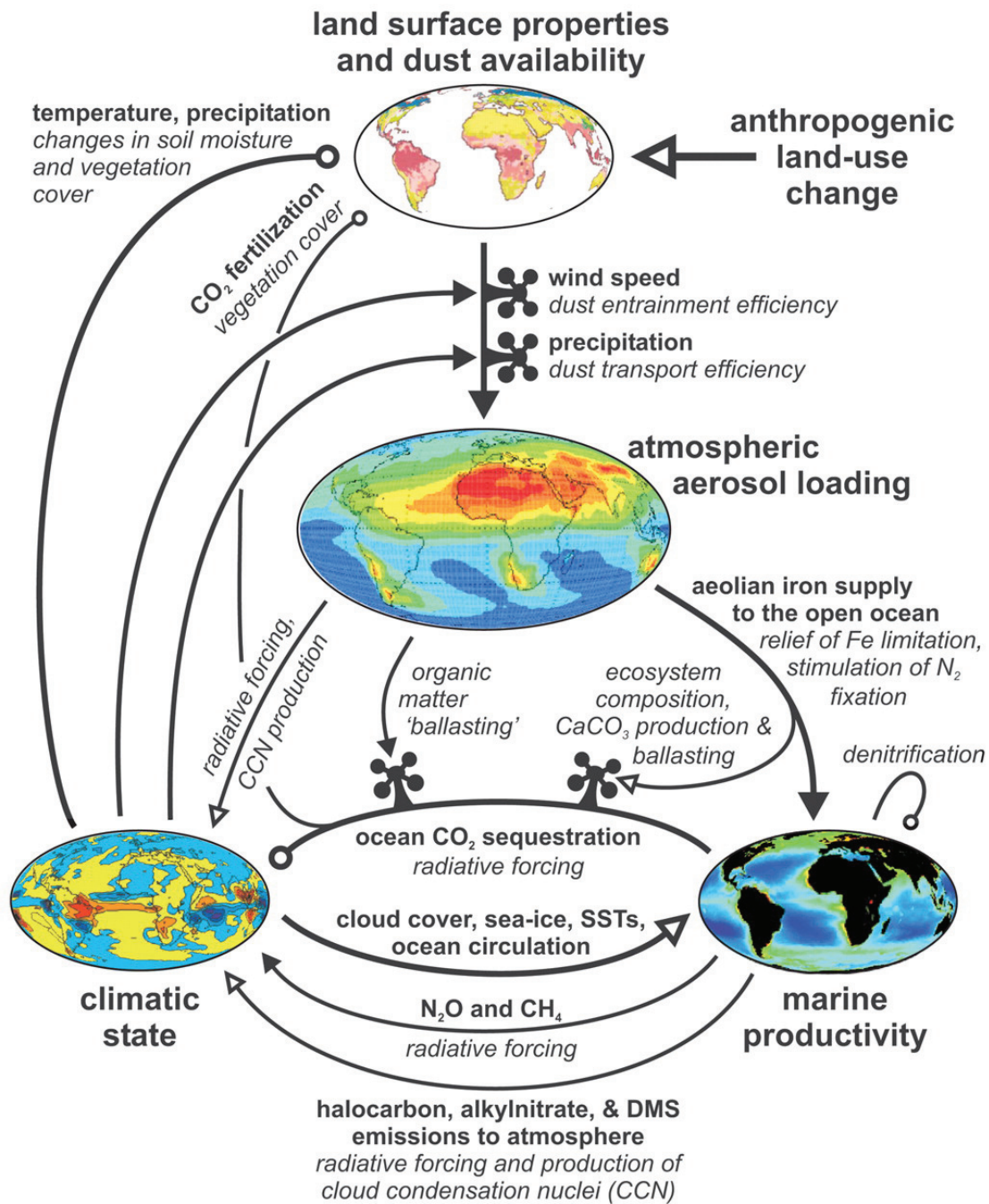


**Figure 1.1:** Scheme of major connections between desert dust, ocean biogeochemistry and climate according to *Jickells et al.* [2005].

Saharan dust outbreaks affects distant regions of the northern hemisphere [e.g. *Harrison et al.*, 2001; *Goudie and Middleton*, 2001]. The tropical and subtropical North Atlantic is subject to the influence of North African dust outbreaks. Transport paths of the North African dust over the North Atlantic are determined by the Saharan air layer (SAL), its northern branches and by the trade winds. Dust deposition plays an important role in biogeochemical processes of the subtropical and tropical North Atlantic Ocean [*Mills et al.*, 2004]. The subtropical oceanic regions are characterized by a usually shallow mixed layer depth, a stable and deep thermo- and nutricline, oligotrophy and low primary production [e.g. *Chavez et al.*, 2011]. Nutrients are entrained into the euphotic zone by mesoscale eddies [e.g. *McGillicuddy et al.*, 1998; *Oschlies*, 2008], fixation of nitrogen [e.g. *Gruber and Sarmiento*, 1997; *Karl et al.*, 2002; *Mahaffey et al.*, 2003] and to a lesser extent by diffusion processes across the thermocline [*Lewis et al.*, 1994; *Chavez and Toggweiler*, 1995]. Additional input of nutrients like phosphorous, nitrogen, silica and iron occurs by dust deposition. Especially nitrogen fixing organisms need iron for enzymatic activity. The subtropical and tropical North Atlantic primary production is limited by iron and phosphorous [*Mills et al.*, 2004], therefore dust outbreaks from North Africa can control biological production and impart particle transport in the ocean.

The vertical transport of particles within the ocean implies the transmission of mass and energy from ocean surface to the sea floor [e.g. *Conte et al.*, 2001; *Waniek et al.*, 2005a]. Fluxes of particles are measured by moored, tethered or free floating sediment traps which intercept particles that sink through the ocean water column [*Honjo and Doherty*, 1988; *Kremling et al.*, 1996; *Buesseler et al.*, 2007]. The interception of those particles increased our understanding of biological, chemical and physical processes in the ocean. Particle formation occurs to a large extent within the euphotic zone of the oceans, where the photosynthetic activity of phytoplankton primary producers is the main process of particle generation. Early sediment trap studies revealed the strong connection between seasonality of deep-sea particle fluxes and seasonal patterns of biogenic particle production in the upper water layer [*Honjo et al.*, 1982; *Deuser and Ross*, 1980; *Deuser et al.*, 1981, 1990; *Asper et al.*, 1992]. Biogenic particles settling through the water column differ in size and composition and hence in settling velocity. The spectrum of particles ranges

from single cells of phytoplankton to large aggregates of biogenic and non-biogenic compounds or zooplankton fecal pellets [e.g. *Waniek et al.*, 2005b]. Those particles can have settling velocities in the range of millimeters to several hundred meters per day, whereby the settling velocity is firstly dependent on the composition of the particle or aggregate and secondly on the size of the particle or aggregate of the same type [*Iversen and Ploug*, 2010]. The descend of particles from ocean surface to the sea floor is linked to the export of organic carbon, but also of chemical elements and even pollutants. Half of Earth's primary production takes place in ocean surface waters. Due to autolysis of dead cells and microbial respiration only 15 % of the organic carbon formed in the euphotic zone reaches the mesopelagial. Only a small fraction (ca. 0.1%) of that reaches the sea floor and is finally buried in the sedimentary record [e.g. *Falkowski and Oliver*, 2007]. The effectiveness of this carbon export is dependent on the biological production in the euphotic zone and the formation of fast settling particles or aggregates. The circumstance, that most unicellular algae naturally form minerals as carbonate (coccolithophores) and opal (diatoms) together with the exudation of sticky polymers lead to the hypothesis of the 'ballast effect'. Those ballast minerals are known to mediate and even accelerate the export of organic carbon from the upper water column [e.g. *Deuser et al.*, 1983; *Armstrong et al.*, 2002; *Klaas and Archer*, 2002; *Fischer et al.*, 2007]. Also non-biogenic particles as lithogenic minerals impart particle and organic carbon export. The ballast effect was proven to be very effective in continental margin and shelf areas, where the ballasting of organic compounds with lithogenic material play a major role in both carbon burial and sedimentation [e.g. *Ittekkot*, 1993; *François et al.*, 2002]. There are some indications, that atmospherically delivered lithogenic particles are also able to ballast organic material in the open ocean regions [*De La Rocha and Passow*, 2007; *Ploug et al.*, 2008; *Sanders et al.*, 2010].

## 1.2 Scientific question

The subtropical North Atlantic is influenced by deposition of dust originating from North Africa, which can be collected and measured in deep-sea sediment traps [e.g. *Chavagnac et al.*, 2007]. This study concentrates on the interannual variability of lithogenic fluxes in the subtropical Atlantic. Study sites are situated in the



northeastern part of the North Atlantic subtropical gyre (Kiel 276, 33°N, 22°W, Chapter 3 and 4) and in the western part of the North Atlantic subtropical gyre (BATS-IOW, 31.76°N, 64.07°W, Chapter 5). The mean cycle of total particle flux, which is dominated by biogenic particles and the mean cycle of lithogenic (clay) flux based on sediment trap material sampled in the 1990ies at Kiel 276, shows a clear difference of flux patterns (Figure 1.2). Total and biogenic particle flux reach its maxima at 2000 m water depth during early spring every year. Although it is known, that the lithogenic particle flux is mediated by biology [e.g. *Deuser et al.*, 1983; *Klaas and Archer*, 2002; *Armstrong et al.*, 2002; *Fischer et al.*, 2007], the flux of lithogenic particles seems to be decoupled from the total particle flux in the subtropical Northeast Atlantic (Figure 1.2).

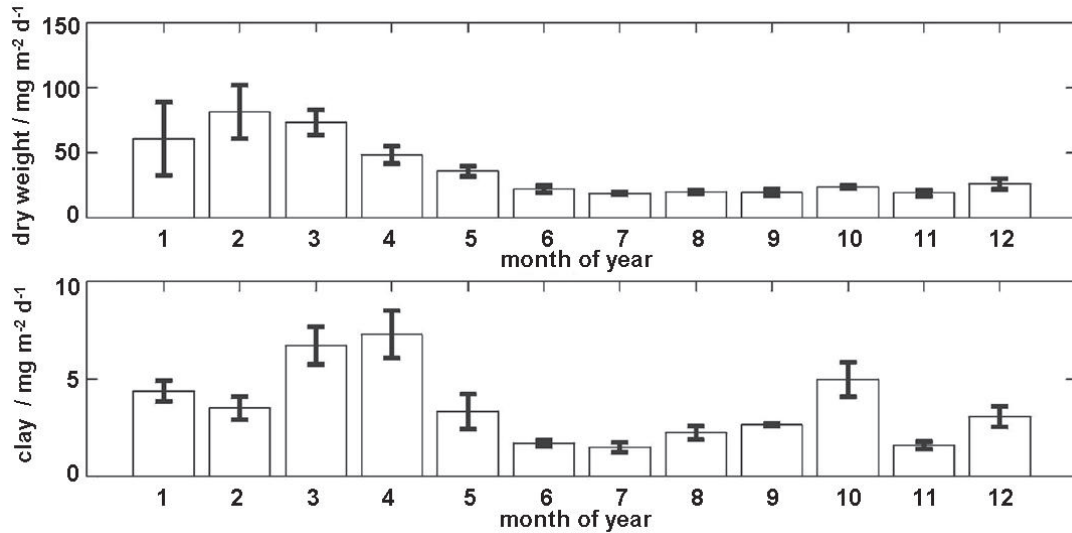


**Figure 1.2:** Annual cycle of total particle flux (upper panel) and clay flux (lower panel) in 2000 m depth at Kiel 276 (33°N, 22°W) in  $\text{mg m}^{-2} \text{d}^{-1}$  (redrawn from *Waniek et al.* [2005b]). Mean monthly fluxes are based on seven year sediment trap sampling. Error bars represent the standard deviation.

This observation arises the question for the reasons of the decoupling between total and lithogenic flux, to which extend North African dust influences the signal of lithogenic flux measured in sediment traps of the subtropical Northeast Atlantic and whether nutrient input due to dust supply impact primary production of surface waters.

Based on the stated primary objective following detailed questions are discussed within the first part of the present work with focus on the eastern subtropical North Atlantic (Chapter 3 and 4):

- What controls the difference between total particle flux and lithogenic or clay mineral flux at Kiel 276?
- How close is the connection between lithogenic particle flux at depth and atmospheric dust deposition in the eastern subtropical North Atlantic?
- Where are the sources of the lithogenic particles?
- Does a dust event affect ocean surface biology in the studied region? Is there an increase of biogenic particles due to fertilization by dust and is it possible to detect enhanced biogenic fluxes at 2000 m depths?

Also the western part of the subtropical North Atlantic is reached by North African dust [e.g. *Carlson and Prospero*, 1972; *Prospero and Carlson*, 1972; *Muhs et al.*, 1990; *Perry et al.*, 1997] and it should be clarified what source areas exist for lithogenic particles trapped at BATS-IOW. Furthermore, the analysis of sediment trap material showed that the authigenic mineral barite, which is formed in connection with biological processes [*Bishop*, 1988; *Dymond and Collier*, 1996; *Paytan and Griffith*, 2007], is present in considerable amounts in BATS-IOW samples and poses the question for the link between barite flux and flux of other biogenic phases.

Following questions are put forward on the BATS-IOW site in the western subtropical North Atlantic (Chapter 5):

- Where do lithogenic particles found in the western subtropical North Atlantic come from?
- Do source areas change within the sampling period from 1998 to 1999 at BAST-IOW?
- What is the seasonal pattern of barite present in the sediment trap material?
- Is the flux of barite linked to the flux of biogenic particles or phases?



The time coverage of sediment trap series at Kiel 276 (2002–2005) and as well at BATS-IOW (1998–1999) allows the comparison of sediment trap samples with satellite data, which was previously not possible due to a gap of satellite observations in the 1990ies. The availability of satellite data supports the understanding of main links and processes between atmosphere, ocean surface and deep ocean. Hence, the present work combines the analysis of qualitative (mineralogy, grain size) and quantitative (mass flux) data of lithogenic and biogenic particle fractions sampled with deep-moored sediment traps with satellite data which indicate dust occurrence over sampling sites and ocean productivity.

## 2 Study sites, methods and additional data

### 2.1 Study sites

The investigation sites are situated in the northern part of the oligotrophic North Atlantic subtropical gyre, far away from continental land masses and from local island influences (Figure 2.1a). The North Atlantic subtropical gyre is a clockwise rotating hydrographic structure driven by the westerlies in mid-latitudes and the easterly flowing trade winds in low latitudes. This oceanic gyre is delimited from west to south by the Gulf Stream, the branches off the North Atlantic Current, the Azores Current, the Canary Current and the North Atlantic Equatorial Current (Figure 2.1a). Equatorial transport of water masses by recirculation occur in the western part of the gyre, though it is also to a lower extent present in the eastern part [e.g. *Stramma and Siedler*, 1988]. The subtropical gyre encompasses several ecological provinces as defined by *Longhurst* [1998], with the North Atlantic Subtropical Gyre Province (NAST) and the North Atlantic Tropical Gyre Province (NATR) covering the largest area of the gyre (Figure 2.1b).

The mooring sites are located in the western (BATS-IOW, 31.76°N, 64.07°W, Chapter 5) and eastern (Kiel 276, 33°N, 22°W, Chapter 3 and 4) parts of the North Atlantic Subtropical Gyre Province (Figure 2.1b) separated by the Mid-Atlantic Ridge. The southern boundary of NAST, between 25°N and 30°N, builds the convergence between trade winds and westerlies [*Longhurst*, 1998]. The deep sea mooring Kiel 276 also referred as L1 [*Waniek et al.*, 2005a,b; *Kuss et al.*, 2010] is situated approximately 240 nautical miles west of Madeira at  $\sim 5200$  m water depth. Surface circulation at the site is characterized by the eastward flowing, meandering Azores Current (AC), an extension of the Gulf Stream, which branches into the Canary Current further east (Figure 2.1a). Mean currents are usually weak at all depth levels and sporadically elevated due to mesoscale events associated with the Azores Current [*Waniek et al.*, 2005a,b].

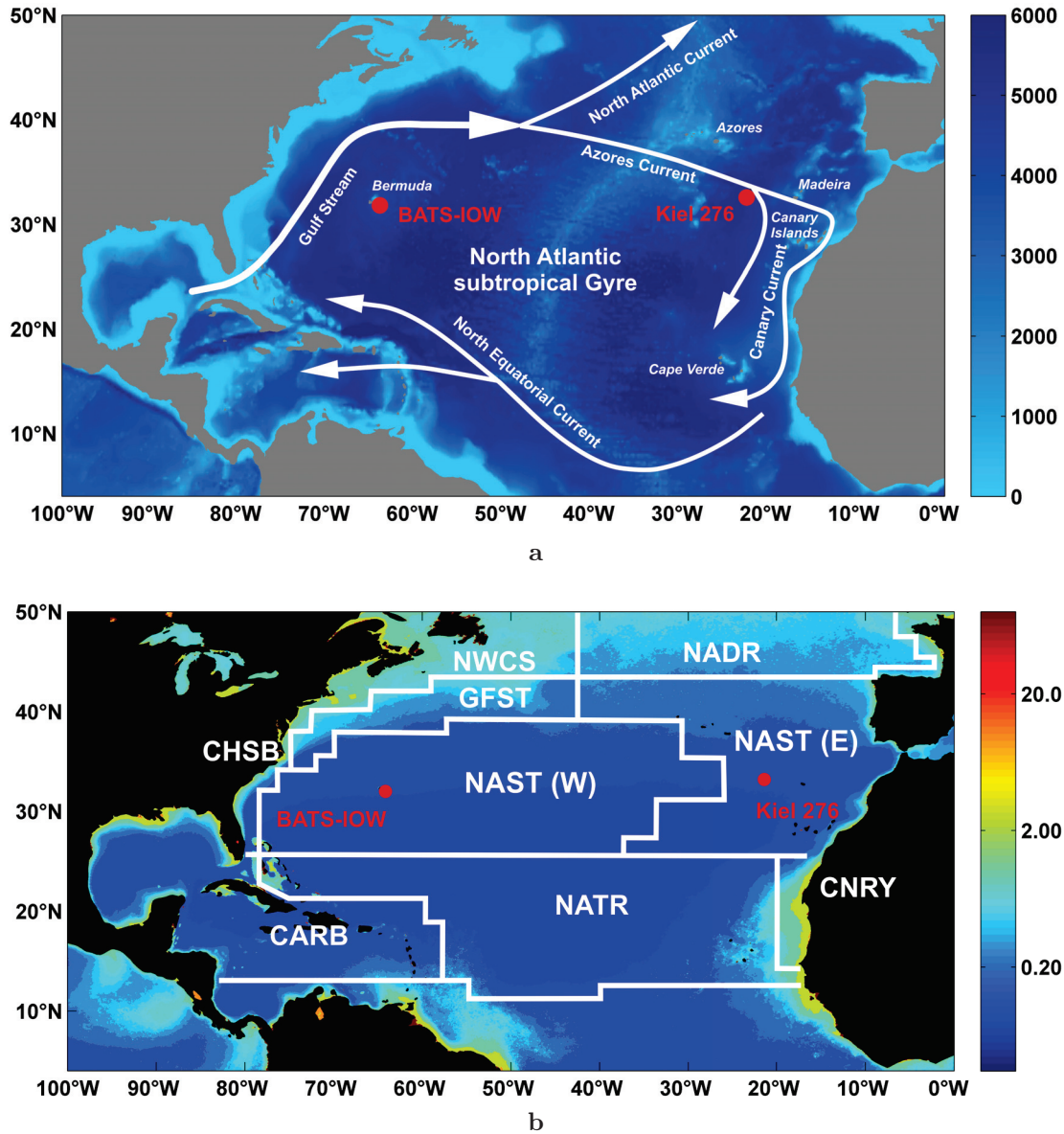


**Figure 2.1:** Location of the sampling sites BATS-IOW and Kiel 276 in the subtropical North Atlantic. a) Main currents of the tropical and subtropical North Atlantic [according to *Rogerson et al.*, 2004]. The color bar indicates bathymetric depth levels in meter. b) North Atlantic ecological provinces after *Longhurst* [1998]. Mean chlorophyll-a concentration from SeaWiFS (average 1997-2010). Displayed chlorophyll-a concentrations (in  $\text{mg m}^{-3}$ ) are indicated in the color bar. CARB: Caribbean Province, CHSB: Chesapeake Bay Province, CNRY: Canary Current Coastal Province, GFST: Gulf Stream Province, NADR: , NAST: North Atlantic Subtropical Gyral Province, NATR: North Atlantic Tropical Gyral Province, NWCS: North Atlantic Shelves Provinces.

The deep sea mooring BATS-IOW is a sampling station of the Bermuda Atlantic Time-series Study (BATS) and located approximately 91 km southeast of Bermuda at 4600 m water depth. A weak recirculation of the Gulf Stream defines the hydrographical patterns at this sampling site. Peak particle fluxes at both study sites are variable, due to their vicinity to bounding northern water masses with biogeochemical characteristics different from the oligotrophic North Atlantic subtropical gyre; and the occurrence of mesoscale eddies (for NAST-E, e.g. *Waniek et al.* [2005a,b]; *Brust and Waniek* [2010]; for NAST-W, e.g. *Deuser et al.* [1981]; *Deuser* [1986]; *Conte et al.* [2001]).

## 2.2 Methods

Sediment trap sampling at both mooring sites was performed by a funnel-type sediment traps with an opening of 0.5 m<sup>2</sup> as described by *Kremling et al.* [1996]. The validity of particle flux measurements by sediment traps, or rather hydrodynamical issues, trapping efficiencies and catchment areas are widely discussed [see, e.g., *Siegel et al.*, 1990; *Gust et al.*, 1996; *Siegel and Deuser*, 1997; *Waniek et al.*, 2000; *Scholten et al.*, 2001; *Siegel and Armstrong*, 2002; *Buesseler et al.*, 2007].

In short, the trap design consists of a fibre glass-reinforced cone with a funnel slope of 34°, a baffle with a honeycomb structure and a rotating sampler assembly holding 21 sampling bottles (400 cm<sup>3</sup> polypropylene cups) (Figure 2.2). Programming of the microprocessor control unit of the sampler assembly allows to sample intervals in the range of 1 min to 1 year. Sampling intervals during sample periods range from days to two months at Kiel 276. During the productive season sampling intervals are normally shorter to get a better temporal resolution of beginning and ending of bloom periods with high particle production. At BATS-IOW sampling intervals are 19-20 days. The sampling period at BATS-IOW lasted only one year (September 1998–August 1999). For Kiel 276, three time series (February 2002–March 2005), each lasting one year, are considered in this study. For treatment of the sediment trap, cleaning procedures and sample cup preparation prior to deployment see section 3.3, [*Kuss and Kremling*, 1999a], *Waniek et al.* [2005b] or *Kuss et al.* [2010]. After trap recovery, sediment trap samples were stored between 4 and 6°C in the dark until laboratory analysis.

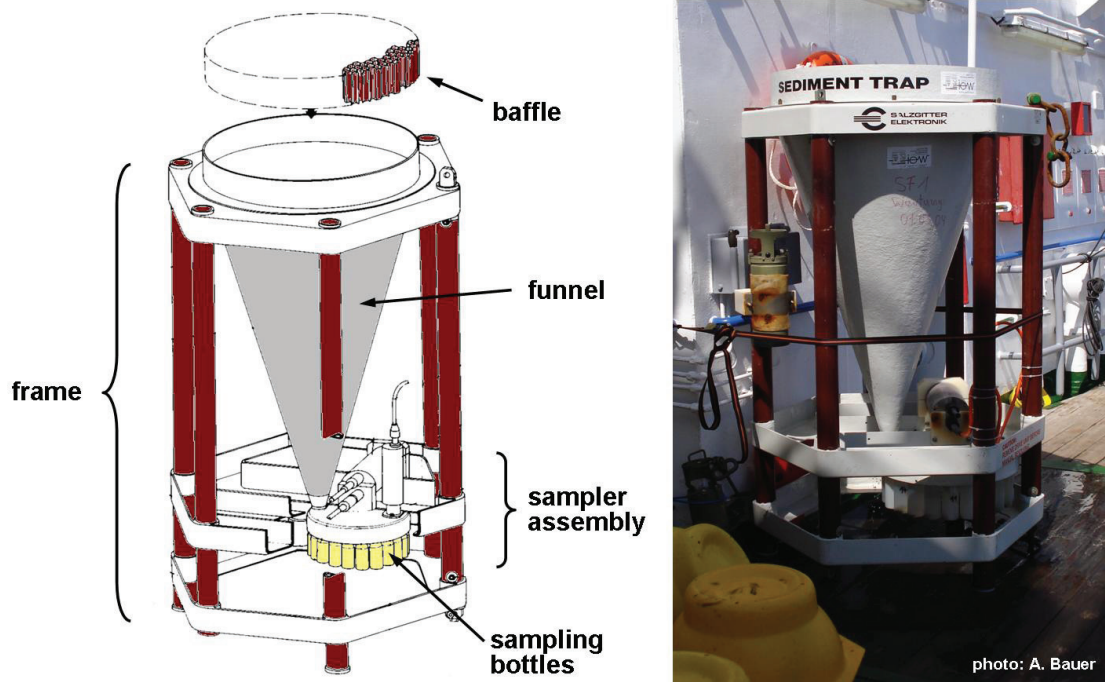


**Figure 2.2:** Simplified sketch of a funnel-type sediment trap according to *Krempling et al.* [1996] (on the left) and photograph of a sediment trap onboard RV Poseidon (on the right). For a detailed description of the trap design see *Krempling et al.* [1996].

Four splits for different analyses were made from each sediment trap sample after the removal of swimmers. The particle flux of each sample was determined from the sea-salt corrected dry weight of sampling material, from trap opening, sampling duration and split factor. The determination of the lithogenic components and major biogenic particle fractions is based on an automated particle analysis with a SEM-EDX (Scanning Electron Microscopy coupled with an Energy Dispersive X-ray spectroscopy) as described in detail in sections 3.3 and 4.6. Generally, the identification of specific minerals is based on the comparison of their elemental composition measured by the EDX with the chemical composition of known (standard) minerals. During the automated particle analysis particles are counted and identified. The result gives a semiquantitative estimate of the particle composition of each sample. Counted minerals are recalculated to mass fluxes of each mineral or particle group. This analytical approach of determining

biogenic (especially opal and carbonate) and lithogenic fraction differs from methods normally used for sediment trap material analysis. Carbonate and opal are normally determined using chemical methods [Deuser *et al.*, 1990; Conte *et al.*, 2001; Waniek *et al.*, 2005a,b]. Whereas the determination of lithogenic fraction in sediment trap material is based on the calculation of a residue mass fraction after subtracting determined biogenic phases or on the aluminium content (Table 3.1). In this study the lithogenic flux is calculated from its relative proportion determined by the SEM-EDX particle analysis (Table 3.1). According to this, the flux of different lithogenic mineral species as quartz, feldspars (potassium feldspar, albite, plagioclase), clay minerals (kaolinite, illite, chlorite, smectite, palygorskite) or metal oxides was determined. The SEM-EDX analysis provides data for biogenic and lithogenic components in one run. Only POC and PON were determined separately according to [Erhardt and Koeve, 1999], because carbon and nitrogen were omitted from analysis. The content and flux of carbonate, opal and other biogenic components (e.g. barite) was determined as described above.

**Table 2.1:** Different ways of determining the lithogenic fraction of sediment trap material.

Determination of the lithogenic fraction	Reference
lithogenic flux = total flux - (opal flux + carbonate flux + 2×POC)	Neuer <i>et al.</i> [1997, 2002, 2004]; Ratmeyer <i>et al.</i> [1999a,b]
lithogenic fraction = total mass - (opal + carbonate + organic matter), organic matter = 2.3×POC	Jickells <i>et al.</i> [1998]; Conte <i>et al.</i> [2001]
lithogenic flux = clay = 10×Al (Al content in clays according to Goldberg and Arrhenius [1958])	Waniek <i>et al.</i> [2005b]
lithogenic flux = Al concentration (8.4% Al content in clays according to Turekian and Wedepohl [1961])	Bory and Newton [2000]; Bory <i>et al.</i> [2002]
lithogenic flux = 12.15×Al(w%)	Honjo <i>et al.</i> [2000]
lithogenic flux = Al flux	Honjo <i>et al.</i> [1995]
lithogenic flux = Al×12.58 (factor according to Wedepohl [1995])	Lamborg <i>et al.</i> [2008]
lithogenic flux = total flux \ 100% × lithogenic fraction%	this study

## 2.3 Additional data

Satellite data products used in this study provide information about atmospheric aerosol content and ocean surface chlorophyll-a concentration. For the observation of atmospheric aerosol occurrences over the mooring positions, the MODIS (Moderate Resolution Imaging Spectroradiometer) aerosol optical depth (AOD) and the TOMS (Total Ozone Mapping Spectrometer) aerosol index (AI) was used. Those aerosols encompass various aerosol types beneath mineral dust. To detect signals of mineral dust over the mooring sites modeled dust AOD data from the GOCART (Goddard Chemistry Aerosol Radiation and Transport model) model [e.g. *Chin et al.*, 2002; *Ginoux et al.*, 2001, 2004] were used.

Shown chlorophyll-a data are SeaWiFS (SEA-viewing Wide Field of-view Sensor) products. Satellite and modeled data are provided by the online portal Giovanni (Goddard Earth Sciences Data and Information Services Center Interactive Online Visualization ANd aNalysis Infrastructure, *Acker and Leptoukh* [2007]). Satellite and modeled data were averaged over the catchment areas of both deep sea mooring sites (explained in Chapter 4 and 5).



### 3 Atmospheric dust contribution to deep-sea particle fluxes in the subtropical Northeast Atlantic

*Brust, J., and J. J. Waniek, published 2010 in Deep-Sea Research I 57, 988–998*

#### 3.1 Abstract

The lithogenic flux of sediment trap material was analyzed from a three year time series (February 2002–March 2005) at 2000 m depth in the Northeast Atlantic (Kiel 276, 33°N, 22°W) with regards to the seasonal and interannual variability of flux intensity and mineralogy - by applying an automated particle SEM-EDX analysis (scanning electron microscope - energy dispersive X-ray analysis). The lithogenic flux shows strong interannual variations with highest lithogenic flux rates occurring during January-February and April-March coupled to the total particle flux. Mean lithogenic flux rates for the sample years are 7.1 (2002–2003), 5.1 (2003–2004) and 16.1 mg m<sup>-2</sup> d<sup>-1</sup> (2004–2005). Mineral assemblages from the three sample years reveal distinct major minerals related to specific source regions. Clay minerals dominate the lithogenic fraction within the years 2002 and 2004 with illite (2002–2003) and palygorskite (2003–2004) being the major clay minerals. During the year 2004–2005, quartz is the major lithogenic mineral accompanied by smectite. The mineral assemblages hint to a mixture of North African source areas with dominant sources in Mauritania and north western parts of NW Africa for the years 2002–2004 and central Sahara (Algeria-Mali) within the year 2004–2005.



## 3.2 Introduction

Airborne mineral dust plays an important role in delivering essential macro- and micronutrients to surface waters of distal ocean regions where no direct continental riverine and coastal or upwelling water nutrient input is available for phytoplankton growth and primary production. The global dust production is estimated to be  $1700 \times 10^6 \text{ t yr}^{-1}$  [Jickells *et al.*, 2005]. Almost the half of it is released from North Africa, where the Sahara and Sahel zone are the key source areas [D’Almeida, 1986; Harrison *et al.*, 2001]. The biggest amount of North African dust is transported within the prevailing wind systems in western direction (Figure 3.1; e.g. Prospero and Carlson [1972]; D’Almeida [1986]). The major wind systems are the Saharan Air Layer (SAL), including its northern branch and the NE trade winds transferring more than one-third of the global eolian dust deposition (to the world oceans) into the North Atlantic (Duce *et al.* [1991]; Figure 3.1).

In the North Atlantic deep sea sediments eolian derived particles make up 10 % to 50 % or more of the non-carbonate fraction [Johnson, 1979; Guerzoni *et al.*, 1997; Chavagnac *et al.*, 2008], which varies with longitude and latitude depending on the spatial and temporal variability of the major wind fields in seasonal (Intertropical Convergence Zone), interannual (North Atlantic Oscillation) and geological time scales. Deep-sea sediment cores as well as ice cores showed that the content and composition (size distribution and mineralogy) of aerosols are affected by climate changes through time [see Rea, 1994, and references therein]. Aerosols and/or mineral dust can have a direct (scattering and absorbing of solar radiation) or an indirect (cloud formation, precipitation, cloud radiative properties) effect on the climate. In terms of climate change and anthropogenic driven desertification and/or deforestation of source regions it is important to investigate and observe aerosol source regions, aerosol production, transport, modification and deposition to quantify its impact on marine biological and geochemical cycles [e.g. Harrison *et al.*, 2001]. Investigations of mineral composition and transport direction of airborne dust were mostly done on aerosol samples [e.g. Prospero and Carlson, 1972; Chiapello *et al.*, 1997; Caquineau *et al.*, 1998]. Lithogenic flux studies with different approaches using sediment trap material exist for the Mediterranean [e.g. Rutten *et al.*, 2000], the Sargasso Sea [e.g. Jickells *et al.*, 1998], for the Pacific [e.g.

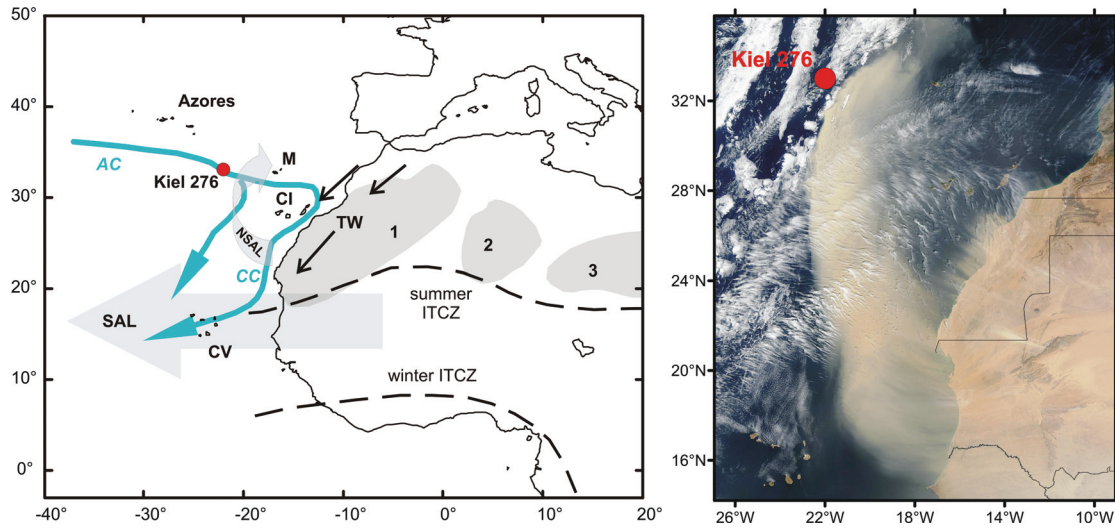


**Figure 3.1:** (left side) Map showing the position of the study site (red dot) and displaying major sea surface currents of the subtropical Northeast Atlantic (blue arrows) and main wind fields over North Africa and the north eastern Atlantic (grey and black arrows). Grey areas indicate major source areas of North Africa (1: Morocco, North Mauritania; 2: South Algeria, Mali, Niger; 3: South Lybia, Chad; *D’Almeida* [1986]; *Molinaroli* [1996]). (AC: Azores Current; CC: Canary Current; SAL: Saharan air layer; NSAL: northern branch of the Saharan air layer; ITCZ: Intertropical Convergence Zone, shown in its summer and winter position; TW: northeast trade winds; M: Madeira; CI: Canary Islands; CV: Cape Verde Islands); (right side) North African dust outbreak approaching study site (Kiel 276) at 33°N, 22°W. (satellite view from 4<sup>th</sup> March 2004, from MODIS; <http://rapid-fire.sci.gsfc.nasa.gov/>)

*Lamborg et al.*, 2008] or the Arabian Sea [e.g. *Ramaswamy et al.*, 1991]. In the Northeast Atlantic, studies of lithogenic particle fluxes exist for the Cape Verde and Canary Islands regions [*Neuer et al.*, 1997; *Ratmeyer et al.*, 1999a,b]. The application of sediment traps attempt to link the atmospheric dust input with the ocean interior processes, additionally providing data within selected time intervals.

Our study focuses on the influx of airborne mineral dust into the deep-ocean of the subtropical Northeast Atlantic, half way between the Azores and the Canary Islands at the mooring site Kiel 276 (33° N, 22° W; Figure 3.1). Mineral composition will reveal source regions as well as interannual compositional differences within the lithogenic sediment trap material. First studies at the mooring site accentuated hydrographic investigations [*Käse and Siedler*, 1982; *Siedler et al.*, 2005],

biogeochemical studies started in the beginning of the 1990ies with the mounting of sediment traps at selected depth during the international Joint Global Ocean Flux Study [*Kremling et al.*, 1996; *Schiebel et al.*, 2002; *Waniek et al.*, 2005a,b]. *Chavagnac et al.* [2007] published sediment trap data of the Kiel 276 mooring encompassing one year period. Analysis of 3000 m sediment trap material showed a NW African origin of the lithogenic material deduced from mineralogy, Sr isotopic composition and REE patterns. Lithogenic flux data were also reported by *Waniek et al.* [2005b] by recalculating aluminium fluxes, but the interannual variations of lithogenic fluxes, especially of the mineralogical composition remain poorly quantified in this part of the Northeast Atlantic. Explicit studies of mineralogy gain even more importance since recent studies have shown the significance of clay minerals and silicates in delivering soluble iron to the sea surface [*Blain et al.*, 2007; *Journet et al.*, 2008]. Beneath a detailed study of single lithogenic mineral flux, its potential supply of solvable iron is used to estimate the impact on primary production over the duration of this study.

### 3.3 Material and Methods

#### Study area

The Kiel 276 mooring is situated at 33° N, 22° W within the Madeira basin (240 nm west of Madeira) at 5500 water depth, in the northeastern edge of the Northern Atlantic Subtropical Gyre Province [*Waniek et al.*, 2005a,b]. The study site is affected by the Azores frontal system of the Azores Current (Figure 3.1), which represents an eastward flowing branch of the Gulf Stream [*Klein and Siedler*, 1989]. Between the cold waters of the northern North Atlantic and the warm subtropical North Atlantic water masses, the Azores Current forms a natural boundary. Further information about the hydrographic conditions at the study site can be found in *Siedler et al.* [2005] and *Waniek et al.* [2005a,b].

#### Sediment trap material

For this study, sediment trap material from 2000 m depth was analyzed covering 3 sampling years (February 2002–March 2005) of the deep sea mooring Kiel 276

(33° N, 22° W). Sampling was performed using a 0.5 m<sup>2</sup> funnel type sediment trap [Kremling *et al.*, 1996]. The trap configuration contains a rotator with sample bottles, allowing a temporal separably sampling procedure with intervals of 14 to 31 days, depending on the seasonality of biological production [Waniek *et al.*, 2005b]. The sampling assembly (cone, rotator and 400 cm<sup>3</sup> polypropylene sampling bottles) was solid cleaned according to the standard procedure for trace elements analysis [Kuss and Kremling, 1999a]. The sampling bottles were filled up with a mixture of 4:1 in-situ seawater and sodium acid (NaN<sub>3</sub> 5 % stock solution in high purity water), added NaCl lead to a final salt content of 38 g l<sup>-1</sup> in the sampling cups [Waniek *et al.*, 2005a, and references therein]. Sampling started after a rinse-period of 1 to 2 weeks. The three investigated time series occupy the years February 2002–April 2003 (series 22), April 2003–March 2004 (series 23) and March 2004–March 2005 (series 24) (see caption of Figure 3.2). Gaps between time series result from the availability of ships for trap recovery and deployment. Gaps between the single sample years were not filled. For more detailed explanations about sample treatment, mass flux determination (given in mg m<sup>-2</sup> d<sup>-1</sup>) and individual sample processing see Waniek *et al.* [2005a,b].

### SEM–EDX analysis

The focal point of this study is the determination of biogenic, authigenic and lithogenic components within the particle association of the trap samples. The scanning electron microscopy coupled with an energy dispersive X-ray micro-analysis (SEM–EDX), chosen here, is a method which facilitates the particle determination of low sample quantities [Bauerfeind *et al.*, 2005]. An alternative method for mineral determination of sediments would be the X-ray diffraction (XRD). The proper analysis of the lithogenic fraction and of clay mineral assemblages with the XRD requires around 1 g of sample material and an intense mechanical and chemical treatment of the samples as homogenization with mortar and pestle, decalcification and removal of opal [Moore and Reynolds, 1997; Sirocko and Lange, 1991] to get reliable mineral data. Due to the low amount of sample material available in sediment trap samples (0.8 g on average) and the low amount of the remaining clay mineral fraction after chemical treatment, we decided to use the SEM–EDX

method for our approach. The SEM–EDX analysis was performed at the IOW using the Quanta FEI 4000 electron microscope and the joined X-ray microanalysis EDAX GENESIS 4000 system. For the SEM–EDX analysis, filters were prepared by filtration of subsamples through  $0.4\text{ }\mu\text{m}$  nucleopore filters (Millipore polycarbonate membrane filter, diameter of 49 mm). Simultaneously, the samples were rinsed with Milli–Q water for desalination. The filters were dried for several hours at  $50^{\circ}\text{C}$ . One filter cutting was stuck on a carrier stub and sputtered with elemental carbon to warrant electric conductivity. During the SEM–EDX analysis, each filter cutting underwent an automated particle analysis, which records morphological (grain size, shape) and chemical parameters (12 main elements) for each measured particle. The method is based on an automated image processing system working with gray–scale limits. Per filter 500 to 2500 particles were distinguished from the filter background and analyzed within a particle size interval of clay to silt size. The 12 elements measured for a single particle are Al, Ca, Cl, Fe, K, Mg, Mn, Na, P, S, Si and Ti. Those elements constitute most common minerals, organic, and inorganic particles and don't show interfering EDX–spectra [Leipe *et al.*, 1999; Bauerfeind *et al.*, 2005]. Element oxides were calculated and normalized to 100 %. The standardization of particle elements enables the identification of minerals and mineral or particle groups according to element boundaries of standard minerals. For the particle determination and quantification, the particle element lists were processed with the mineral classification program "mineral" (© W. Zahn). Within the particle spectrum more than 20 minerals and mineral/particle groups were identified. The biogenic fraction involves carbonates, opal and other biogenic minerals (e.g. barite, apatite) and the lithogenic fraction comprises quartz, feldspars, clay minerals (illite, smectite – specifically montmorillonite, chlorite – Mg- to Fe-rich chlorites, kaolinite, palygorskite) and element oxides and hydroxides (Fe, Al, Mn). The counts of the identified minerals were again normalized to 100 %, since in every sample a different number of particles was identified, and recalculated with the mass flux values of the appropriate sample, leading to mass flux data ( $\text{mg m}^{-2}\text{d}^{-1}$ ) for single identified minerals or particles for each sample of the time series. This semiquantitative approach is based on the assumption that

all particles represented by counts have similar grain sizes and densities<sup>1</sup>, independent from mineral species varieties. This assumption is supported by the grain sizes of the samples (see section 3.2). Samples were not homogenized at any time prior to the analysis.

### Repeatability

The reproducibility of the SEM–EDX analysis was tested by means of 5 repeated measurements of one sample. Three filter compounds were produced from one sample and from one of these filter samples 3 stub cuttings were prepared. The 6th measurement of this sample was analyzed in line with the series measurements. The single sample results, analyzed within the measuring processing of the series, show a stronger deviation from the repeated measurements (Table 3.1). One reason for the measured variability is the differing amount of sample material used for the analysis. For the repeated measurements a higher sample amount was dispersed for filter preparation, whereas for the series measurements only a spatula tip of sample was dispersed. The higher value of analytical uncertainty gives a more realistic view of the analytical reproducibility, leading to variations of  $\pm 9\%$  of the lithogenic fraction and  $\pm 6\%$  of the clay minerals (Table 3.1).

## 3.4 Results & Discussion

### Lithogenic fluxes from February 2002 to March 2005

Typically, the main particle flux occurs between February and May in every year, with mid-February and mid-April presenting the periods with highest flux rates [Waniek *et al.*, 2005a,b; Storz *et al.*, 2009]. Through the year biogenic calcium carbonate deposition dominates the particle flux. The highest particle flux rates are coupled to the late winter bloom period of coccolithophores in this part of the Atlantic. The main peaks as well as the yearly values are highly variable in strength of mass flux between years [Waniek *et al.*, 2005a,b]. This is also seen in the particle flux rates for the investigated years of sampling (Figure 3.2a). Series 22 starts with

---

<sup>1</sup>densities in  $\text{g cm}^{-3}$  of major mineral phases: calcite: 2.6–2.8, quartz:  $\sim 2.65$  and clays: 2–3 (for further information see standard textbooks for mineralogy)

**Table 3.1:** Results of the repeated measurements of one sample (series 23/9) given in  $\text{mg m}^{-2}\text{d}^{-1}$ . The other biogenic group includes: barite, Ca-P mineral, and organics. The other lithogenic group involves Fe oxides, bauxite, Ti minerals and an unspecified Fe-Al-Si mineral. The contribution of illite, smectite, chlorite, kaolinite and palygorskite to the clay minerals is also listed. Standard deviations for listed particle groups and minerals are shown in parenthesis.

Particle class	single series measurement	repeated measurements	repeated double measurements
biogenic particles			
carbonates	18.47	12.15 (1.46)	13.20 (2.71)
opal	0.58	1.57 (0.34)	1.40 (0.48)
other biogenic	0.29	0.47 (0.10)	0.44 (0.11)
lithogenic particles			
quartz	0.26	1.57 (0.32)	1.35 (0.57)
feldspars	0.23	0.85 (0.18)	0.74 (0.28)
clay	4.51	7.32 (0.92)	6.85 (1.35)
illite	0.13	1.90 (0.47)	1.61 (0.79)
smectite	0	0.10 (0.05)	0.08 (0.06)
chlorite	0.03	0.39 (0.09)	0.33 (0.16)
kaolinite	0.23	0.56 (0.27)	0.51 (0.28)
palygorskite	4.12	4.37 (0.69)	4.32 (0.63)
other lithogenic	0.10	0.50 (0.15)	0.44 (0.20)

relatively high particle flux rates (March and April), which are reduced over the rest of the year and remain also low during the following year of sampling (series 23; *Storz et al.* [2009]). An abrupt increase of the mass flux occurs at the beginning of the 2004–2005 sampling period (series 24). This year is also characterized by high mass flux rates, compared to the sampling years of series 22 and 23. As seen in previous studies, the total particle flux pattern resembles the seasonal pattern between 2002 and 2004 [*Storz et al.*, 2009]. Interannual variabilities of the particle flux rates in this region and reduced seasonality at times (eg. in series 23) are often linked with the displacement of the Azores Current frontal system [*Schiebel et al.*, 2002; *Waniek et al.*, 2005a] which has an effect on the catchment area and on local ocean surface productivity, by keeping low nutrient waters of subtropical origin above the mooring position.



The lithogenic flux pattern shows a similar picture, highest lithogenic particle fluxes often appear to be coupled with highest total particle flux rates (Figure 3.2a). In series 22 the lithogenic flux follows that of the total flux with highest values in April ( $27.5 \text{ mg m}^{-2}\text{d}^{-1}$ ) and May ( $16.1 \text{ mg m}^{-2}\text{d}^{-1}$ ), but shows a stronger decrease for the rest of the year and a peak prior to the February maximum of total particle flux (Figure 3.2a,b). During the following series 23, the lithogenic particle flux increases until June ( $10.7 \text{ mg m}^{-2}\text{d}^{-1}$ ) and drops until the end of the sampling year to a minimum  $0.2 \text{ mg m}^{-2}\text{d}^{-1}$  (April 2004), whereas the total particle flux shows a second maximum during January and February. Highest lithogenic flux rates occur in May 2004 ( $42.5 \text{ mg m}^{-2}\text{d}^{-1}$ , series 24) concur with the April–May maxima of the total particle flux. For the rest of the year, both, the lithogenic and the total flux shows strong alterations from sample to sample or month to month. After a clear decline of the flux rates during end of May and mid-June 2004, the total flux generally increases again. The lithogenic flux shows an apparent decrease and again a major peak during March 2005 ( $40.3 \text{ mg m}^{-2}\text{d}^{-1}$ , Figure 3.2b). It is remarkable that the highest percental contribution of the lithogenic fraction doesn't go along with highest lithogenic mass fluxes (Figure 3.2a). The lithogenic contribution averaged over each single sampling year vary from year to year with 12.7 (series 22), 20.1 (series 23) and 13.4 % (series 24). Series 24 exhibits the highest average lithogenic flux rate ( $16.1 \text{ mg m}^{-2}\text{d}^{-1}$ ), whereas series 22 and 23 show lower lithogenic fluxes with mean values of  $7.1$  and  $5.1 \text{ mg m}^{-2}\text{d}^{-1}$  respectively. These values are higher than previously published lithogenic particle flux rates for this region [e.g. *Kuss and Kremling*, 1999a; *Wanick et al.*, 2005a,b].

The lithogenic fraction given here encompasses quartz, feldspar, clays and oxides determined by the SEM-EDX analysis. Published data of lithogenic flux rates are estimated from measured aluminium contents and therefore represent clay flux rates only [*Wanick et al.*, 2005a,b]; nevertheless, the aluminum content also involves feldspars which are tectosilicates incorporating aluminium atoms in its crystal lattice. The comparison of our clay flux rates with the published values for lithogenic (clay) fluxes reveal a good agreement. Calculated mean clay flux values of  $3.7$  (series 22),  $4.2$  (series 23) and  $3.1 \text{ mg m}^{-2}\text{d}^{-1}$  (series 24) are in line with clay fluxes of  $3.4$  and  $4.2 \text{ mg m}^{-2}\text{d}^{-1}$  given for the period from 1993 to 1996 [*Wanick et al.*, 2005b] and the given percental contribution to the total flux of around 10 %



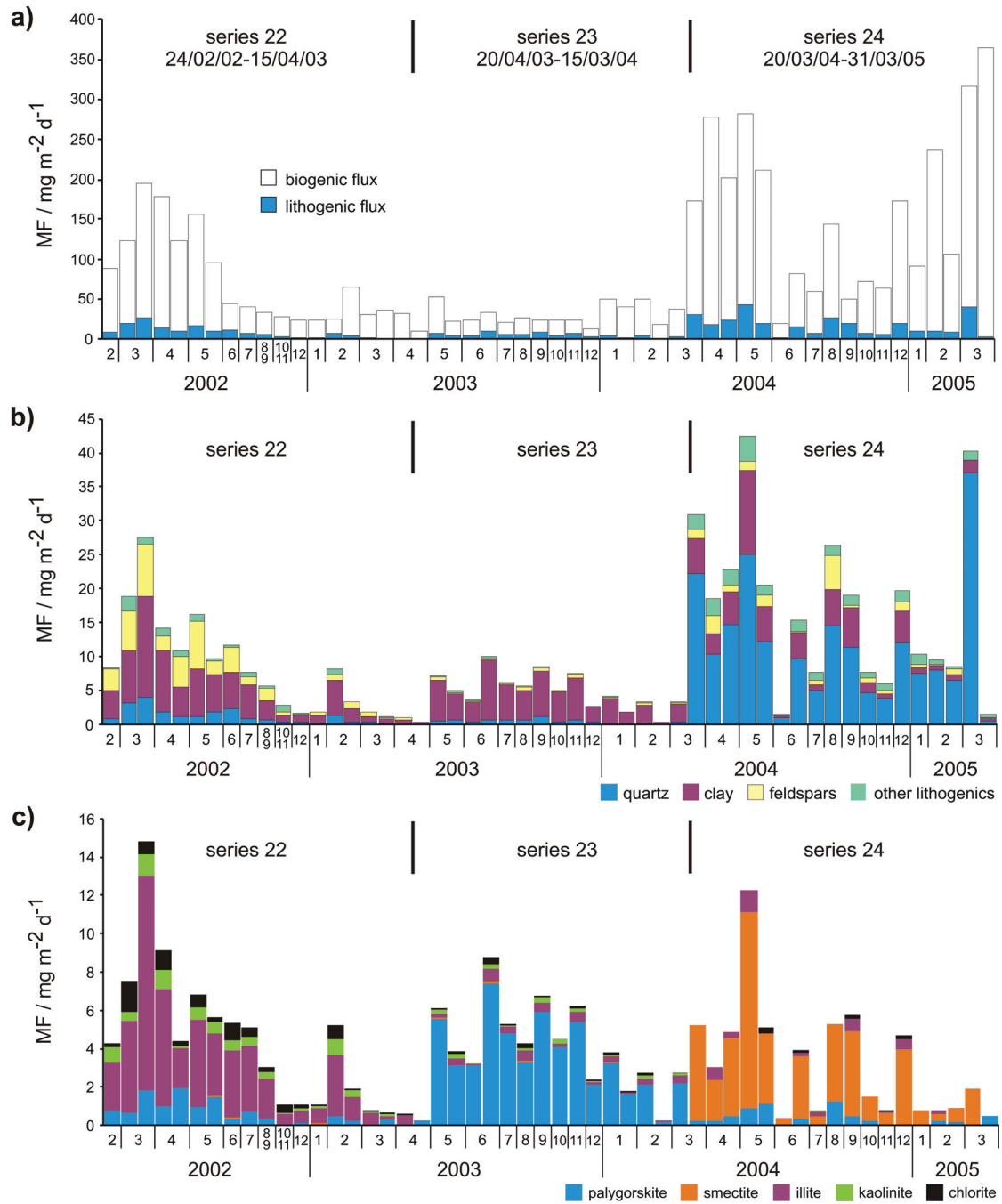


**Figure 3.2:** a) Total particle flux of investigated time series. b) Lithogenic particle flux showing the fluxes of main lithogenic particle groups. c) Clay mineral flux of individual clay minerals. (The flux of particles is given in  $\text{mg m}^{-2} \text{d}^{-1}$ .)

[Kuss and Kremling, 1999a; Waniek *et al.*, 2005a]. Moreover, several samples from series 23 contain lithogenic percentages of considerably more than 11 %, but the clay flux rates for the individual samples stay mostly below  $10 \text{ mg m}^{-2}\text{d}^{-1}$  (Figure 3.2c). The clay content dominates the lithogenic flux during 2002–2003 and 2003–2004, at an average accounts for 52 and 84 % of the lithogenic flux respectively, shared with feldspar mineral contribution in series 22. Within the particle flux of the year March 2004–March 2005 quartz is the major component of the lithogenic fraction, being lower during the other years of sampling (Figure 3.2b).

The quartz contribution average out 64 % of the lithogenic flux, whereas the average clay content makes up to 19 % of the lithogenic fraction of series 24. This means that at this site the non-clay minerals as quartz play an important role in defining the lithogenic flux or even dominate the lithogenic flux. The applied particle analysis reveals that the lithogenic flux can be underestimated if only the clay minerals are considered, because of the occurrence of non-clay minerals.

### Grain size distribution of particles

The SEM–EDX analysis provides grain size data for every particle under investigation within the measured grain size interval. Grain size analysis of the investigated trap time series show mean grain sizes of 1.8 to  $2.8 \mu\text{m}$ , with samples of series 24 representing the slightly coarser particles (Figure 3.3). The average mean grain size of the lithogenic particles of  $2.3 \mu\text{m}$  comprise equally sized clay and feldspar minerals (some  $2.2 \mu\text{m}$ ) and somewhat coarser quartz grains (about  $2.9 \mu\text{m}$ ). Generally the lithogenic particle groups (clays, feldspars, quartz) of series 24 are about  $1 \mu\text{m}$  larger in the mean grain size than in series 22 and 23 (Figure 3.4). The detected grain sizes infer an atmospheric long-range transport of particles carried in high altitudes. Most of the lithogenic particles range between 1.3 and  $4.8 \mu\text{m}$ , only few quartz and clay particles have maximum sizes of 31 or  $44 \mu\text{m}$ . Reported grain sizes of aerosols over the North Atlantic range mostly between 0.1 to  $10 \mu\text{m}$  [Jickells *et al.*, 2005] and in a worldwide view aerosol particles are basically smaller than  $5 \mu\text{m}$  [see Péwé, 1981, and references therein]. Commonly, the coarse fraction ( $5\text{--}10 \mu\text{m}$ ) decreases within long range transport of 1000 to 2000 km [Schütz, 1989]. Reported aerosol grain size distributions on the Canary Islands circa 300

km off the African coast at 2000 m altitude show a similar main grain size range of 0.6-5  $\mu\text{m}$  [Torres-Adr3n *et al.*, 2002] compared to the samples presented here, collected 1200 km away from the African coast.

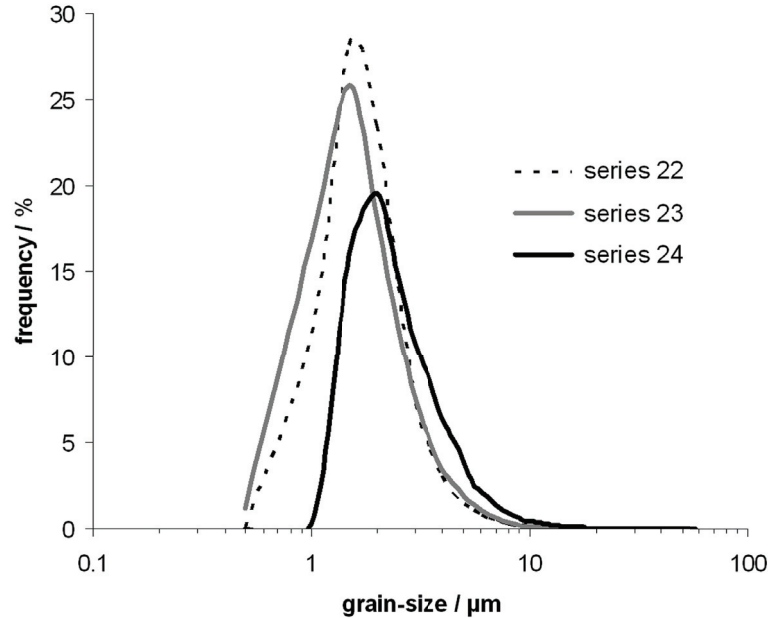


**Figure 3.3:** Grain size distributions retrieved from SEM-EDX analysis of investigated sediment trap series. Note that particles of series 24 are slightly coarser than particles of series 22 and 23.

Characterized by a mostly platy flake-like (e.g. kaolinite, smectites) to fibrous (palygorskite) morphology and small grain sizes, clays can be deflated easily (depending on wind-strength) from soils in poorly vegetated arid to sub-arid regions and travel very far through the atmosphere [Chamley, 1989]. Whereas it is known that clay assemblages are unaffected by gravitational settling within atmospheric long-range transport, the contribution of quartz within aerosols decreases with distance from the source due to gravitational scavenging. The slightly larger quartz particles might be delivered from another (higher) altitude, settling earlier than the clay minerals. Ratmeyer *et al.* [1999b] noted a seasonal dependence in grain size distribution of sediment trap material at a Cape Verde site (11°29.0'N, 21°01.0'W) connected to summer time high altitude Saharan Air Layer (SAL) transport leading to coarser mean grain sizes and lower altitude transport within the trade wind

regime during winter and spring. Similar processes might occur at the study site presented here. The trade wind dust contribution to sediment trap flux is more important than the SAL dust input at Cape Verde as well as Canary Islands [Ratmeyer *et al.*, 1999a]. This fact could also explain the comparatively high quartz content in samples of series 24 (Figure 3.2b). An other possible influence on lithogenic mineral composition in sediment traps is the organic material linked transport of clay-sized terrigenous particles, which is explained by the "ballast hypothesis" [Armstrong *et al.*, 2002; Klaas and Archer, 2002]. Because of the small grain sizes of measured lithogenic particles (mostly smaller than  $4.8 \mu\text{m}$ ), a fractionation within the water column during lateral transport is presumably insignificant (see Ratmeyer *et al.* [1999a]). Lateral transport processes within the ocean interior via currents might have an influence on the mineral composition in sediment trap samples, but not compulsory to grain sizes. Current meter data revealed moderate current velocities at the sampling site. Generally, the mean current velocities at all depth levels of the study site are low interrupted by strong mesoscale events (maximum speeds up to  $25 \text{ cm s}^{-1}$ ) lasting 1–3 months [Waniek *et al.*, 2005a]. The current velocities decrease from surface to bottom - up to 1000 m depth current velocities range between 20 and  $25 \text{ cm s}^{-1}$ , below 1000 m current velocities decrease to  $5 \text{ cm s}^{-1}$  [Waniek *et al.*, 2005a] - deducing a low contribution of lateral advection of particles.

### Mineralogy and origin of the lithogenic particles

As stated in many publications, the mineral assemblage of aerosol dust and deep-sea sediments are characteristic for different source regions [e.g. Chamley, 1989; Avila *et al.*, 1997; Caquineau *et al.*, 1998]. Especially the clay mineral assemblage provides information about dust sources. Lange (1982) illustrated that the different species of clay minerals are qualitatively distributed ubiquitously on the North African continent, differences appear in prevalence of particular clay mineral species or associations at distinct geographic settings; conditioned by the petrography of the bedrock and prevailing climatic situations. The investigated sediment trap time series show clear differences in presence of dominant clay minerals. Illite, palygorskite and smectite are the major minerals characterizing 50% of the

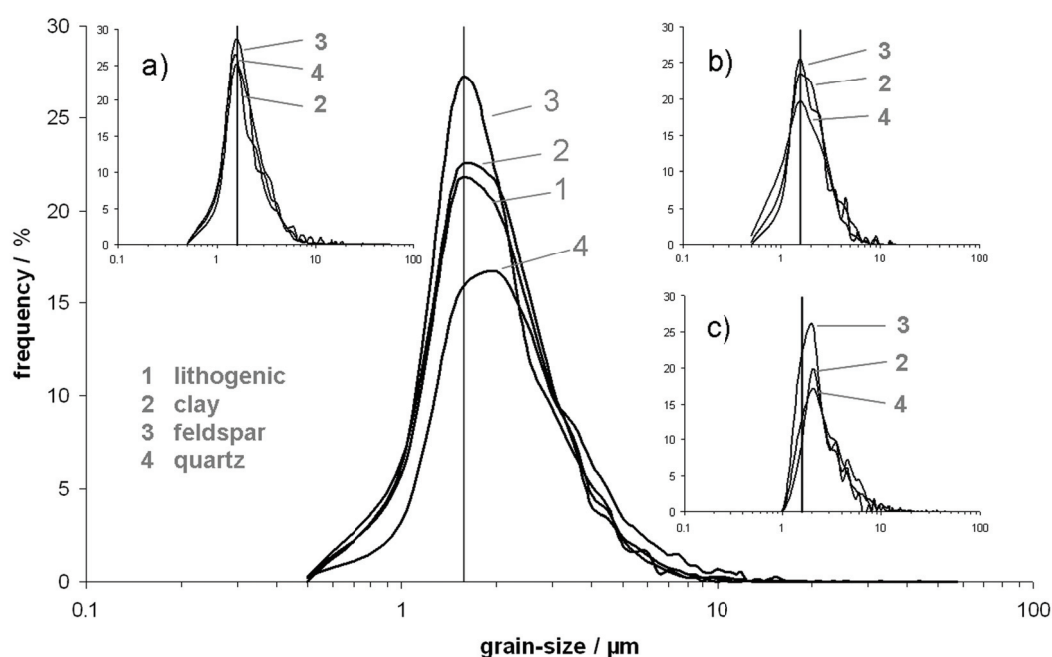


**Figure 3.4:** Grain size distributions of lithogenic particle groups of the whole data set (samples of all sample years are involved) and for single years of sampling (a) series 22, b) series 23 and c) series 24). The vertical line marks the main peak of the lithogenic flux distribution (all samples are involved), also shown in sub-diagrams.

clay mineral fraction of one sample year in each case (see Figure 3.2c). Kaolinite is also present but its contribution becomes less important from 2002 to 2005 and lacks in almost all samples of series 24. *Caquineau et al.* [1998, 2002] approves the illite-to-kaolinite ratio for deciphering dust sources. In the first instance, the ratios, pictured in a quartz-illite-kaolinite-ternary diagram (Figure 3.5a), exhibit a Northwestern Saharan source for the samples of series 22 and 23 characterized by values higher than 2. Only few samples might be interpreted to be delivered from the south and central Sahara sources as defined by I/K ratios of 0.5 to 1. Generally, illite is the most abundant clay mineral in aerosols transported over the North Atlantic and in related deep-sea sediments, followed by the presence of kaolinite [Prospero, 1981; Chamley, 1989]. The conjoint occurrence of both clay minerals

is dependent on latitude as kaolinite is characteristic for low latitudes where hydrolytic weathering prevailed [Griffin *et al.*, 1968; Thiry, 2000]. Below 15° N west of Africa kaolinite forms the dominant clay mineral in eastern Atlantic sediments. Assuming a North African source of eolian lithogenic detritus within sediment trap samples, source areas south of 15° N can be excluded regarding the I/K ratio. The ternary diagram also shows that the content of illite and kaolinite declines from year to year, challenging reliable propositions of the source area of investigated samples by means of that ratio. Another tracer mineral for north African dust is palygorskite [Avila *et al.*, 1997, and references therein], a Mg-bearing clay mineral which is present in samples of all investigated years. It is the main clay mineral in series 23. During this year the other clay minerals pale in comparison to series 22 and 24. The SEM–EDX particle analysis method is sensitive to interaction effects ascribed to abundance of certain particle groups (T. Leipe, IOW, pers. comm.) and the high palygorskite content might be due to the overlay of magnesium rich particles as magnesium carbonate of open origin which is frequent in samples of this series. The effect of the overlay can influence the identity of clay mineral species, but doesn't control the presence of clay minerals. Behind the high incidence of palygorskite, other clays are probably masked since during mineral classification clays are distinguished by cations whereas the silicon and aluminium contents are similar. Illite or other clay mineral contents are possibly higher within samples of series 23 which would reveal a higher similarity to clay mineral assemblages of series 22. But even though, the presence of palygorskite is evident and indicates northwest African dust sources, especially of west Mauritania [Reiff *et al.*, 1986].

Similar information is given by the I/K ratios plotted against the palygorskite content as introduced by Bout-Roumazelles *et al.* [2007] where the samples cluster clearly around proposed end-members which are determined to be sources of the lithogenic sediment trap material. Differences between end-members and measured clay mineral contents are apparent (Figure 3.5b). Those discrepancies are possibly due to the application of different methods. Data for clay mineral contents in sediments and derived relative percentages of mineral species or deduced mineral ratios given in literature are mostly based on X-ray diffraction analysis. Although there might be potential discrepancies in data evaluation and comparison with X-ray diffraction data, the trends of the sediment trap samples are well exposed in the

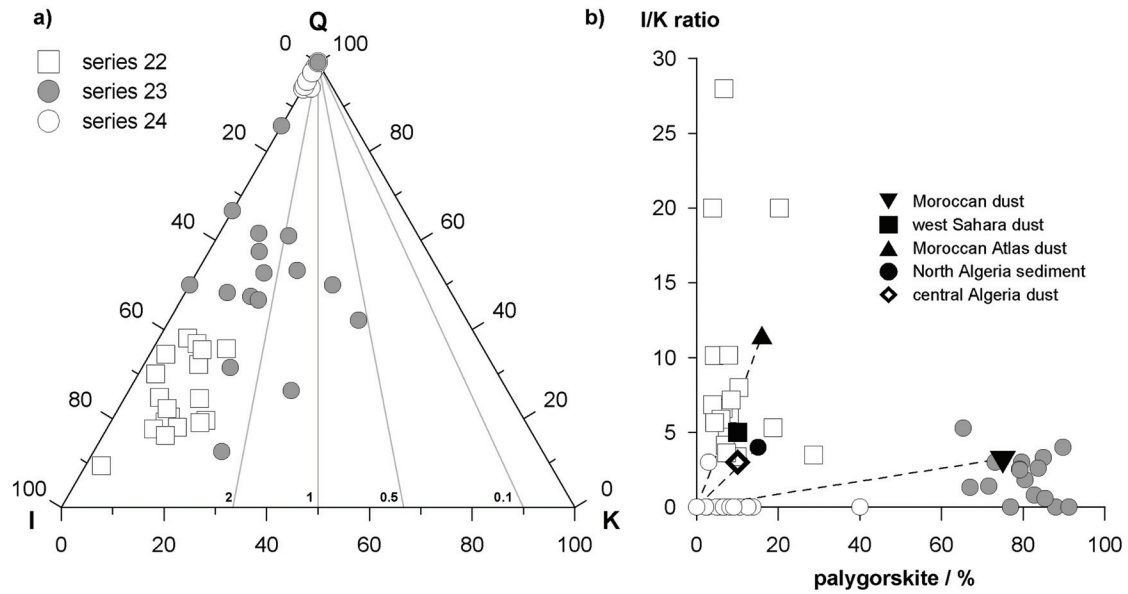


**Figure 3.5:** a) Ternary diagram (after *Caquineau et al.* [2002]) displaying illite/kaolinite ratios (I/K) of investigated samples. I/K values define possible source areas according to sectors of origin as defined by *Chiapello et al.* [1997],  $I/K > 1$ : north and west Sahara source,  $I/K \approx 0.5$ : south and central Sahara,  $I/K \approx 0.1$ : Sahel. b) Illite/kaolinite ratios (I/K) plotted against the palygorskite content (% from clay mineral species) of the investigated samples. The relevant end-members are redrawn from *Bout-Roumzeilles et al.* [2007].

diagrams. *Chavagnac et al.* [2007] proposed a North African dust source coming from the Anti-Atlas Moroccan chain for lithogenic material of the 3000 m depth trap during 2003–2004 (series 23) based on Sr isotope data together with the high prevalence of palygorskite and smectite going along with an absence of kaolinite. The series 23 of the 2000 m trap samples investigated here, does have kaolinite even though in low amounts, but samples almost lack in smectite. This fact is not a contradiction to the results presented by *Chavagnac et al.* [2007]. Sediment trap studies have shown that traps at different depth within a mooring array can have variable concentrations or even assemblages of clay minerals [*Honjo et al.*, 1982] or particle flux rates [*Neuer et al.*, 1997] due to lateral advection from continental slopes or coasts. An influence of resuspension of slope material can be neglected at the Kiel 276 site as it is more than 450 km away from neighboring islands or submarine rises and over 1000 km off the African coast. Differences in mineralogy



between 2000 and 3000 m trap material might be the result of a variety of processes, e.g. the natural variability of samples, transport processes occurring between both depth levels or the method based insecurity of particle analysis may play a role. Beyond that, the extend of the catchment area might be also determining. The catchment area of the 2000 m trap at Kiel 276 station is estimated to be 100 km<sup>2</sup> for an average sinking speed of 100 m d<sup>-1</sup>, involving particles circa 280 km away from the sampling site into the statistical funnel [Waniek *et al.*, 2005a,b]. Catchment areas of 3000 m traps possess larger radii, mostly exceeding more than 100 km<sup>2</sup> compared to 2000 m traps [Waniek *et al.*, 2000]. Based thereon, the 3000 m trap probably receives additional or even miscellaneous material, coming from aerosols deposited on the ocean surface afar the catchment area of the 2000 m trap and causing differences in mineralogy. Admixtures of kaolinite in the 2000 m (this study) trap samples or smectite in 3000 m trap samples [Chavagnac *et al.*, 2007] don't question the deduced source areas from palygorskite presence which are the North Mauritania and the Morocco regions within this sampling period (2003-2004).

Sample year of series 24 differs clearly from the two previous years. This is obvious in the lithogenic flux (see 3.1) and also in the mineral assemblages of the samples. During the year 2004–2005 smectite is the most prominent detected lithogenic mineral among the clay fraction. Smectite is known from eolian dust investigations in Israel, transported by winds coming from Libya and Egypt [Ganor, 1991; Ganor and Foner, 1996] and from dusts over Spain, being the main constituent in aerosols from Tunisia-Libya and Algeria [Avila *et al.*, 1996, 1997]. According to Paquet *et al.* [1984] smectite is a characteristic mineral in aerosols derived from South Hoggar and Tanezrouft (Algeria and Mali). Those studies also show that the high smectite content in the aerosols is always associated with another major lithogenic mineral such as kaolinite [Ganor, 1991; Ganor and Foner, 1996; Avila *et al.*, 1996, 1997]. Though kaolinite is mostly absent in samples of series 24 and play a minor role during the other years of sampling (see above). Smectite rather seems to be associated with quartz. Quartz is an omnipresent mineral in desert dust and the leading non-clay mineral of aerosols and sediments of the North Atlantic [Prospero, 1981]. In aerosols detected off the North African coast quartz makes 15 % up to 20 % within northeast trade wind dusts [Chester and Johnson,



1971a,b; *Chester et al.*, 1972] and deep-sea sediments of the Atlantic ocean have about 13 % quartz on a carbonate-free basis [*Windom*, 1976], ranging on average between 11 and 21 % from the Equator to mid-latitudes. Samples of series 24 differ remarkable from those average values. Other studies have shown that quartz is a dominant component in aerosols derived from Africa exceeding the clay mineral content [*Molinaroli*, 1996; *Guerzoni et al.*, 1997]. Smectite rich aerosols with a quartz-smectite co-occurrence were observed during a dust event in the French Pyrenees originating from sources of northwestern Saharan areas (northern Algeria, *Bücher et al.* [1983]). On African soil maps [*Reiff et al.*, 1986; *Molinaroli*, 1996] a further smectite rich soil source is present in the northwestern edge of the African continent along the Rif mountains. Concerning the samples presented here, the predominance of smectite and presence of illite in low amounts in series 24 samples, favor an origin for lithogenic detritus from southern Algeria - northern Mali sources (South Hoggar and Tanezrouft). A mixture of African dust sources during wind transport is possible [e.g. *Schütz*, 1989] as palygorskite, which occurs mainly in the Morocco and north Mauritanian area, is also present in samples of series 24.

An other clay mineral detected within the lithogenic particle assemblages throughout the years is chlorite, which is present in samples of series 22 and also frequent in series 23, but mostly lacks in series 24. The average chlorite content of all samples is about 6 % ( $\pm 20\%$ ;  $2\sigma$ -confidence limit) of the clay fraction. In aerosols collected over the western Mediterranean Sea, chlorite represents 8 to 10 % of the clay fraction [*Guerzoni et al.*, 1997]. The latter authors also observed a kaolinite-to-chlorite ratio (K/Cl) smaller than 2 in all collected aerosols. K/Cl greater-than-or-equal 2 are known to be characteristic for desert dust and were used as a further proxy to distinguish European background dust from African (Saharan) dust in the Mediterranean area [*Molinaroli*, 1996]. *Avila et al.* [1996] reported a lack of chlorite in aerosols from North Africa over Spain but noted a locally characteristic abundance of chlorite in soils of Northeastern Spain. Due to its sensitivity to hot and humid weathering, chlorite plays a minor role in the lower, tropical and subtropical latitudes in Atlantic deep-sea sediments and aerosols and is also a minor constituent in aerosols over the Mediterranean. Thence, the chlorite distribution of global surface deep-sea sediments opposes the kaolinite dispersal [*Griffin et al.*,

1968]. Chlorite is common in high latitudes associated with physical weathering of plutonic and metamorphic rocks and therefore displays a primary mineral which is released by mechanical breakage [Griffin *et al.*, 1968; Prospero, 1981]. The  $< 2 \mu\text{m}$  fraction of aerosols distributed close to the North African coast has abundantly occurring chlorite in the whole mineral assemblage and 12 to 19% chlorite in the clay mineral assemblage [Chester and Johnson, 1971a,b]. Kaolinite exceeds the chlorite content in samples from these authors, resulting in K/Cl ratios of 1.5 to 2.3 (calculated from Chester and Johnson [1971a,b] data). K/Cl values observed in samples of the Kiel 276 time series range from 0.3 to 7. In five samples of series 24 the ratio becomes zero, where chlorite is present and kaolinite lacks. All these facts demonstrate the wide range of variability of this ratio. One reason for that can be the origin of chlorite rich aerosols from the Atlas Mountains [Lange, 1982]. Close to the African coast the chlorite content overruns kaolinite to a factor of 3 [Lange, 1982]. Moderate weathering and tectonic uplift preserved little altered source rocks, still containing primary minerals as chlorite. A chlorite rich band spreads along the North African coast, controlled by water currents and basically by the African wind systems [Lange, 1982]. Consequently, the presence of chlorite in series 22 and 23 supports the idea of source areas from the Atlas Mountains and Morocco and the lack of kaolinite and occurrence of chlorite affirms the presence of mixing effects during aerosol formation and in the ocean interior.

### Link between biogenic and lithogenic flux

One of the main issues in ocean biogeochemistry is the question for a link between aerosol input into remote ocean areas and phytoplankton bloom and how tiny particles of biogenic and lithogenic origin can settle the water column fast. Hence, lithogenic particles have two effects on particles in the ocean surface, these are (1) particle formation and (2) particle transport. Firstly, important nutrients required for plankton growth (nitrogen, phosphorous and iron) are supposed to be transported with lithogenic material - which are clay minerals, metal oxides and hydroxides (detrital or on coated quartz grains), feldspars, phosphates (e.g. apatite), etc. - to the oceans. A sufficient supply of nutrients by lithogenic particles would (indirectly) increase the amount of (biogenically formed) particles and their

flux to the deep ocean. The second assumption is that detrital mineral flux increases the downward flux of biogenic material by "ballasting" [Klaas and Archer, 2002]. Both processes are supposed to influence the export of organic carbon from ocean surface to the deep ocean. Iron and phosphorous supply is connected with mineral dust deposits in the subtropical and tropical North Atlantic [Mills *et al.*, 2004]. At least iron exhibits a good correlation with lithogenic particle flux ( $r^2=0.66$ ) within the studied sample collective ( $n=52$ ), whereas between phosphorous and lithogenic flux no significant correlation was found ( $r^2=0.43$ ). Within Kiel 276 samples flux of both elements (Fe and P) exhibit a positive relation to the biogenic particle flux (Figure 3.6a), being best demonstrated for the series 22 (Figure 3.6b). Another micronutrient as zinc (a cofactor in phosphatases), which is transported together with phosphorous within mineral dust, is supposed to be responsible for leastwise cyanobacteria growth [Mills *et al.*, 2004] beneath Fe and P. Thus, P is effectively associated with biogenic particle flux then with the lithogenic particle flux. Likewise Fe (Figure 3.6b), P is also positively related with particulate organic carbon ( $r^2=0.85$ ), showing the important biogeochemical connection between both elements and organic carbon. Within the sample years Fe and P show fluxes of 2.1 and 144  $\mu\text{mol m}^{-2} \text{d}^{-1}$  (iron) and 0.8 and 133  $\mu\text{mol m}^{-2} \text{d}^{-1}$  (phosphorous) (Figure 3.6a). Concerning the delivery of iron to the sea surface Journeet *et al.* [2008] found out that clay minerals as illite and smectites play a greater role in delivering soluble iron, incorporated in clay lattice interlayers, instead of iron oxides and hydroxides. This result is a key clue to biogeochemical models comprising soluble iron in ocean surface processes indicating the necessity of involving aerosol mineralogy. Enhanced lithogenic particle, P and Fe flux and biogenic flux in series 24 arises the question for a link between nutrient input and surface ocean productivity in the Northeast Atlantic. As already illustrated (see 3.1) the lithogenic flux follows superficially main peaks of total and biogenic flux within the time series 2002 to 2005. This is also valid for Fe and P flux, which accompany the main peaks of biogenic particle flux, being lowest during series 22 and highest within series 24 (Figure 3.6a).

Flux of particulate iron (Figure 3.6a) leads to a theoretical organic carbon flux of 0.02 to maximal 1.3  $\text{g C m}^{-2} \text{d}^{-1}$  during the sample years, applying the Redfield Ratio based  $\text{C/Fe} = 122/2.6 \times 10^{-5}$  relation and assuming a solubility of iron

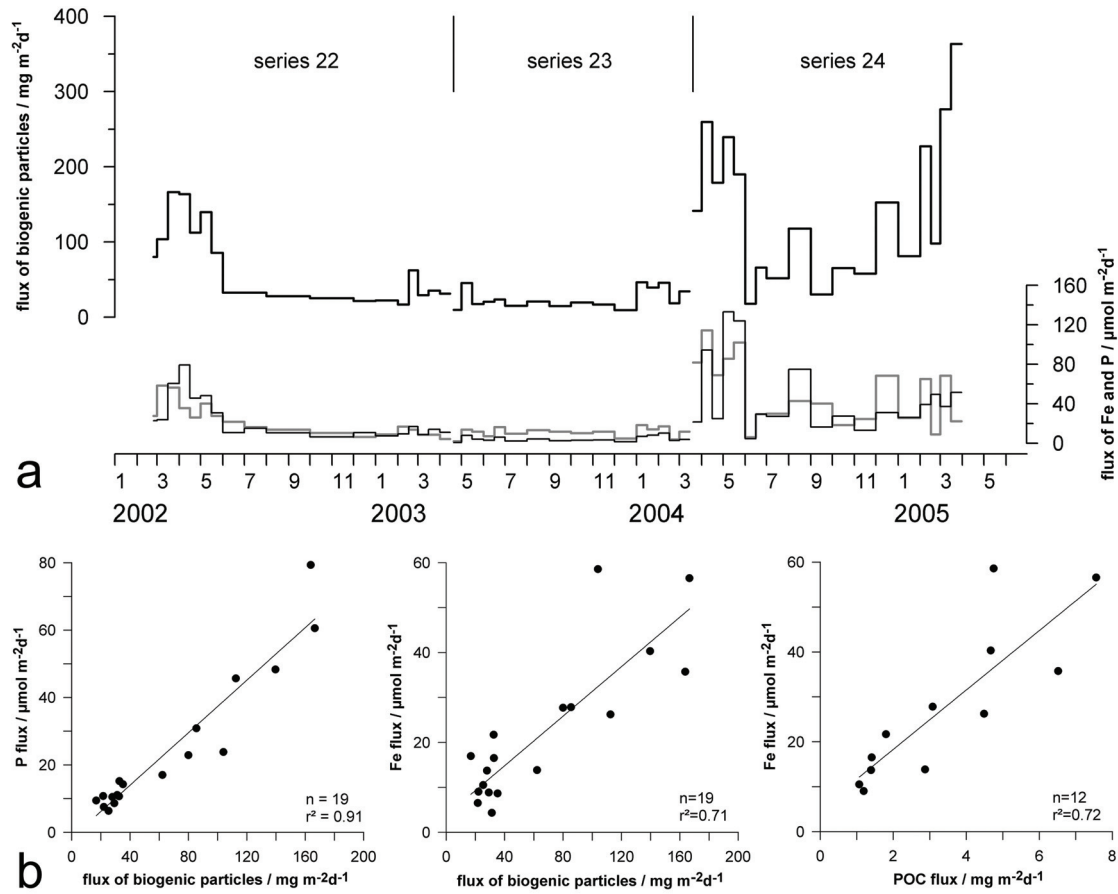


**Figure 3.6:** a) Comparison of the flux of biogenic particles (involves opal, carbonates, barite, organic particles; upper black solid line) and flux of iron (grey line) and phosphate (black line). The element fluxes were derived from the SEM-EDX measurements. Mean Fe flux values of the sample years are 18.7 (series 22), 11.1 (series 23) and  $46.1 \mu\text{mol m}^{-2} \text{d}^{-1}$  (series 24). b) Relation between P and biogenic particle flux, Fe and biogenic particle flux and Fe and POC flux showcased for series 22. (Particulate organic carbon (POC) was analysed according to *Waniek et al.* [2005a])

from particulate matter of 2% and a bioavailability of 1% dissolved Fe [*Kuss and Kremling*, 1999b; *Chavagnac et al.*, 2007]. Average values of Fe determined organic carbon fluxes for the sample years are 0.21 (series 22), 0.13 (series 23) and  $0.52 \text{ g C m}^{-2} \text{d}^{-1}$  (series 24). Assuming a continues additional iron-dependent C production for the month of bloom period (usually 3 month in this region), additional C production leads to 19 (series 22), 11 (series 23) and  $47 \text{ g C m}^{-2} \text{season}^{-1}$

(series 24). This leads to a primary production of 161 to 197 g C per  $\text{m}^{-2} \text{y}^{-1}$ , which means an increased primary production of 7 to 31 %, if the primary production in the study area is assumed to be at  $150 \text{ g C m}^{-2} \text{y}^{-1}$  on average (based on satellite chlorophyll concentrations, *Waniek et al.* [2005b]).

The efficiency of carbon export is usually expressed by the rain ratio, which is represented by the relation of organic carbon and inorganic carbon or carbonate respectively. Carbonate is known to be the main ballast mineral causing downward flux of organic carbon (Klaas and Archer, 2002). This was also shown by sediment trap studies which revealed positive correlations between organic carbon and carbonate flux [e.g. *Neuer et al.*, 1997; *François et al.*, 2002; *Fischer et al.*, 2007]. This is also true for the POC and  $\text{CaCO}_3$  flux in Kiel 276 samples ( $r^2=0.93$ ). A positive correlation between particulate organic carbon (POC) and lithogenic material was also found in Kiel 276 samples ( $r^2=0.76$ ). *Passow* [2004] and *Passow and De La Rocha* [2006] noted that sole correlations between organic carbon and (ballast) mineral flux are not explicit enough to clarify either ocean surface processes nor particle transport mechanisms. They concluded a POC constrained downward flux of lithogenic and biogenic mineral particles, while organic carbon catches minerals from sea surface until its repletion in particle load is reached. The samples of Kiel 276 seem to reflect this behavior in a similar way (Figure 3.7), but care should be taken because no organic carbon is considered here. Biogenic particles (carbonates, opal, etc.) are considered to be proxy for POC, as its origin is strongly related to organic carbon production. Relations between lithogenic mass flux and its percentaged contribution (relative content) to the total mass flux reveal two distinct characteristics within the Kiel 276 samples. There are samples, which show a "saturation curve" between lithogenic flux and relative lithogenic content (samples of series 22 and 24). For those samples with higher total particle flux (section 3.1), the biogenic particle flux keeps up with lithogenic dust input. That means with increasing lithogenic input, the formation of biogenic particles also increases. Which suggests that lithogenic minerals might have triggered an enhanced phytoplankton bloom. Nevertheless, such causal effects remain still uncertain and need further validation. The other group of samples (series 23, some samples of series 22 and 24), which exhibit an almost linear increase of relative lithogenic content attendant with lower lithogenic flux values, lithogenic dust

input increases whereas biogenic particle flux remains. Those samples have relatively low lithogenic particle and total particle flux rates (see 3.1). The apparent linear relation might reflect a ballasting of lithogenic and biogenic particles, but no saturation of carrying capacity of particles as proposed by *Passow* [2004] can be observed. A deficit in these assumptions is the lack of available sea surface POC data for each sampling interval. The comparison of lithogenic flux, biogenic flux and/or POC of the sediment trap samples is only an indirect approach. A carrying saturation of organic carbon for minerals, which was observed during laboratory studies [*Passow and De La Rocha*, 2006], will be possibly never reached in the subtropical Northeast Atlantic due to intermittent dust input, its low quantity and its circulation via currents in ocean interior.

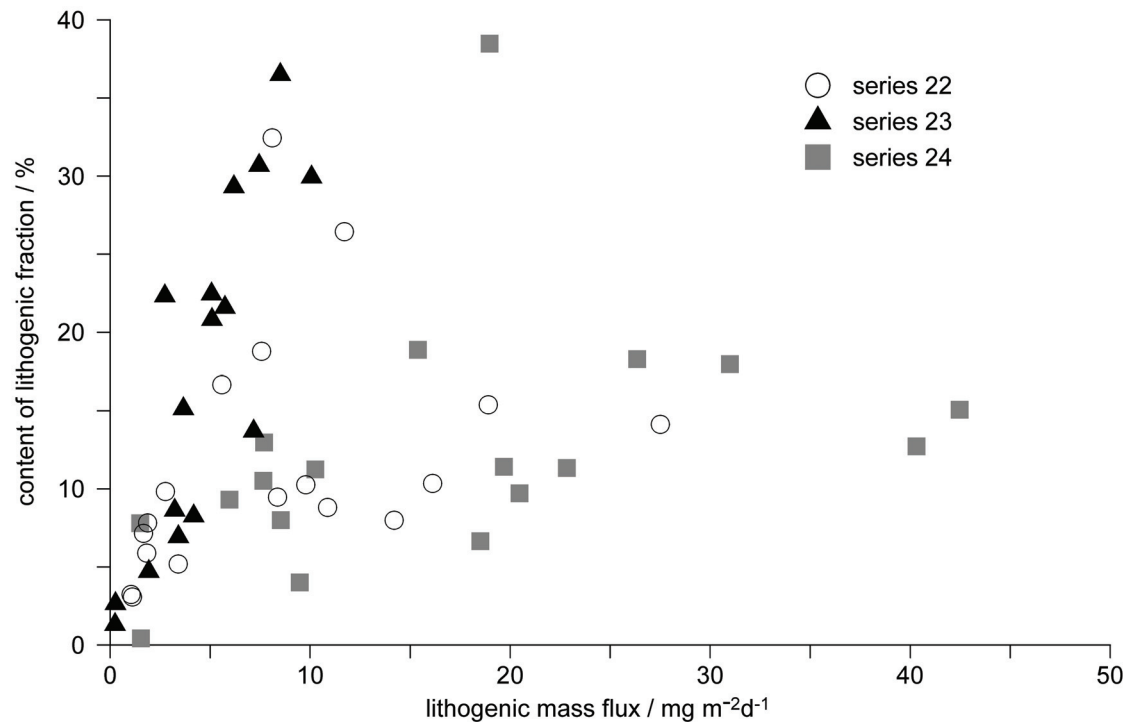


**Figure 3.7:** Relationship between content of lithogenic fraction referred to mass flux and lithogenic flux.

### 3.5 Conclusions

The flux of lithogenic particles observed in sediment trap samples of the subtropical Northeast Atlantic differs seasonally and interannually and seems to be independent from the biogenic flux except during the 2002-2003 sampling interval. The amount of lithogenic and clay flux is in line with previously found lithogenic mass fluxes at the sample site. Lithogenic particle grain sizes of investigated samples concur with observed aerosol grain size distributions off Northwest Africa, approving an eolian source of lithogenic minerals. The flux of single lithogenic minerals or mineral assemblages show rather interannual than seasonal variations. Those observed minerals and mineral assemblages are characteristic for different North African source regions. Predominantly northwestern African sources (Mauritania and Morocco) delivered lithogenic material during 2002 to 2004. Those findings are in good agreement with deduced source areas for the 3000 m trap of series 23 (Chavagnac et al., 2007). During 2004-2005 sampling interval lithogenic mineral assemblages exhibit more inland situated sources (Algeria and Mali). A mixture of sources during aerosol formation, deposition on ocean surface and during eolian transport and transport processes within the ocean can not be excluded. The influence of the Azores current frontal system, its shift in position relative to the sample site, also determines the particle flux at the sampling site and possibly impacts lithogenic composition and flux. Despite that, tropical and subtropical open ocean regions are influenced by aerosol delivered nutrient input. Determined on eolian Fe flux of three sampling years average, an average additional C production of  $26 \text{ g m}^{-2} \text{ season}^{-1}$  organic carbon can be reached, which would result in a 17 % increase of primary production in this region.

### 3.6 Acknowledgements

Thanks to master, crew and scientists who assisted and supported our work during sampling campaigns aboard RV POSEIDON, to T. Leipe and R. Bahlo from IOW for their assistance during sample processing and SEM-EDX measurements and to D. Schulz-Bull (IOW) and three anonymous referees for comments on earlier versions of this manuscript. This work is financially supported by DFG (contract number WA2157/2-1 and WA2157/3-1).

## 4 Descending particles: from the atmosphere to the deep ocean – A time series study in the subtropical NE Atlantic

*Brust, J., D. E. Schulz-Bull, T. Leipe, V. Chavagnac, and J. J. Waniek,*

*published 2011 in Geophysical Research Letters*

### 4.1 Abstract

The transport ways of organic matter into the deep ocean are still under debate. Lithogenic particles deliver nutrients to the surface, boost biological production, and impact on carbon export. This study focuses on the transfer of lithogenic particles from the atmosphere to the deep ocean and its physical and biological interactions during their descent through the water column. A clear coupling between atmospheric dust occurrence and deep-sea lithogenic particle fluxes at 2000 m depth was observed in the subtropical NE Atlantic (33° N, 22° W). This has never been demonstrated before for this site, far away from the African continental slope and with no lateral influx of particles present. The atmospheric signal transmission to the deep ocean lies in the range of one to two months. The presented data demonstrate the dependence of lithogenic deep-sea fluxes on the positioning in the ocean and on particle residence times in the water column.

### 4.2 Introduction

Mineral aerosols are known to have an impact on climate by influencing a variety of processes in the atmosphere (e.g. affecting earth's radiation budget, cloud formation and properties, *Kaufman et al.* [2002]) and the ocean [*Duce et al.*, 1991; *Bishop et al.*, 2002; *Jickells et al.*, 2005]. Climate change scenarios predict spreading of



desert areas, increasing wind strength and enhanced mineral aerosol production which is also relevant for oceanic primary production as aerosols carry essential nutrients to the ocean (e.g. phosphorous, nitrogen, iron; [Duce *et al.*, 1991]). Fertilization and ballasting are the major effects eolian mineral detritus have on ocean biogeochemistry and particle flux [e.g. Jickells *et al.*, 2005; Armstrong *et al.*, 2009; Iversen *et al.*, 2010]. Hence, mineral aerosols deposited in the ocean indirectly affect the carbon export. However, the fate of particles that descend from the atmosphere to the deep ocean is still under debate.

Signals of lithogenic dust in the air, at the sea surface and in the deep ocean are mediated by biological processes within the ocean, where both coupling [Jickells *et al.*, 1998; Migon *et al.*, 2002] and decoupling [Buat-Ménard *et al.*, 1989; Migon *et al.*, 2002] of the signals was reported. Comparative studies of dust concentrations and marine sediment fluxes were carried out at different sites off NW/W Africa [Bory and Newton, 2000; Neuer *et al.*, 2004], which were additionally influenced by lateral advection of continental slope/shelf material. Yet those studies showed a close relation between the atmospheric dust and the marine lithogenic flux signal.

In this study, we will compare the amount of aeolian particles deduced from satellite images to that identified at depth in the open ocean water column. The aim is to determine the fate of lithogenic particles from the atmosphere to the deep ocean and to identify their link to primary production.

### 4.3 Sampling material and methods

Particle flux was obtained from a 2000 m deep sediment trap at the deep-sea mooring site Kiel 276 (33° N, 22° W, Figure 4.1a), located at the northern fringe of the oligotrophic North Atlantic Subtropical gyre region [Waniek *et al.*, 2005a,b]. Sampling intervals ranged from 5 to 62 days, between February 2002 to March 2005. The fraction of lithogenic material was determined by an automated particle analysis via scanning electron microscopy coupled with an electron dispersive X-ray system (SEM-EDX) (see section 4.6 for further information).

For a comparison of lithogenic flux data with estimates of atmospheric input, we chose the satellite retrieved Aerosol Optical Depth (AOD) at 550 nm as a proxy for aerosol concentration in the atmospheric column [Kaufman *et al.*, 2002]. Satellite

derived AODs – such as the MODIS AODs of the Terra and Aqua satellites used here – comprise sea salt aerosols, sulphur aerosols, carbonaceous aerosols, and the mineral dust component (see section 4.6). Since only mineral dust accounts for the lithogenic particle flux of the sediment traps, we have additionally chosen the simulated dust AODs (AOD<sub>dust</sub>) from the GOCART model [Ginoux *et al.*, 2004] (see section 4.6). Those AODs gave reliable results compared with dust fractions derived from the MODIS AOD [Kaufman *et al.*, 2005]. Area averaged MODIS AOD and GOCART AOD<sub>dust</sub> data are provided by Giovanni [Acker and Leptoukh, 2007] in daily and monthly resolutions. The area selected for averaging covers the catchment area for the 2000 m sediment trap. This was deduced from the statistical funnel, where particles collected in the trap originate from up to 280 km away from the mooring position [Waniek *et al.*, 2005a] (Figure 4.1a). For a comprehensive comparison of the lithogenic particle flux and the AOD time series, monthly and half-monthly flux and aerosol values were computed and cross-correlated. The cross-correlation analysis was carried out by using the Pearson correlation coefficient ( $r$ ) and the Spearman's rank correlation coefficient ( $\rho$ ), preferable for small sample sizes with outliers and differing scales of compared parameters [Helsel and Hirsch, 2002].

## 4.4 Results and discussion

Lithogenic particle fluxes are variable throughout the years and range between 0.2 and 42.5 mg m<sup>-2</sup> d<sup>-1</sup>, with a mean contribution to the total particle flux of about 15 % [Brust and Waniek, 2010]. The average annual lithogenic particle flux (9.5 mg m<sup>-2</sup> d<sup>-1</sup>, on the basis of the sampling period) at Kiel 276 implies a sedimentation of 3 t mineral dust per km<sup>2</sup> per year at 2000 m water depth. Compared to dust deposition reported for the Canary Islands area at 1000 m water depth [Ratmeyer *et al.*, 1999a]. This means a 30 % lower dust deposition and a weakened dust transport to the northwestern Atlantic region. Several studies have shown that lithogenic detritus delivered to the study area originates from North African dust sources [Chavagnac *et al.*, 2007; Brust and Waniek, 2010]. Dust outbreaks emitted from North Africa and propagating in western directions are mainly confined between 5° and 20° N as defined by the position of the Intertropical Convergence

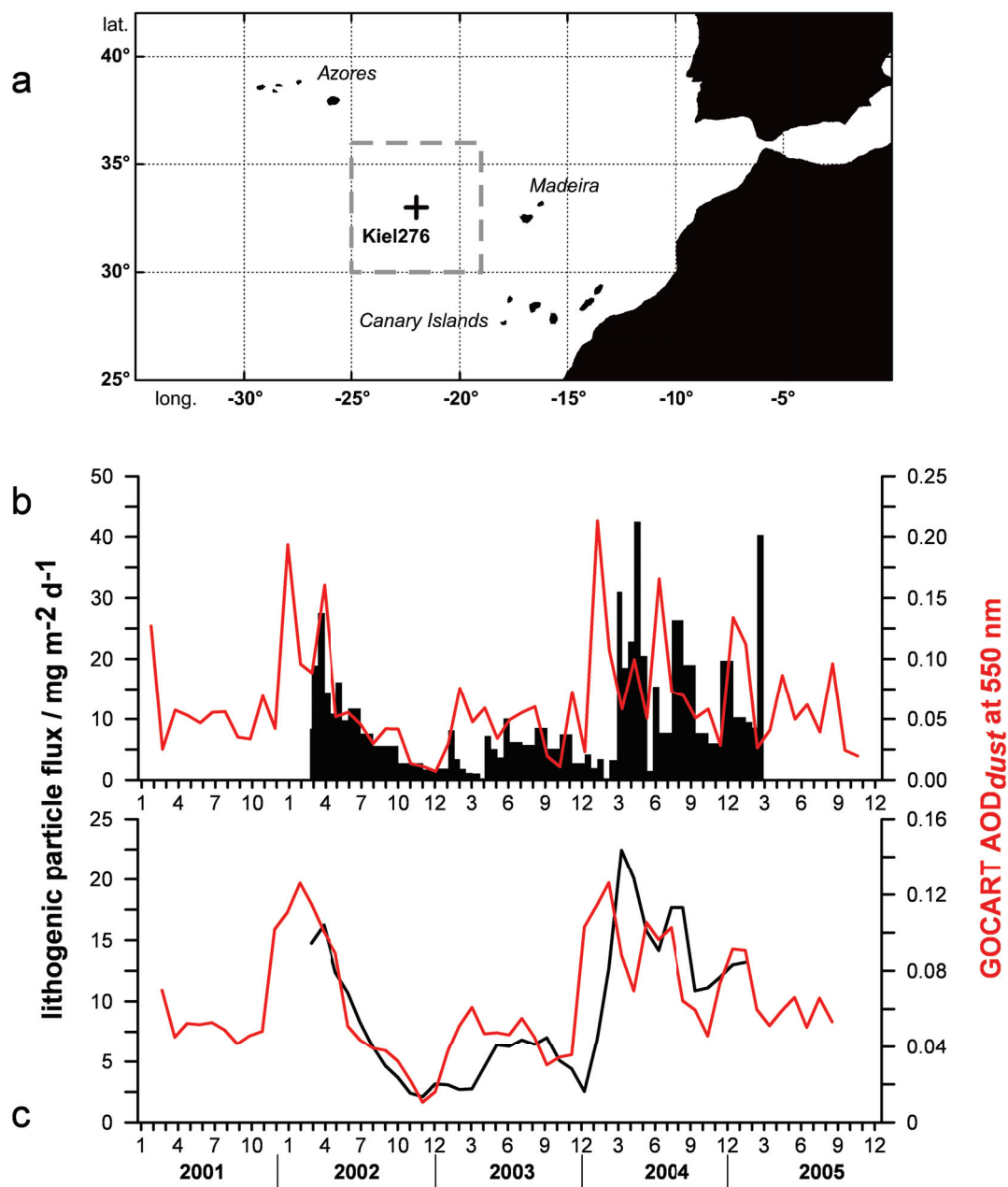


**Figure 4.1:** a — Position of the sampling site in the subtropical NE Atlantic. The grey box covers the area of averaged AOD data, based on the catchment area of a sediment trap deployed at 2000 m depth. b — Lithogenic particle flux (black bars) versus GOCART dust aerosol optical thickness (red line), area averaged based on the catchment area. c — Moving averages (3 points) for lithogenic flux (black line) time series and GOCART AOD time series (red line), based on monthly values.

Zone [Moulin *et al.*, 1997] and only occasionally spread to 35°N [Cachorro *et al.*, 2006; Chavagnac *et al.*, 2008].

Lithogenic flux and AOD time-series exhibit obvious similarities in the occurrence of main peaks, but with a visible time lag (Figure 4.1b). This remarkable similarity is highlighted by smoothing both time series with a moving average as exemplified by the GOCART AOD<sub>dust</sub> vs. lithogenic flux (Figure 4.1c).

Calculated correlation coefficients between the lithogenic flux and the AODs are generally below 0.7. The correlation coefficients between MODIS AOD and lithogenic flux are lower compared to correlations between lithogenic flux and the GOCART AOD<sub>dust</sub> (Table 1), possibly due to the MODIS AOD including all aerosol types affecting the radiation extinction. Although there are only medium correlations, both monthly and half-monthly  $r$ - and  $\rho$ -coefficients imply a shift of 1.5 months between atmospheric aerosol deposition and lithogenic flux at 2000 m depth (see Table 4.1).

**Table 4.1:** Pearson ( $r$ ) and Spearman’s rank ( $\rho$ ) correlation coefficients between lithogenic flux at 2000 m water depth and MODIS AOD and GOCART AOD<sub>dust</sub> values given in monthly ( $n=37$ ) and half-monthly ( $n=74$ ) resolution. Superscript numbers at highest correlation coefficients (bold) codify confidence limits: 1: 95%, 2: 99%, 3: 99.9%. The MODIS aerosol data comprise AOD retrievals from the Terra (24/02/2000–03/07/2002) and Aqua (03/07/2002–2010) satellites. Only positive lags were considered, moving the AOD time series temporally forward. For calculating half-monthly values each month was split into a 15 day interval from the beginning to the 15<sup>th</sup> of the month and the rest of the month beginning with the 16<sup>th</sup> of the month until the end, defining intervals of 13 to 16 days.

lag	MODIS AOD				GOCART AOD <sub>dust</sub>			
	monthly		half-monthly		monthly		half-monthly	
	<b>r</b>	$\rho$	<b>r</b>	$\rho$	<b>r</b>	$\rho$	<b>r</b>	$\rho$
4	-0.12	-0.06	<b>0.35</b> <sup>2</sup>	0.22	0.09	0.39	0.37	<b>0.42</b> <sup>3</sup>
3	0.02	0.04	<b>0.33</b> <sup>2</sup>	<b>0.26</b> <sup>1</sup>	0.42	0.49	<b>0.47</b> <sup>3</sup>	<b>0.43</b> <sup>3</sup>
2	<b>0.49</b> <sup>2</sup>	0.27	0.27	0.25	<b>0.63</b> <sup>2</sup>	<b>0.63</b> <sup>2</sup>	0.36	0.40
1	0.40	<b>0.35</b> <sup>1</sup>	0.15	0.004	<b>0.55</b> <sup>2</sup>	<b>0.65</b> <sup>2</sup>	0.22	0.32
0	0.08	0.09	-0.09	-0.07	0.17	0.39	0.10	0.29

This is a fast time response of lithogenic particle transport from the atmosphere inferred from the atmospheric dust AOD signal to the deep ocean. The net settling velocities range between  $32 \text{ m d}^{-1}$  (2 months) to  $44 \text{ m d}^{-1}$  (1.5 months). *Neuer et al.* [2004] found a 14-day-time lag (9.5-day-time lag) between dust signal and particle flux at 500 m (330 m) depth, which results in a net settling velocity of  $35 \text{ m d}^{-1}$ , comparable to net settling velocities observed in this study. Underlying the deviation from a perfect coherency between AOD and lithogenic flux in the study area could be a variety of processes, such as the accuracy of sample analysis [*Brust and Waniek*, 2010]. The transport path of lithogenic particles from the atmosphere to the ocean involves different aspects of transport mechanisms. This is (1) the time, the transport process and path from atmosphere to ocean surface, (2) the time the particle remains in the mixed layer and (3) the time the particle is descending through the ocean water column and its particular trajectories. These processes determine the net settling velocity of particles.

A major uncertainty concerns the amount of dust being deposited from the atmosphere to the surface ocean. The mineral aerosol fraction of AOD is a proxy for dust concentrations in the atmosphere but deposition rates are difficult to obtain where ground based measurements of surface dust fluxes are lacking. Two main mechanisms, dry and wet deposition, cause dust deposition [*Duce et al.*, 1991]. In the Canary Island region, dry deposition exceeds wet deposition, being in line with global estimates for dust deposition [*Torres-Padrón et al.*, 2002]. During summer the Saharan Air Layer is located in high altitudes, in winter the dust transport occurs mainly in the lower atmospheric layers within the trade winds [*Ratmeyer et al.*, 1999a]. The deposition of aerosols is considered to be a linear process at least for dry deposition, whereas non-linear relations are considered for wet deposition and fall-out from high altitudes [*Schepanski et al.*, 2009]. The fraction deposited from the dust plume carries some uncertainty as well. We assume that particles distributed in the atmosphere over the catchment area descend within days (less than one week) [*Jaenicke*, 1980] to the ocean surface when the mean diameter of lithogenic particles is around  $2 \mu\text{m}$  [*Brust and Waniek*, 2010]. Uncertainty arises also from the unknown site of deposition within the catchment area of the trap and the estimated residence time of the dust particles in the surface layer. *Deuser et al.* [1983] calculated residence times for clay particles within the surface

water (0–100 m) ranging from two weeks to 80 days. This accords to recently observed residence times of lithogenic particles in surface waters (0–200 m) of 40 days [Buat-Ménard *et al.*, 1989; Bory and Newton, 2000] and residence times of dust-derived iron of 6–62 days [Croot *et al.*, 2004]. Residence times vary due to various influences: grain-sizes of the lithogenic particles, resuspension within the mixed layer, seasonality [Migon *et al.*, 2002], interaction with organic compounds and biology, and moreover the manner and time required for particle aggregate formation [Iversen and Ploug, 2010]. Particles are displaced by surface currents while remaining in the upper water layer. Mean near surface currents in SE direction are low ( $< 5 \text{ cm s}^{-1}$ ) at Kiel 276. Below the mixed layer depth ( $\sim 50$  to 200 m) [Waniek *et al.*, 2005a,b], particles start sinking but are less exposed to current-controlled displacements. Settling speeds are in the order of  $100 \text{ m d}^{-1}$  [Waniek *et al.*, 2005a]. Assuming a direct descent of particles from ocean surface to 2000 m depth, particles would reach the trap in 20 days. Still, settling velocities can also vary below the mixed layer due to scavenging and release through organic matter decomposition. Decreased settling velocities and/or longer routes of transport increase the time the particle needs to reach the trap position, e.g. particles from 280 km afar need around 65 days presuming current velocities of  $5 \text{ cm s}^{-1}$  to reach the sampling site. This is slightly longer than the lag of 1.5 to 2 months visible between AODs and lithogenic particle flux and might be one explanation for the deviation from a better correlation.

There is also the fact that there is a range of sinking velocities of particles caught in a sediment trap, rather than a single sinking velocity [Armstrong *et al.*, 2009]. The assumed settling velocity of  $100 \text{ m d}^{-1}$  points towards short residence times in surface waters from 25 to 40 days.

Chlorophyll-a concentrations derived from SeaWiFS satellite (see section 4.6), used as a proxy for primary production in surface waters, were compared with GO-CART AOD<sub>dust</sub> and biogenic particle flux at 2000 m depth (Figure 4.2b). The station Kiel 276 is located in a section of the Atlantic Ocean which is not influenced by coastal upwelling processes. However, satellite derived chlorophyll-a rarely shows a response to dust input [Waniek *et al.*, 2005b]. Primary production peaks during winter/early spring when nutrients from deeper water layers are resupplied by deepening of the mixed layer ( $\approx 200 \text{ m}$ ) (Figure 4.2a). Typically, the biogenic

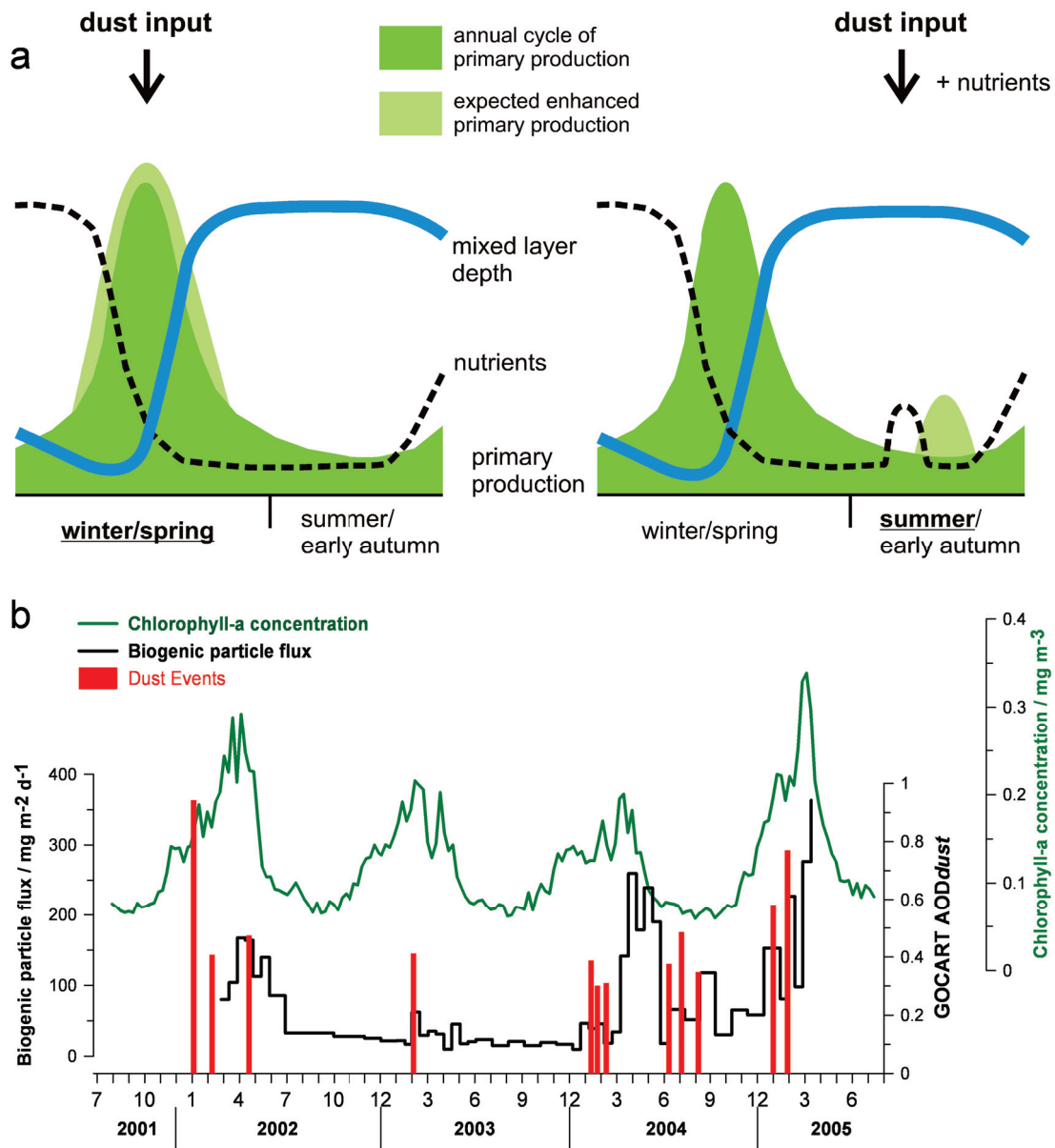


**Figure 4.2:** a — Scenarios of dust deposition during winter (left-hand figure) and summer (right-hand figure) and its possible effects on primary production. b — Area averaged data of 8-day mean SeaWiFS chlorophyll-a values shown together with biogenic particle flux from the 2000 m sediment trap. The biogenic particle flux was determined by SEM-EDX automated particle analysis and encompasses biogenic mineral phases (e.g. calcite, opal, barite) [Brust and Waniek, 2010]. Red bars indicate dust events determined by an aerosol optical depth (AOD) threshold of mean AOD plus standard deviation [Ohde and Siegel, 2010] for MODIS and GOCART AOD data in comparison with satellite views. Dust events last 2 to 5 days, shown bars mark the first day of a dust event over the sampling site.



particle flux follows the satellite chlorophyll-a signal within one month, expressed both in an increase of surface water chlorophyll-a between December and March and by high biogenic particle fluxes occurring between March and April [Waniek *et al.*, 2005a,b; Brust and Waniek, 2010] (see Figure 4.2b). A dust event during winter/early spring increases nutrient concentrations and may increase primary production (Figure 4.2a). During summer, the nutrients are depleted in the shallow mixed layer ( $\leq 50$  m) compared to winter, leading to low primary production during these months. Therefore, a clear impact of atmospheric dust input on the primary production should be expected in summer: nutrient limitation is relieved by mineral dust input and associated bioavailable compounds which would support biologic production with a delay of days to weeks (Figure 4.2a). From January 2002 to May 2005, the combination of true color VIS satellite pictures and AOD dust signals indicate the occurrence of at least 12 dust events (Figure 4.2b), taking place essentially in winter and spring (2002–2005) and occasionally during summer 2004. The incidence of the dust events is variable throughout the years for example, in 2003 only one strong event was observed, while in 2004 six events occurred. These numerous dust events are evidenced by high lithogenic fluxes in 2004–2005. In general, chlorophyll a concentrations are marginally coupled to dust inputs and seems to be mainly seasonally controlled by the deepening of the mixed layer during winter, leading to a renewal of nutrients from below. However, a dust-derived enhancement of biological production during winter/early spring could be masked by the natural variability of primary production intensity in this region (Figure 4.2b). Summer dust events have a strong impact on the amount of lithogenic particles collected at depth, but do not affect surface chlorophyll-a concentrations (Figure 4.2b) and thus primary production. Effects can be masked by the deep chlorophyll maximum (at 120 m depth) present in this part of the Atlantic and not registered by satellite sensors [Waniek *et al.*, 2005b]. Neuer *et al.* [2004] infer potential fertilization via aerosols during summer months in the Canary Island region, based on aerosol samples, water column and sediment trap measurements. In summer 2004, when dust events occurred in July and August, the flux of biogenic particles was also elevated (Figure 4.2b) without an increase of surface chlorophyll-a concentrations as based on satellite images. This hints to an effect missed by satellite observations. For a better understanding of these



processes further investigations are needed with longer lasting sediment trap time series and simultaneous satellite aerosol optical data to observe more summer dust events within this region and their impact on primary production.

## 4.5 Acknowledgments

We thank R. Prien, I. Stottmeister and T. Ohde from the IOW for giving helpful comments and the two reviewers for their suggestions to improve the manuscript. We also would like to acknowledge NASA GES-DISC scientists and associated personnel for the production and online provision of the data used in this research effort. This work is a contribution to three DFG funded projects (WA2157/2-1, WA2157/3-1 and WA2157/4-1).

## 4.6 Auxiliary material

### Study area

The deep-sea mooring Kiel 276 (33°N, 22°W) is located in the Madeira Basin (240 NM west of Madeira) at 5500 m water depth. The station is situated in the eastern part of the North Atlantic Subtropical Gyre Province (NAST, *Longhurst* [1998]), where it is influenced by the Azores Current, an eastward propagating branch of the Gulf Stream [*Klein and Siedler*, 1989]. The Azores Current delimits the cold waters of the northern North Atlantic and the saltier, more oligotrophic, and warmer water masses of the subtropical North Atlantic, which has its origin in the Sargasso Sea. Between Madeira and Canary Islands the Azores Current couples with the Canary Current, where surface waters of low-latitude origin are recirculated to the south [*Sy*, 1988]. Generally, the Azores Current occupies a water depth of more than 1000 m with a width of 50 km [*Gould*, 1985] and moves spatially between 32° and 36°N [*Klein and Siedler*, 1989]. Accompanying meanders and eddies of the frontal system result in intense recirculation and subduction across the Azores Front [e.g. *Käse and Siedler*, 1982; *Gould*, 1985]. The sampling site is influenced by the outflow of Mediterranean deep water at 1000 m depth and the North Atlantic Deep Water below 1600 m depth. The main thermocline (270 m) is characterized by current amplitudes of 20 to 25 cm s<sup>-1</sup> [*Waniek et al.*, 2005b], which is also valid for the 1000 m niveau. Between 1000 and 1600 m

current amplitudes show a strong decrease. Mean currents within the Aanderaa current meters-measured depth intervals (100 m, 300 m, 550 m, 1000 m, 2050 m and 3500 m) are weak ( $5 \text{ cm s}^{-1}$ ), with maximum amplitudes of  $25 \text{ cm s}^{-1}$  [Waniek *et al.*, 2005a,b]. Those mesoscale events occur sporadically with periods of 1 to 3 months and are associated with the meandering Azores Current frontal system [Waniek *et al.*, 2005a,b]. During the studied time series the mean current velocities in the 240 m and 500 m depth level were below  $5 \text{ cm s}^{-1}$ .

## Material and methods

Marine particulate material was sampled by using a funnel type sediment trap with a funnel slope of  $34^\circ$  and an opening aperture of  $0.5 \text{ m}^2$  as described by Kremling *et al.* [1996]. Prior to deployment, the trap components (cone, rotator and  $400 \text{ cm}^3$  polypropylene sampling bottles) were cleaned, following the standard procedure for trace elements analysis after Kuss and Kremling [1999a]. The sampling bottles contain a mixture of 4:1 in-situ seawater, sodiumacide ( $\text{NaN}_3$  5 % stock solution in high purity water) and additional NaCl (final salt content of  $38 \text{ g l}^{-1}$ , see Waniek *et al.* [2005a], and references therein). Separate temporal sampling of sediments in the 18 sample bottles is steered by the rotator control unit; sampling intervals are adapted to seasonal biological particle production [Waniek *et al.*, 2005b]. After deployment, the sampling program started after a 1-2 week rinse-period. The recovered sediment-trap samples were stored at 4 to  $6^\circ\text{C}$  in a dark environment until analysis. Determination of mass flux started with removal of zooplankton "swimmers" from samples by means of Teflon tweezers. Four equal splits for different analysis purposes were made. The supernatant was removed from the splits, chemically analyzed and compared to blank solution with the aim to estimate redissolved amounts of particulate material [Lundgreen *et al.*, 1997]. The solid residues were freeze-dried prior to analysis. The particle flux (given in  $\text{mg m}^{-2} \text{ d}^{-1}$ ) was calculated from the salt-corrected dry weight, the split factor (1/4), the opening area of the trap and the duration of the sampling interval. For the Scanning electron microscopy (SEM) and energy dispersive X-ray microanalyses (EDX) analysis a small amount of the sample powder was dispersed in Milli-Q water and filtrated through  $0.4 \mu\text{m}$  nucleopore filters (Millipore polycar-

bonate membrane filter, diameter of 49 mm). Simultaneously, the samples were rinsed with Milli-Q water for desalination and the filters were dried for several hours at 50 °C. Filter cuttings (about 1 cm<sup>2</sup> of filters) were glued on aluminum stubs and sputtered by elemental carbon (vacuum sputtered) to assure electric conductivity. The automated SEM-EDX multi-element analysis was performed on a FEI Quanta 400 microscope connected to an EDAX-Genesis system (at the Leibniz-Institute for Baltic Sea Research in Warnemünde) under following measurement conditions: high vacuum; 15 kV electron beam; working distance: 10 mm; BSE and EDAX-Econ IV detector. During the automated particle analysis morphological (grain size, shape) and chemical parameters (12 main elements: Al, Ca, Cl, Fe, K, Mg, Mn, Na, P, S, Si and Ti) of each particle are recorded. Around 2000 particles per filter stub were measured within a particle size interval of clay to silt size. The method is based on an automated image processing system working with gray-scale limits and the identification and quantification of the elements follows the ZAF-correction. The 12 elements measured are main constituents in most common natural minerals, organic, and inorganic particles and do not show minor peak overlapping EDX-spectra [Leipe *et al.*, 1999; Bauerfeind *et al.*, 2005]. Element oxides were calculated and normalized to 100 % for each particle, which enables the identification of minerals and mineral or particle groups according to element boundaries of standard minerals. The determination and quantification of particles in each sample was processed with the mineral classification program "mineral" (©W. Zahn), where more than 20 minerals and mineral/particle groups were identified. The lithogenic fraction comprises quartz, feldspars, clay minerals (illite, smectite, chlorite, kaolinite, palygorskite) and element oxides and hydroxides (Fe, Al, Mn). The counts of the identified minerals were recalculated with the mass flux values of the respective sample, leading to mass flux data (mg m<sup>-2</sup> d<sup>-1</sup>) for the lithogenic fraction of each sample. This semiquantitative approach is based on the assumption that all particles represented by counts have similar grain sizes and densities, independent from mineral species varieties [Brust and Waniek, 2010]. Five measurements (including 3 subsections of one filter) from one sample were performed to test the reproducibility of the SEM-EDX analysis and a 6th measurement of this sample was analyzed in line with the series measurements [Brust and Waniek, 2010]. The reproducibility of the method according to Brust and Waniek

[2010] is for the lithogenic fraction  $\pm 23\%$ . Lithogenic flux rates are highly variable throughout the sampling years and vary between  $2.24$  and  $42.5 \text{ mg m}^{-2} \text{ d}^{-1}$  (see *Brust and Waniek* [2010] for further information) and the annual average lithogenic flux is about  $9.5 \text{ mg m}^{-2} \text{ d}^{-1}$  (see article text) with a standard deviation of  $\pm 8.8 \text{ mg m}^{-2} \text{ d}^{-1}$ . For further information about the method used, see *Brust and Waniek* [2010].

### Satellite and GOCART data

Aerosol optical depth (AOD) and chlorophyll-a data were downloaded from Giovanni (GES-DISC (Goddard Earth Sciences Data and Information Services Center) Interactive Online Visualization ANd aNalysis Infrastructure), which is a Web-based platform for visualization, analysis, and access of NASA missions remote sensing data. The data are available from the website: <http://disc.sci.gsfc.nasa.gov/giovanni/> and accompanying web links. Two products were used for aerosol optical depth estimates, the MODIS (Moderate-Resolution Imaging Spectroradiometer) AOD at 550 nm and the dust AOD fraction of the GOCART (Goddard Chemistry Aerosol Radiation and Transport) model. MODIS instruments are aboard the Terra and Aqua satellites, which provide views of the entire Earth's surface within 1 to 2 days in 36 spectral bands. The bands 3 to 7 give information about land, cloud and aerosols properties, where data of band 4 (550 nm) are used in this study. Daily and monthly MODIS AOD data (MYD08\_D3 products) provided by Giovanni are available in  $1^\circ \times 1^\circ$  (longitude and latitude) spatial resolution. For further information about MODIS see <http://modis.gsfc.nasa.gov/>. Average half-monthly and monthly MODIS AODs were calculated from daily MODIS AODs. The comparison of ground-based AERONET (AERosol RObotic NETwork) sun/sky-radiometers and MODIS AOD measurements show an uncertainty of  $\tau = 0.03 \pm 0.05\tau$  ( $\tau$ , synonym for AOD) MODIS aerosol optical thickness over the ocean [*Remer et al.*, 2005]. *Zhang and Reid* [2006] state an error in MODIS  $\tau$  at 550 nm by 10-20 %, which is also based on the comparison of AERONET and MODIS data. Combined daily Terra and Aqua MODIS AODs (covering the sampling interval 2002-2005) reveals on average 27 pixels (maximum 88 pixels) per day within the averaged area ( $30^\circ$ - $36^\circ$  N,  $19^\circ$ - $25^\circ$  W), where half of the days AODs

data consists of over 23 pixels (7 % of the days lack AOD pixel information).

The Goddard Chemistry Aerosol Radiation and Transport (GOCART) model simulates major tropospheric aerosol components. These are sulfate, dust, black carbon, organic carbon, and sea-salt aerosols. GOCART aerosol data are available in monthly or daily temporal resolution and in a  $2.5^\circ \times 2^\circ$  (longitude and latitude) spatial horizontal resolution, provided by Giovanni. Data used for the GOCART model generated aerosol components are the assimilated meteorological fields of the Goddard Earth Observing System Data Assimilation System (GEOS DAS), produced by the Goddard Global Modeling and Assimilation Office. For a detailed description of the GOCART (Goddard Chemistry Aerosol Radiation Transport) model we refer to the papers of *Chin et al.* [2002] or *Ginoux et al.* [2001] and the website <http://acdb-ext.gsfc.nasa.gov/People/Chin/gocartinfo.html>.

SeaWiFS (SEA-viewing Wide Field-of-view Sensor, onboard of Orb-View-2) chlorophyll-a (Chl-a) concentrations (5.2 reprocessed data) were downloaded from the Giovanni web sites (<http://reason.gsfc.nasa.gov/OPS/Giovanni/ocean.swf8D.shtml>). The SeaWiFS data used here consist of Chl-a from 8-day global standard mapped images (SMI). The SeaWiFS products have a resolution of about 9 km ( $0.083^\circ \times 0.083^\circ$ ) at the equator. Mean monthly pixel counts of SeaWiFS Chl-a data (<http://disc.sci.gsfc.nasa.gov/giovanni/>) are in the order of 5314 pixels per month within the studied time interval and the chosen area for averaging. The comparison of SeaWiFS Chl-a data with in-situ data, taken in the vicinity of the study area and in a temporal relation close to the studied time interval shows a median ratio of 1.45 and a median difference between the SeaWiFS Chl-a and in-situ concentration of 52 % (<http://seabass.gsfc.nasa.gov/>; slope statistics: 4, slope = 0.4, intercept = -0.47,  $R^2=0.97$ ). Although, differences between SeaWiFS Chl-a and in-situ data are quite large (e.g. among others due to limited available in-situ data), SeaWiFS Chl-a data are useful to show changes in chlorophyll-a concentrations in the upper water column [e.g. *Signorini et al.*, 1999; *Davenport et al.*, 2002].

## 5 Barite and North African dust in 3200 m deep sediment trap material southeast of Bermuda

*Brust et al., manuscript, to be submitted to Deep-Sea Research I*

### 5.1 Introduction

The area around the island of Bermuda faces a long history of interdisciplinary investigations. Due to its position miles away from continental landmasses and the steep topography of the Bermuda Rise the island was recognized to be an ideal base for expeditions, the deployment of long-term deep-sea moorings with sediment traps [Michaels and Knap, 1996; Phillips and Joyce, 2007] and atmospheric investigations [e.g. Jickells et al., 1982; Arimoto et al., 1992, 1995]. Ongoing marine time series programs are the Hydrostation S, the Bermuda Atlantic Time-series Study (BATS) and the Oceanic Flux Program (OFP). Bermuda is situated in the northwestern edge of the North Atlantic subtropical gyre or Sargasso Sea, south of the Gulf Stream. Oceanographic time-series programs provided a fundamental understanding of marine biological and chemical processes of this area [e.g. Deuser et al., 1981; Deuser, 1986; Conte et al., 2001]. A weak Gulf Stream recirculation prevails south of Bermuda [Michaels and Knap, 1996] with mean velocities less than  $5 \text{ cm s}^{-1}$  at 500 m and less than  $1 \text{ cm s}^{-1}$  below 1500 m water depth [Siegel and Deuser, 1997]. The net Ekman downwelling, which is a distinctive feature of the gyre center [McClain and Firestone, 1993] reaches rates of  $4 \text{ cm d}^{-1}$  south of Bermuda. The area between  $25^\circ$  and  $32^\circ \text{ N}$  is a transient zone between different water masses. Relatively eutrophic water masses are present in the North, where the subtropical mode water is formed due to convective mixing between  $31^\circ \text{ N}$  and the Gulf Stream during the winter time [Talley, 1982]. In the south comparatively oligotrophic subtropical and permanently stratified water masses occur, which overly the nutrient-rich mode water [Steinberg et al., 2001]. The biological pro-

duction of the upper water column in the Sargasso Sea is controlled by seasonal changes of major physical parameters as heat flux and wind stress, which define the availability of nutrients in the euphotic zone [Steinberg *et al.*, 2001]. Nitrate limitation south of Bermuda results in picoplankton dominance with nitrogen-fixing cyanobacteria, whereas the nutrient richer waters north of Bermuda promote the bloom of diatoms and coccolithophores in early spring [Michaels and Knap, 1996, and references therein]. These patterns can be observed over the deep-sea mooring sites present south of Bermuda [Michaels and Knap, 1996]. Usually, a weak, short lasting spring bloom occurs in February–March, when the wintertime convective mixing reaches its maximum with depth of 150–250 m [Huang and Conte, 2009].

Conte *et al.* [2001] pointed out the interannual variability in timing and strength of particle fluxes in the Sargasso Sea, where the general maximum of particle fluxes measured in sediment traps south of Bermuda can be observed between January and April. In the time between April and October the Bermuda–Azores high causes seasonal heating and the development of a shallow, stratified and nutrient-poor mixed layer. Generally low particle fluxes are observed in sediment traps during this time. Major components of the particulate material found in Sargasso Sea waters are biogenic carbonate and silicate [Deuser *et al.*, 1981; Conte *et al.*, 2001]. Usually the mean carbonate content of sediment trap material of the Sargasso Sea makes 50 up to 75 % [Deuser, 1986; Deuser *et al.*, 1981; Conte *et al.*, 2001] and the contribution of opal to the total mass flux ranges between 8 and 29 % [Conte *et al.*, 2001]. Major species contributing to the carbonate flux are coccolithophores [Haidar *et al.*, 2000]. Lithogenic minerals accounts for the minor fraction of particle fluxes in the Sargasso Sea [Deuser *et al.*, 1981; Conte *et al.*, 2001]. The flux of lithogenic particles is mainly controlled by the input of mineral dust [Jickells *et al.*, 1998] and subsequently by laterally advected continental shelf/slope sediments, which are supplied by the Gulf Stream to the Sargasso Sea [Huang and Conte, 2009]. Jickells *et al.* [1998] have shown that there is a strong annual variability in lithogenic particle flux due to the efficiency of dust transport from North African source regions. The main atmospheric features, which determine the direction of air flow to this area are the Intertropical Convergence Zone (ITCZ) and the semi-permanent "Bermuda" high pressure center [Perry *et al.*, 1997]. It is well known that dust coming from North Africa is transported to the Caribbean [e.g. Carlson



and Prospero, 1972], to the eastern coast of the United States [Perry *et al.*, 1997] and also to the central United States [Gatz and Prospero, 1996]. High aluminium concentrations in aerosols showed the presence of African dust also at Bermuda [Arimoto *et al.*, 1992, 1995]. Dust coming from the United States is common during spring and is minimal during the summer months [Gillette and Hanson, 1989]. Dust from North Africa carried to Caribbean and the eastern coast of the United States, Bermuda and Bahamas is defined by the location and strength of the clockwise-rotating "Bermuda" high pressure center and occurs mostly during summer. Also soil profiles of western Atlantic islands show the presence of North African dust within longer time scales [e.g. Muhs *et al.*, 1990; Herwitz *et al.*, 1996]. Referred to aluminium contents in sediment trap material the major contribution of lithogenic particles to deep-sea mass fluxes can be found in summertime in the Sargasso Sea, in particular when dust outbreaks from North Africa strengthen [Jickells *et al.*, 1998].

This study presents the chemical and mineralogical composition of a one-year (1998-1999) sediment trap time series at 3200 m depth with the aim of deciphering the sources for lithogenic particles. The study site is a German contribution to the Bermuda Atlantic Time-series Study (BATS) program which is part of the U.S. Joint Global Ocean Flux Study (JGOFS). This BATS-IOW (to avoid confusion with the BATS sampling site *sensu stricto*) sampling site is positioned several kilometers southeast of the OFP and northeast of the original BATS site. The analysis of major lithogenic elements as aluminium, iron and silicon together with the contribution of major source-indicative clay minerals supplements earlier investigations of lithogenic material found in sediment traps in the Sargasso Sea. The chemistry and mineralogy of BATS-IOW samples will be analyzed in relation to observations from these other study sites and to other published data concerning aerosol and sediment composition. Another major aim of this study is to decipher the relation of barite as an important biogenic compound to the biological production in the upper water column. The seasonal development of major biogenic and lithogenic components will be discussed in comparison with satellite chlorophyll-a and aerosol data.



## 5.2 Material and Methods

### Sediment trap material and SEM–EDX analysis

The sampling site BATS-IOW is located circa 91 km southeast of Bermuda in the Sargasso Sea (Figure 5.1) within almost 4600 m water depth. Sediment trap material from 3200 m water depth was obtained by a funnel-type sediment trap with an opening of  $0.5 \text{ m}^2$  [Kremling *et al.*, 1996]. The temporal resolution of sample intervals spanned 19 and 20 days, covering the time 5th of September 1998 to 29th of August 1999. Precise details of sampling procedure and treatment of sample material after trap recovery are given in the literature [Waniek *et al.*, 2005a,b; Kuss *et al.*, 2010].

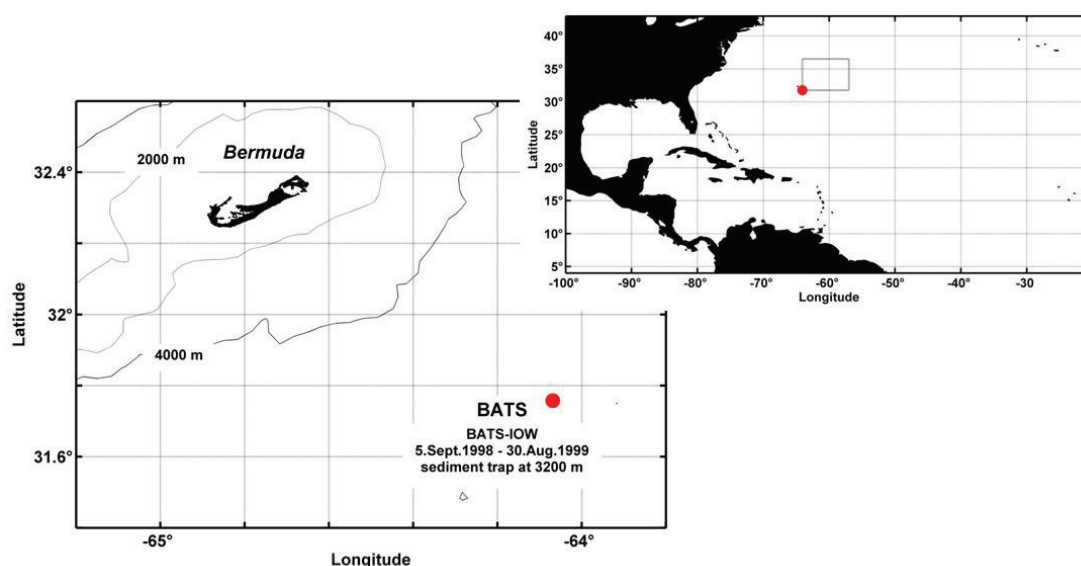


**Figure 5.1:** Position of the sediment trap sample site BATS-IOW southeast of Bermuda (map on the left) and location of the BATS-IOW sampling site (red circle) within the North Atlantic (map on the right). The catchment area (grey dashed box) of the 3200 m sediment trap based on the statistical funnel of the 3200 m deep OFP sediment-trap for particle sinking with  $100 \text{ m d}^{-1}$  [Siegel and Deuser, 1997]. Bathymetry is based on ETOPO2 data (<http://www.ngdc.noaa.gov/mgg/global/etopo2.html>).

The mass flux was determined after removing zooplankton "swimmers" from the sample material by dividing the dry weight by trap area and exposure time. The

mass flux was corrected for sea salt by subtracting the salinity present in the wet weight from the dry weight. The analytical approach of this study includes the determination of particulate organic carbon (POC) and particulate organic nitrogen (PON) and the analysis of biogenic and lithogenic mineral phases. Both, POC and PON were measured with the CHN Elemental Analyser according to *Erhardt and Koeve* [1999], whereby carbonate was removed with dilute hydrochloric acid prior to analysis. The fraction of biogenic and lithogenic mineral phases was analyzed by an automated particle microanalysis using the Scanning Electron Microscopy coupled Energy Dispersive X-ray system (SEM-EDX) [*Bauerfeind et al.*, 2005; *Brust and Waniek*, 2010]. Prior to analysis, the samples were desalinized by rinsing with Milli-Q water. Thinly coated Nucleopore filters were prepared for each sample [*Brust and Waniek*, 2010] and covered with elemental carbon to ensure electrical conductivity. For any particle measured on the filter, three morphological parameters (average diameter, area, shape) and the weight percentage of 12 main chemical element oxides were determined by the automated SEM-EDX analysis. The chemical data set of an automated particle analysis of a filter sample is comparable to a chemical bulk analysis. Biogenic and lithogenic particles and particle groups were classified according their elemental ratios by a comparison with standard minerals [*Bauerfeind et al.*, 2005; *Brust and Waniek*, 2010]. The lithogenic fraction involves quartz, feldspars, different clay minerals and metal oxides. Determined biogenic particles include carbonates, opal, barite, apatite and others. Barite is identified indirectly, because a direct barium determination had to be omitted from the the automated SEM-EDX particle analysis due to the overlapping of Ti and Ba EDX peaks. This has no influence on the determination of the mineral 'barite', as sulfur is another element measured within the automated particle analysis. Hence, a particle which is composed of Ti and S is a barite because no Ti-S minerals exist naturally. Double measurements of three samples revealed consistency concerning major chemical and particulate constituents (Figure 5.2). Major differences are seen in elements and particle groups, which are present in low amounts (e.g. S, Cl, Ti, Mn). The variation of the main elements as Si and Al, and Fe are relatively low and vary with 3 to 12 % around mean values. Therefore, these elements and its ratios (Si/Al, Fe/Al) were chosen for further considerations.

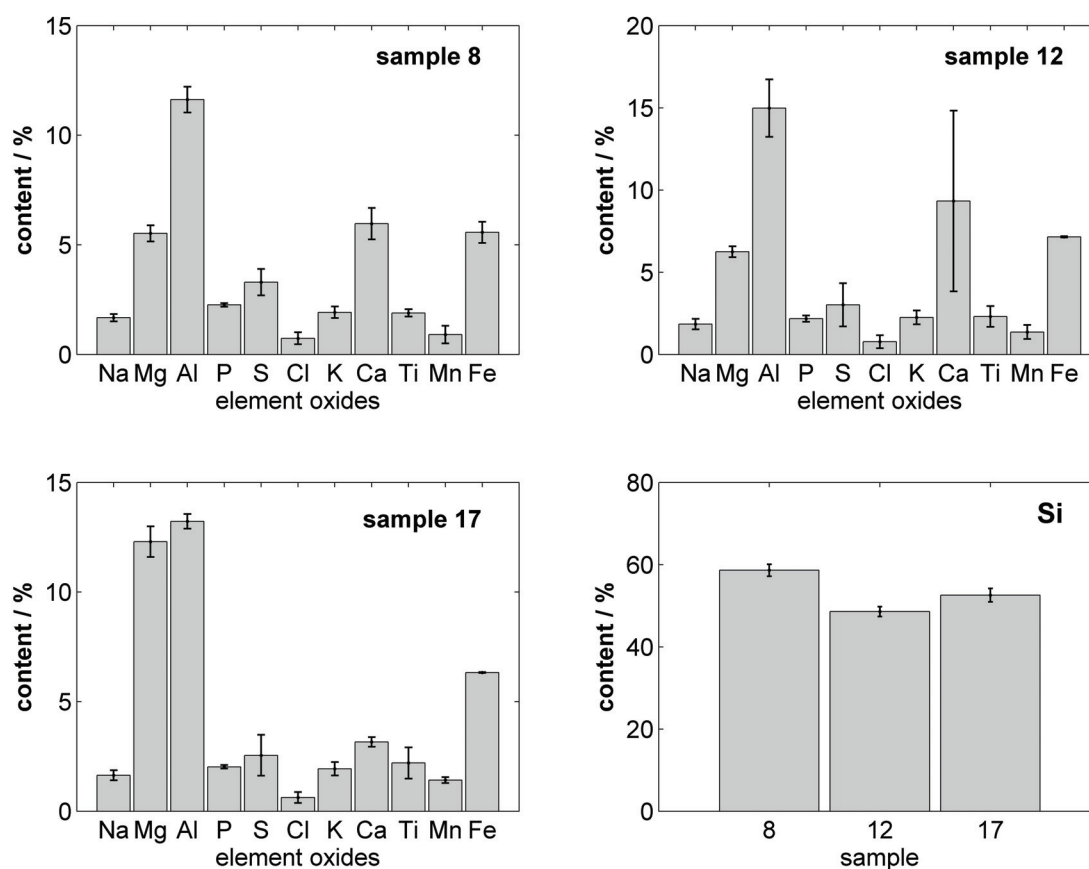


**Figure 5.2:** Comparison between double measurements, showing the reproducibility of the determination of the chemical composition (element oxides in %) of three samples (sample 8: 23/01–11/02/99; 12: 13/04–02/05/99, 17: 22/07–10/08/99). The contribution of Si is presented separately. Note the different scales.

### Catchment area

Recording Current Meter (RCM) data in three depth levels reveal current velocities of maximum  $20 \text{ cm s}^{-1}$  (Figure 5.3). Mean current velocities stay well below  $5 \text{ cm s}^{-1}$ , which is in line with earlier observations in this region [Siegel and Deuser, 1997]. Southwesterly flow directions prevail (Figure 5.3), which is an expression of weak Gulf Stream recirculation in this area. This circulation pattern hints to a catchment area NE of the sediment trap. Based on the comparison of Coastal Zone Color Scanner (CZCS) chlorophyll concentrations with simultaneous sedi-

ment trap carbon fluxes in 3200 m water depth, *Deuser et al.* [1990] deduced a catchment area for the OFP site extending a few hundred kilometers NE of the mooring position within a region of 200 km x 200 km. Another approach to determine the catchment area of sediment traps in the Sargasso Sea involving the flow field, particle sinking rates and trap depth was made by *Siegel and Deuser* [1997]. According to their data, the statistical funnel for the 3200 m sediment trap related to particles with sinking speeds of  $100 \text{ m d}^{-1}$  occupies a catchment area, which is located up to 600 km north of the OFP site. Because of the similar flow pattern at BATS-IOW with southward currents, it is therefore likely that a similar catchment area exists for the studied site (Figure 5.1).

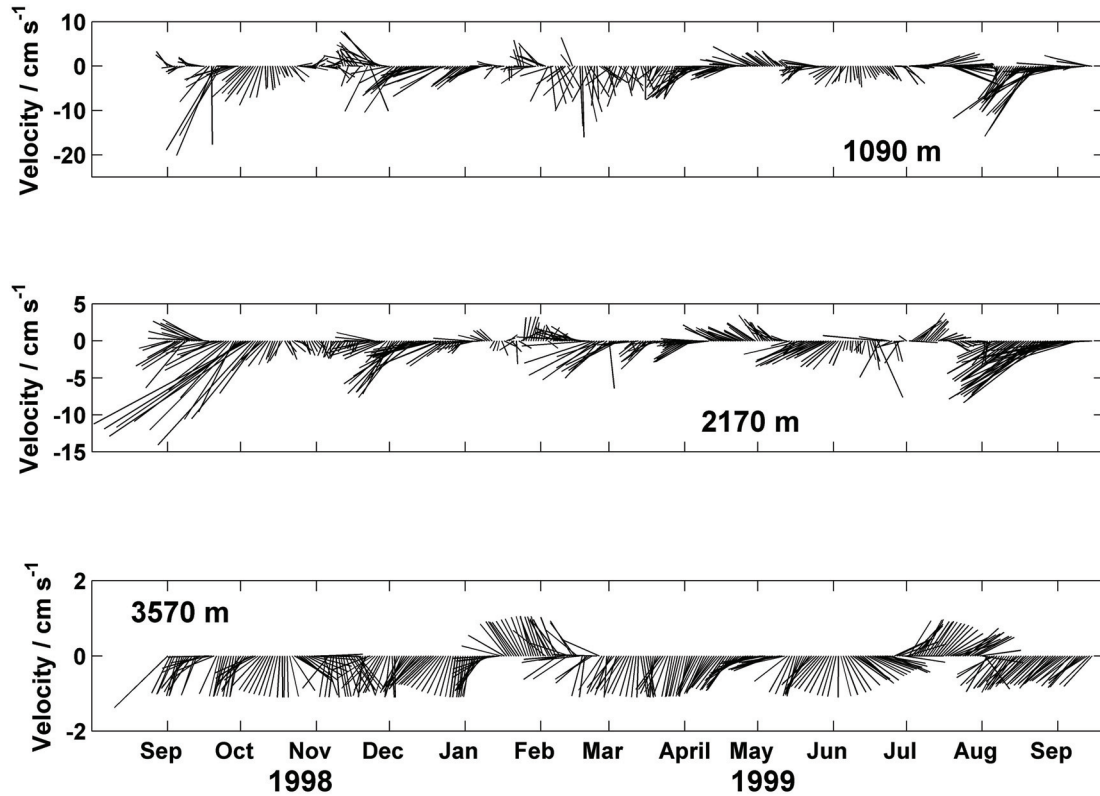


**Figure 5.3:** Currents in 1090 m, 2170 m and 3570 m depth levels (in  $\text{cm s}^{-1}$ ) measured between 1998 and 1999 at the BATS-IOW site.

## Satellite data

Biological particle fluxes and the lithogenic contribution to the particle flux are compared with satellite data, which provide information about chlorophyll-a concentrations of ocean surface waters and the presence of aerosols in the atmosphere over the Sargasso Sea. Chlorophyll-a products are derived from SeaWiFS (Sea-viewing Wide Field-of-view Sensor) onboard the GeoEye's OrbView-2 satellite (data coverage, 1996-2010). The aerosol index (AI) of TOMS (Total Ozone Mapping Spectrometer, see <http://toms.gsfc.nasa.gov/index.html>) onboard Earth Probe is chosen to reveal the presence of mineral aerosols in the atmosphere. The aerosol index is a qualitative measure of near-UV absorbing aerosol, which include mineral dust, smoke and soot aerosols caused by biomass burning [e.g. *Herman et al.*, 1997; *Chiapello et al.*, 1999], but not sulfate aerosols. Daily, 8-day mean and monthly satellite products are provided by Giovanni (<http://disc.sci.gsfc.nasa.gov/giovanni>). Chlorophyll-a concentrations derived from SeaWiFS are available in 8-day mean and monthly resolution with a spatial resolution of  $0.083^\circ \times 0.083^\circ$ . TOMS Aerosol indices (AI) are provided in  $1.0^\circ \times 1.25^\circ$  gridded daily products (data coverage, 1997-2005). For a comparison with sediment trap data, 8-day mean chlorophyll-a and daily AI data were averaged over the catchment area ( $600 \times 600$  km, Figure 5.1) for the time span of sampling. For comparability, 20-day AI averages were calculated, which cover the time of individual sediment trap sampling intervals.

## 5.3 Results and Discussion

### Particle flux and biogenic fluxes

The particle flux measured at the BATS-IOW site in 3200 m depth ranges between 4.1 and  $73.2 \text{ mg m}^{-2}\text{d}^{-1}$  (Figure 5.4) with an average mass flux of  $\sim 33 \text{ mg m}^{-2}\text{d}^{-1}$ . This value agrees with the general long-term average flux of  $35.2 \pm 16.9 \text{ g m}^{-2}\text{d}^{-1}$  observed at the OFP site (range: 10–97  $\text{mg m}^{-2}\text{d}^{-1}$ , *Conte et al.* [2001]). Highest mass fluxes occur in October/November 1998 and in January/early February 1999 (Figure 5.4). Whereas the autumn and winter time 1998/1999 is characterized by 'continuously' elevated particle fluxes, particle fluxes of spring and summer 1999

show more variability.

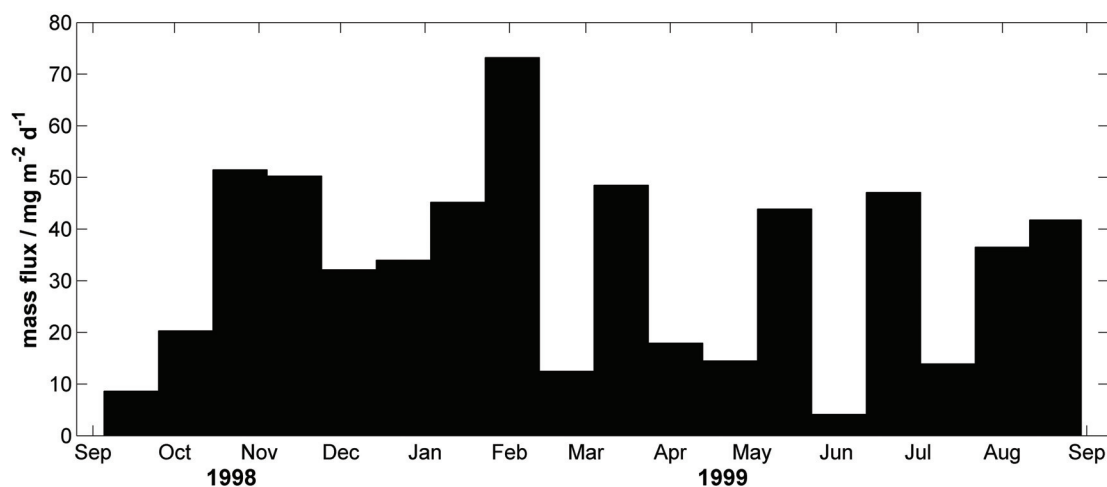


**Figure 5.4:** Total particle flux at the BATS-IOW site from 5<sup>th</sup> September 1998 to 30<sup>th</sup> August 1999 (in  $\text{mg m}^{-2} \text{d}^{-1}$ ).

This pattern is also present in the POC and PON flux and in the flux of barite (Figure 5.5). The presence of barium and/or its chemical compound barite in marine sediments is known to be an indicator for recent and paleo-productivity in the water column [e.g. *Dehairs et al.*, 1980; *Bishop*, 1988; *Dymond and Lyle*, 1992; *Dymond and Collier*, 1996; *Paytan and Griffith*, 2007]. Barite ( $\text{BaSO}_4$ ) is an authigenic mineral produced in the water column or sediment by chemical precipitation of barium. There is some evidence that barite forms in microenvironments which are related to the decay of organic matter [*Dehairs et al.*, 1980]. The BATS-IOW sediment trap samples show a pronounced seasonal cycle of barite (Figure 5.5). This cycle is obviously closely linked to the flux of biogenic particles and organic matter, which have similar flux patterns during the sampling period and is expressed by the close relation between barite, POC and PON (Figure 5.6). *Huang and Conte* [2009] showed that the flux of barium in OFP sediment trap samples increases two-fold between 500 and 1500 m and remains almost constant between 1500 and 3200 m water depth. These authors also outlined the connection of barium flux with the flux of opal. This is explained by the formation of barite within microenvironments of interstices of diatom frustules [*Bishop*, 1988]. The relationships between opal and POC, opal and PON and between barite and opal of the

BATS-IOW samples support the linkage between opal and biogenic phases in the water column and the close relation to barite (Figure 5.6).

POC, PON, barite and opal as important representatives for the biological production in the euphotic zone exhibit very similar seasonal patterns during the sampling period and can be related to satellite chlorophyll-a concentrations. The chlorophyll-a concentrations as a proxy for primary production in the catchment area show an increase between October 1998 and April 1999, when the chlorophyll concentrations reach its maximum with an abrupt decay of the bloom (Figure 5.5). In general, this increase is also present in the flux of biogenic particulates, but the biogenic fluxes already decrease while the chlorophyll-a concentrations are still at a high level (Figure 5.5).

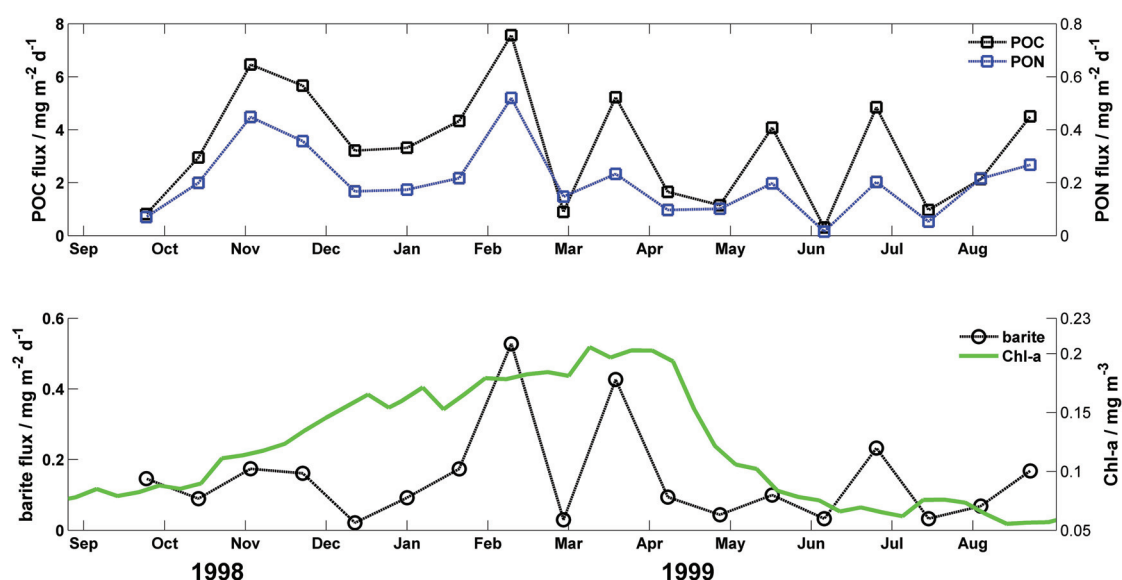


**Figure 5.5:** Flux of POC and PON (upper panel), and flux of barite (from SEM-EDX, lower panel) shown together with chlorophyll-a concentrations ( $\text{mg m}^{-3}$ ) in the upper water column (SeaWiFS data, area averaged). Note, that the flux values are plotted at the end of each sampling interval. One sampling interval lasts 19 or 20 days. The particle flux is given in  $\text{mg/m}^{-2} \text{d}^{-1}$ .

The comparison of satellite CZCS chlorophyll pigment concentrations with the long-term flux of POC at 3200 m water depth revealed a lag of 1.5 months between the biological processed of the ocean surface and the flux at depth in the Sargasso Sea [Deuser *et al.*, 1990]. A similar temporal difference was also observed



in the eastern part of the subtropical North Atlantic Gyre at  $33^{\circ}$  N,  $22^{\circ}$  W. Based on satellite and modeled aerosol optical depth data and lithogenic particle fluxes at 2000 m depth, a time lag of 1.5 to 2 months was observed between atmospheric dust occurrence and marine lithogenic flux [Brust *et al.*, 2011]. There is no clear time lag visible between biogenic fluxes and chlorophyll-a concentrations throughout the sampling period 1998/1999. But the general trend of increasing chlorophyll-a concentrations in November/December 1998 can be related to the increase of biogenic fluxes starting in January 1999, which indicates a lag of 1 or 2 months. The peak of biogenic fluxes in January and March 1999 is interrupted in February 1999, whereas chlorophyll-a concentrations are still elevated until April (Figure 5.5).

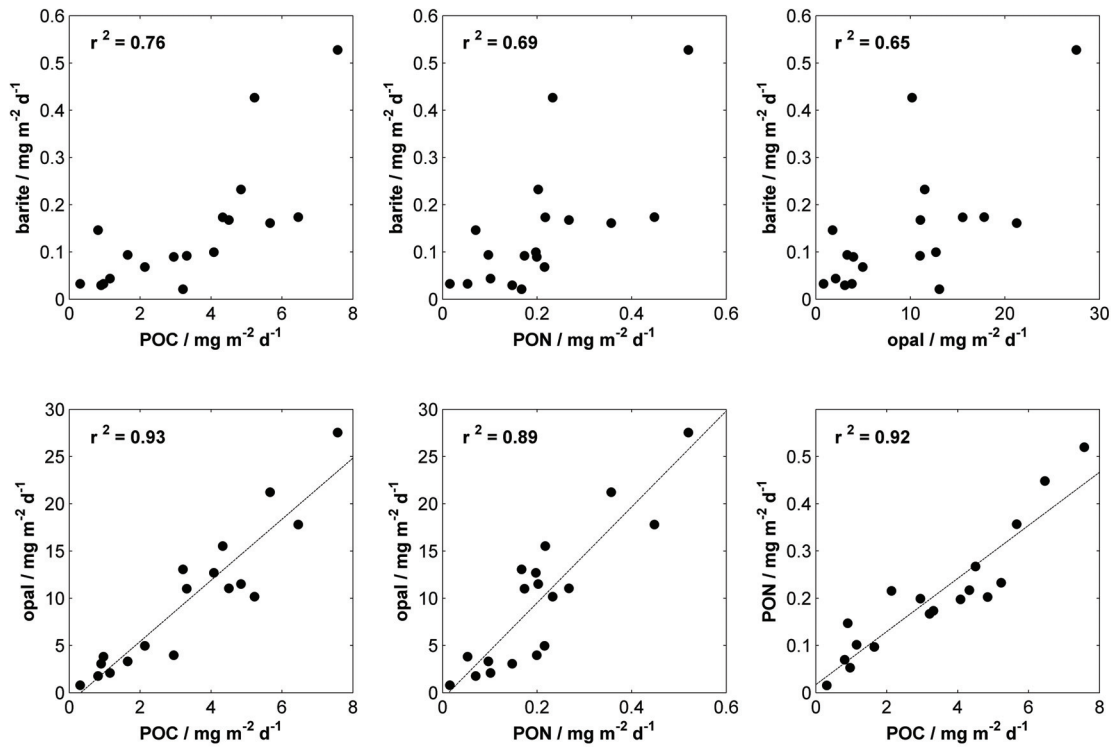


**Figure 5.6:** Relationships between barite, POC, PON and opal (mg m<sup>-2</sup> d<sup>-1</sup>). The Pearson correlation coefficient ( $r^2$ ) between respective biogenic particulates is also given.

One reason for this discontinuity might be given in current directions and velocities during this time interval. A reverse in current directions occurs at all three



depth levels in January/February 1999 (Figure 5.3). The reverse from southward to northward flow directions is clearly discernable at the 3570 m depth level and also present, but less pronounced at 2170 m and 1090 m depth level. A change in the origin of water masses over the trap depth could have led to the supply of different amounts of particles to the trap. These flow conditions might also explain the decrease of fluxes during end of April 1999 (Figures 5.4, 5.5) and the decoupling of ocean-surface chlorophyll pigments and biogenic fluxes during this period. Currents in 2170 m and 1090 m depth are coming from south in April and early May 1999 (Figure 5.3), which changes the catchment area and transfers other water masses and different particle assemblages to the mooring site during this time. The lack of enhanced biogenic particulates in southern water masses can be explained by the earlier termination of the bloom period in the southern sea since the bloom propagates from south to north [Conte *et al.*, 2001]. South of the BATS-IOW mooring position the bloom reached its maximum in February 1999 and decayed in March 1999 as seen in chlorophyll-a data (not shown). Enhanced fluxes (Figures 5.4, 5.5) in May 1999 might reflect the chlorophyll-a peak of early April again, shortly before the bloom decays in the northern catchment area. Such observations of discontinuous particle fluxes within the ocean can also be explained by the patchiness of biological production in the ocean surface and the sediment trap position relative to the descent of particles or the bloom as discussed by Siegel *et al.* [1990]; Waniek *et al.* [2000]. Temporal and spatial mesoscale physical structures as eddies can therefore also play a major role in particle export flux from ocean surface to the deep ocean. Mesoscale eddies are frequent hydrographic features in the sea area south of Bermuda and often induce nutrient injections from below into the euphotic zone, which support blooms in late spring and during the summer time [Steinberg *et al.*, 2001]. The peaks of biogenic fluxes in May and June 1999 (Figure 5.5) might be caused by such processes.

### **Lithogenic composition, aerosol contribution and sources**

Past studies have demonstrated that the area around Bermuda is mainly influenced by North African mineral dust [e.g. Arimoto *et al.*, 1992, 1995; Jickells *et al.*, 1998]. North African sources for lithogenic material are also confirmed by Fe/Al ratios

(Figure 5.7) of BATS-IOW sediment trap samples. Aluminium is one of the major elements of earth's crust [e.g. *Taylor and McLennan*, 1985] and generally referred as a tracer of crustal origin in aerosols and its sediments. As the concentration of aluminium is almost independent from rock type [*Dymond et al.*, 1997], accompanying elements (e.g. Si, Fe, Ti) are usually normalized to aluminium with the aim of deciphering sources of aerosols. Aluminium and silicon are major elements in silicates (e.g. clay minerals, feldspars, quartz), which are tracers of North African dust. Iron is associated with feldspars and clays, in which Fe is incorporated in the crystal lattice or occurs as iron oxide (hematite,  $\text{Fe}_2\text{O}_3$ ) and/or hydroxide (goethite,  $\text{FeO-OH}$ ) surface coatings. The Fe/Al ratio of North African soil sources range between 0.52 and 1.24 [Table 2a in *Formenti et al.*, 2010]. Possible other sources for lithogenic material could also be derived from areas in North America, which are prone to aerosol production, for example the Great Plains. A study of the red clayey paleosols found on Bermuda revealed that Zr/Y and Zr/La ratios are very similar to the ratios of North African dust in the  $< 2 \mu\text{m}$  fraction, whereas no similarity to possible North American sources (Great Plains loess, Mississippi Valley loess) was found [*Herwitz et al.*, 1996]. Chemical analysis of loess soils in the Mississippi River Valley and the Great Plains reveal Fe/Al values, which lie in the range of 0.3 and 0.6 (calculated from given Si, Al and Fe contents listed in: *Pye and Johnson* [1988]; *Muhs and Bettis III* [2000]; *Muhs et al.* [2001]). Fe/Al ratios of BATS-IOW sediment trap samples (0.7–0.9) coincide with North African Fe/Al ratios. Figure 5.7 illustrates a compilation of published Fe/Al and Si/Al ratios with North African provenance. The data show a wide scattering of ratios, which might be caused by different sample types (soils, aerosols, rain samples), different North African sources, time and location of sampling (Table 5.1), which also controls sources and modifications during transport, and analytical methods. However, most of the published data appear in the field of North African sources and are concentrated in a narrow range of Fe/Al values (between 0.5 and 1). Unexpectedly, the average Fe/Al ratio given for dust over the North Atlantic, calculated according to the average annual atmospheric deposition of Fe and Al (and Si) to the North Atlantic (data given in *Duce et al.* [1991]), occurs outside the North African field. Interestingly, the local originating aerosol and soil samples are limited to Fe/Al ratios of 0.6–0.7, although the Si/Al ratios vary between 2 and 5.5.

Furthermore the Si/Al-Fe/Al diagram shows a clustering of data with Si/Al ratios of 2.5 and Fe/Al ratios of 0.65. These data encompass local North African aerosol [Formenti *et al.*, 2008] and rain [Desboeufs *et al.*, 2010] samples, North Atlantic aerosol samples [Formenti *et al.*, 2003; Buck *et al.*, 2010], Mediterranean [Bergametti *et al.*, 1989b] aerosol and European [Bonelli *et al.*, 1996] aerosol samples. Formenti *et al.* [2010] stated the low significance of Si/Al ratios to discriminate source regions in North Africa with the exception of the Bodélé Depression. Si/Al ratios of most North African dusts have a low variability around 2.3 [see Formenti *et al.*, 2010, and references therein]. Dusts derived from the Bodélé Depression (Chad, south Sahara) reach Si/Al values of 4 due to the mobilization of freshwater diatoms of the dried-out Mega-Lake Chad [Formenti *et al.*, 2010].

Studied sediment trap samples clearly plot in the field of North African dust sources with mean Fe/Al ratios of 0.75 and Si/Al ratios of 4 (Figure 5.7), hence North African sources for the lithogenic fraction are most likely. Compared to the BATS-IOW samples, other sediment trap data of the subtropical North Atlantic (Figure 5.7), namely the OFP site [Huang and Conte, 2009] and the Kiel276 deep sea mooring (33°N, 22°W; Brust and Waniek [2010]), demonstrate greater deviations in Si/Al ratios. The wide range of Si/Al ratios in sediment trap samples can be attributed to the presence of biogenic silica or opal, which shifts the Si/Al ratio to higher values. Silicon-aluminium ratios of OFP site data are above 8

**Figure 5.7 (following page):** Scatter plot of Si/Al versus Fe/Al mass ratios. BATS-IOW series shown together with literature data: \* soil samples taken in North Africa and local dust samples, + dust samples taken in the Mediterranean area, off the West African coast and the central Atlantic, ° sediment trap samples and SPM taken in the North Atlantic ocean. The average Si/Al and Fe/Al ratios for dust over the N Atlantic were derived from the average atmospheric deposition of Al, Fe and Si to the ocean after Duce *et al.* [1991]. Gray shaded areas mark the general range of Fe/Al values taken from literature data (light gray: Fe/Al ratios for North African sources, provided by Formenti *et al.* [2010]; dark gray: Fe/Al ratios of North American soils, which are prone to dust mobilization. North American soil data from Pye and Johnson [1988], Muhs and Bettis III [2000], Muhs *et al.* [2001] and Bettis III *et al.* [2003].) The lower panel shows mean values of given literature data for more clarity. see Table 5.1 for further information on the referenced data.

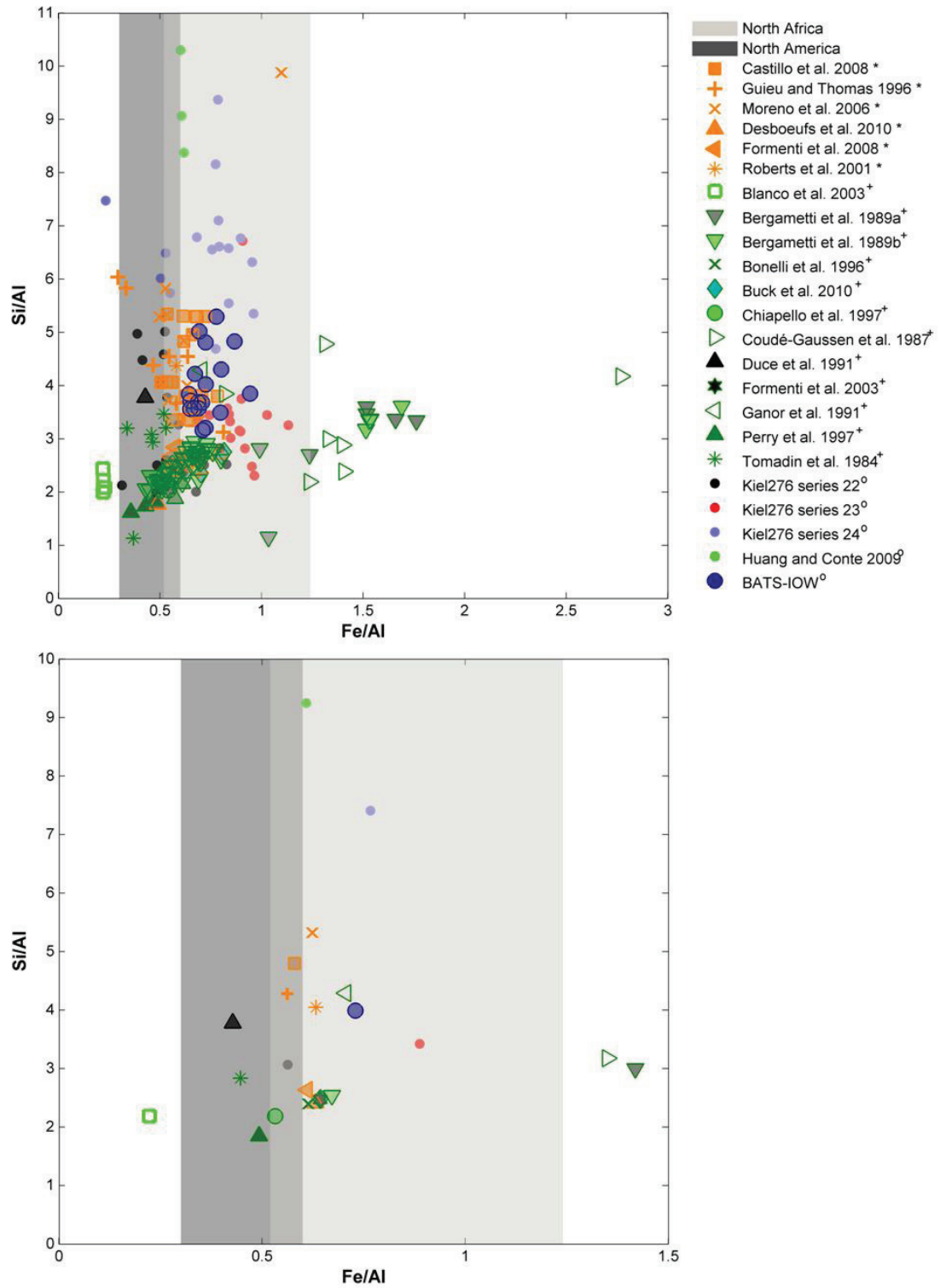


**Table 5.1:** List of references which provide chemical data of soil and aerosol samples with North African provenance. Sampling location, sampling time and sample type of distinct North African soil and aerosol samples of referenced data in Figure 5.7 are listed. First section: local sources, second section: aerosol samples with North African origin taken off North Africa.

Reference	Sampling location	Sample type	Source	Sampling time
<i>Castillo et al.</i> [2008]	Sahara-Sahel dust Corridor	aerosol, soil samples	Sahara-Sahel	early 2000s
<i>Guieu and Thomas</i> [1996]	Algeria, North Africa	soil samples	local	December 1991
<i>Moreno et al.</i> [2006]	Sahara-Sahel dust Corridor	soil, road and aerosol samples	local	
<i>Desboeufs et al.</i> [2010]	Niger	rain samples	south-eastern Saharan sources	June–July 2006
<i>Formenti et al.</i> [2008]	North Africa	aerosol	North Africa	January–February, August 2006
<i>Roberts et al.</i> [2001]	Central African rain forest, Congo	aerosol	Mineral dust, N Africa (coarse fraction)	November–December 1996
<i>Blanco et al.</i> [2003]	Lecce, southeast Italy	aerosol	northwestern Sahara, Chad, Niger, Algeria and Lybia	April–June 2002
<i>Bergametti et al.</i> [1989a]	Canary Islands	aerosol	North Africa, Sahel and Morocco	July 1985
<i>Bergametti et al.</i> [1989b]	Capo Cavallo, Corsica	aerosol	N Africa	1985
<i>Bonelli et al.</i> [1996]	Stelvio National Park, north Italy	aerosol	North Sahara	March 1991
<i>Buck et al.</i> [2010]	North Atlantic, ship transect off Africa	aerosol, rain samples	Sahara (according to air trajectories)	June 2003
<i>Chiapello et al.</i> [1997]	Sal, Cape Verde	aerosol	Sahel, central Sahara, north Sahara	October to April 1991 and 1992
<i>Coudé-Gaussen et al.</i> [1987]	Fuerteventura, Canary Islands	aerosol	southern Morocco	April 1984
<i>Formenti et al.</i> [2003]	over the Atlantic Ocean, between Cape Verde and Senegal	aerosol (aircraft samples)	North African dust mixed with anthropogenic European/ N American sources	September 2000
<i>Ganor et al.</i> [1991]	Israel	aerosol	North African and Arabian Desert	1968–1987, 23 dust storms
<i>Perry et al.</i> [1997]	central to eastern United States (East US, Virgin Islands)	aerosol	North Africa	1992–1995, selected dust events
<i>Tomadin et al.</i> [1994]	ship transect Adria, Italy	aerosol	Sahara	1981

for the years 2002–2005 in three different depth levels (*Huang and Conte* [2009]; Figure 5.7). The differences in Si/Al ratios between sediment trap in 1998/1999 and 2002–2005 highlight interannual differences of biological production (opal) and atmospheric input of lithogenic particles to the study area, which are present between sediment trap series in Kiel276 as well (Figure 5.7; *Brust and Waniek* [2010]). Whereas the amount of land-derived biogenic opal, as for instance aeolic contributions of diatom opal from the Bodélé Depression, is probably vanishingly small. Nevertheless, it is remarkable that, despite these differences, Fe/Al values between trap samples in the Northeast Atlantic are similar and appear in the North African–Fe/Al–field. Exact North African sources are not detectable with the Si/Al and Fe/Al ratio alone. Several studies have shown that other elements and its ratios to aluminium are also important indicators for source regions, such as the Ca/Al ratio. The potential of the Ca/Al ratio as a discriminator of distinct North African sources has long been recognized [e.g. *Bergametti et al.*, 1989a; *Chiapello et al.*, 1997] and its ability to detect aerosol sources is positively discussed at present [*Formenti et al.*, 2010]. As a result of Ca-poor source areas and modifications during the atmospheric transport (e.g. due to acidic rain water), North African dust which reaches North America and the Caribbean can be depleted in calcium. Mineral aerosols from North America by contrast have relatively high Ca contents and *Perry et al.* [1997] suggest the Ca/Al ratio as a characteristic distinction between North American (local) and North African dust sources at least for North American settings. Due to the dominance of biogenic originated carbonates in marine sediment trap material and the difficulty in distinguishing those biogenic from the allochthonous carbonate within the particle analysis, the Ca/Al ratio is not applicable in this study. Calcium rich aerosols from North Africa occur mainly together with specific minerals as palygorskite and have been occasionally observed at Barbados [*Caquineau et al.*, 2002]. Minerals and especially clay minerals are important indicators for lithogenic sources in North Africa. The presence of specific clay mineral species (e.g. palygorskite) and also clay mineral ratios as the illite-to-kaolinite ratio (I/K) are indicative for distinct source areas [*Formenti et al.*, 2010]. In BATS-IOW samples the lithogenic fraction is dominated by clays ( $58 \pm 9\%$ ), quartz ( $30 \pm 9\%$ ) and feldspars ( $7 \pm 2\%$ ) (Figure 5.8). Clay minerals contribute more than half to the lithogenic flux. An unusual high clay content is

seen in July, where clay minerals contribute over 80 % to the lithogenic particle flux (Figure 5.8). The major clay mineral in BATS-IOW sediment trap samples is illite, which contributes  $56 \pm 14$  % to the clay mineral flux, followed by kaolinite, palygorskite, chlorite and smectite. The relative contribution of palygorskite to the clay mineral flux dominates during the summer months 1999 without an increased lithogenic particle flux. In these samples, palygorskite even dominates the total lithogenic particle flux. The palygorskite content increases with the beginning of July 1999 and reaches a maximum end of July. The contribution of palygorskite to the clay mineral flux reflects the input of mineral dust to the Sargasso Sea at that time. Higher palygorskite rates are also present end of April and in May 1999 (Figure 5.8, 5.9), but without enhanced fluxes.

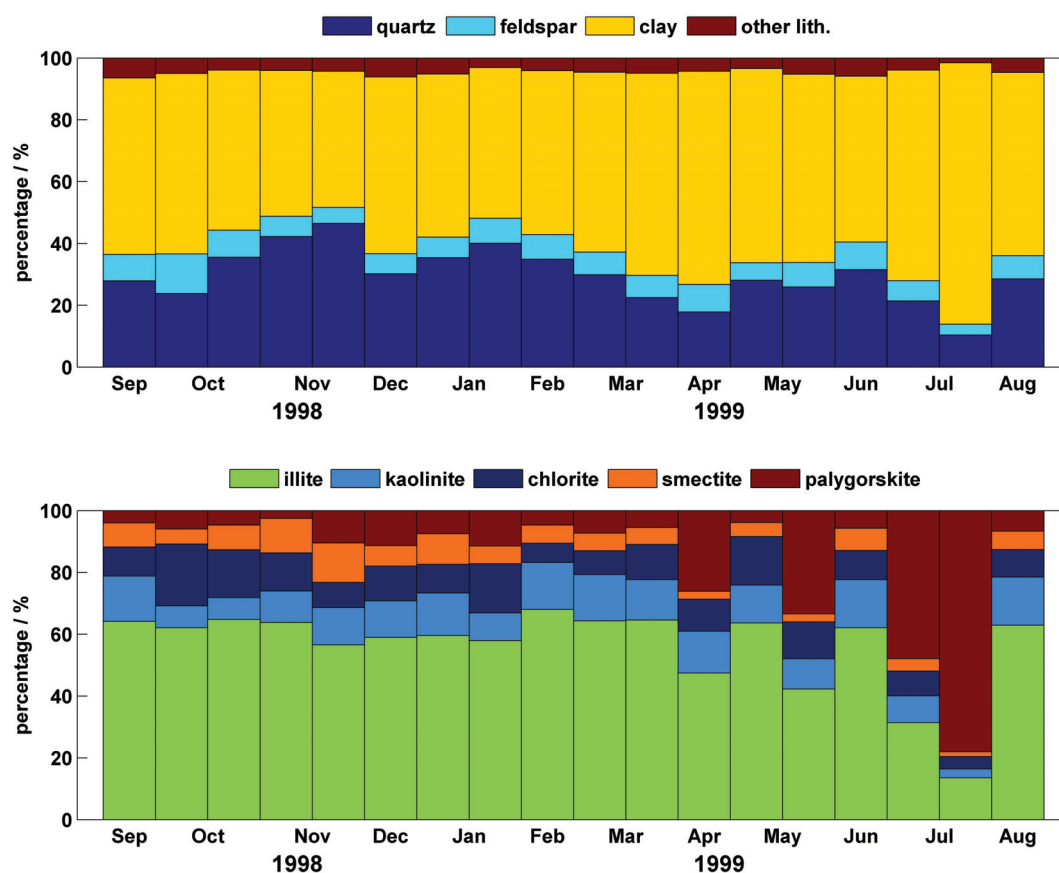


**Figure 5.8:** Proportion (in %) of main lithogenic particle groups within the lithogenic fraction (upper panel) and proportion (%) of clay minerals within the clay fraction (lower panel).



This general increase of palygorskite from spring to summer 1999 corresponds to the TOMS aerosol index (AI), which indicates an increase of atmospheric aerosols from March to September 1999 (Figure 5.9).

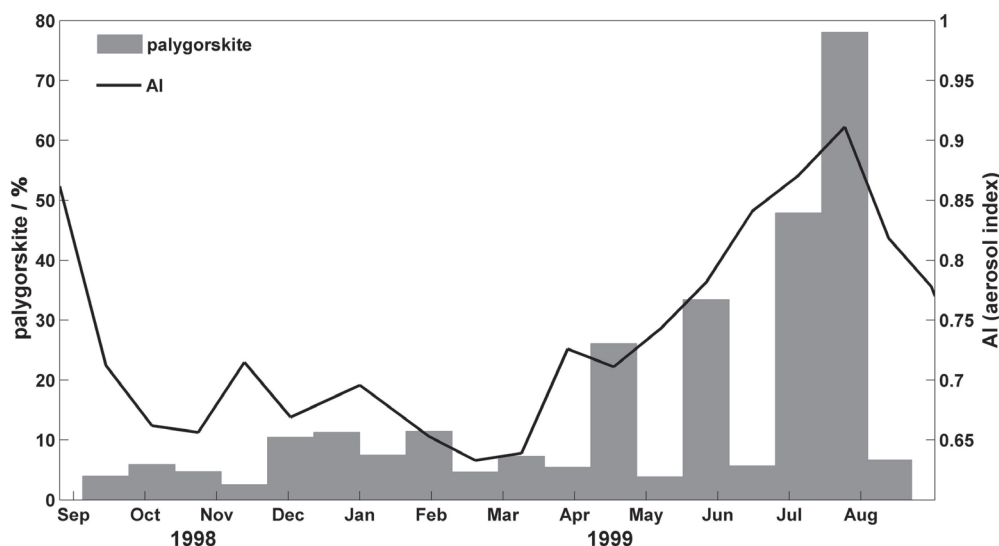


**Figure 5.9:** Contribution of palygorskite to clay mineral flux (in %) and TOMS aerosol index (AI, unitless).

As has already been pointed out between chlorophyll-a concentrations and biogenic fluxes, there is also no obvious time lag between dust occurrence and clay flux. Similar to the biogenic fluxes, the lithogenic flux and the contribution of palygorskite to the total, lithogenic and clay fraction (Figure 5.8, 5.9) is not continuous or responds without cease to the aerosol occurrence. Biogenic fluxes have shown that the reversing of current directions in January/February, April/May and July 1999 account for lower particle fluxes in distinct time intervals. The main transport route of lithogenic material within the ocean is associated to biogenic particles [e.g. *Klaas and Archer, 2002*]. A lower contribution of lithogenic material and distinct mineral species to the particle flux can therefore be explained by a smaller efficiency of particle transport due to lower amounts of aggregates forming biogenic compounds in the water column. The distribution of aerosols in the atmosphere over the western subtropical Atlantic supports this idea. Aerosol indices south of Bermuda are generally higher and decrease to the north as mineral aerosols coming from North Africa are approaching the study site from southeast. Palygorskite is



a typical clay mineral for western North African source areas [*Bout-Roumazeilles et al.*, 2007, and references therein] and prod to western North African sources for the lithogenic fraction in BATS-IOW sediment trap samples. I/K ratios of the samples have constantly values above 2 (Figure 5.10), which is likewise an indication for north and west Sahara sources as defined by *Caquineau et al.* [1998, 2002]. The I/K-palygorskite diagram (Figure 5.10) shows a development of the lithogenic fraction between 1998 and summer 1999 from western (Morocco Atlas, western Sahara) to more central (Morocco, Algeria) sources of the northwestern part of North Africa (Figure 5.10).

Aerosol indices are also elevated prior to sampling in September 1998. But the contribution of mineral dust is comparatively small at the beginning of the sediment trap time series. The clay mineral fraction is controlled by illite in 1998, palygorskite is present, but in low amounts. Therefore main sources must be identified in palygorskite depleted areas of North Africa (south and central Sahara). Mixtures of mineral dust from different African origins probably led to the presence of palygorskite. Dust samples taken on Barbados are dominated by south and central Sahara signatures of I/K ratios, which also imply mixtures of dust from different source areas [*Caquineau et al.*, 2002]. Some mineral aerosols which contain palygorskite and calcite were also detected at Barbados during October 1992 and July 1994 [*Caquineau et al.*, 2002]. Based on I/K ratios and satellite imagery two distinct source areas were identified for those dust events, an Egyptian origin in October 1992 and a source area situated across the Libyan-Tunisian border for July 1995. I/K ratios of Egyptian aerosols are smaller than 1, therefore this source region for lithogenic material of the BATS-IOW sediment trap can be ruled out. Palygorskite-bearing sources with high I/K ratios such as the area around the Libyan-Tunisian border, but also North African sources situated further west (e.g. central Algeria, West Sahara, Morocco) are possible dust sources for lithogenic particles found at BATS-IOW.

Beneath the eolian input of lithogenic material to the Sargasso Sea lateral sources are also suggested to contribute to lithogenic particle flux at depth [*Huang and Conte*, 2009]. Especially hurricanes are known to have an impact on particle fluxes in the Sargasso Sea by resuspension of slope material from the Bermuda Rise [*Conte*, 2005; *Weber et al.*, 2006; *Huang and Conte*, 2009]. During the Hurri-

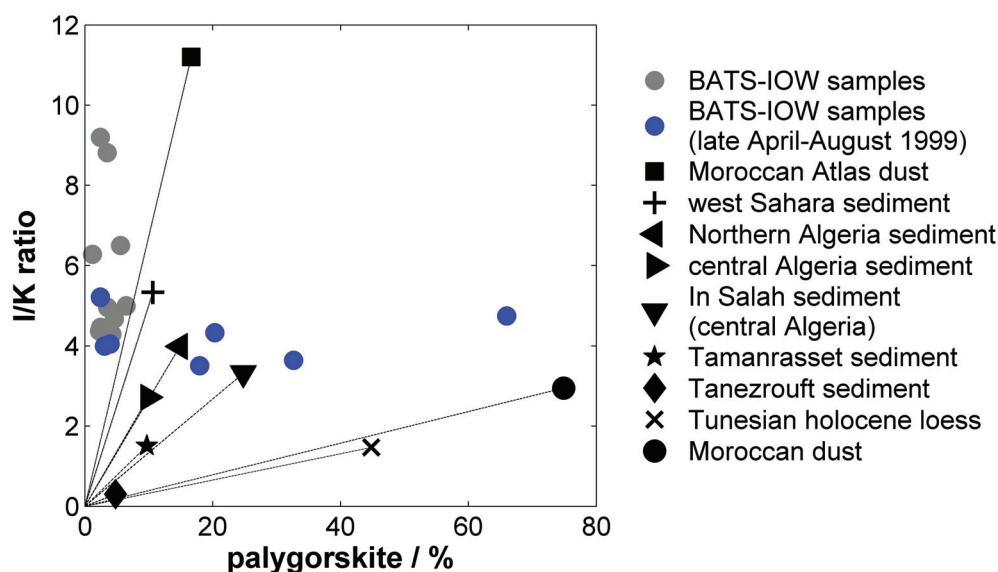


**Figure 5.10:** Illite/Kaolinite ratios (I/K) plotted against the palygorskite content (% of the lithogenic fraction) present in BATS-IOW sediment trap samples. Samples of late spring to summer 1999 (13. April – 30. August) are marked in blue. The relevant end-members are redrawn from *Bout-Roumazeilles et al.* [2007].

cane seasons of 1998 and 1999 three Hurricanes passed Bermuda, Daniell (24.08.–03.09.1998), Karl (23–28.09.1998) and Arlene (11–18.06.1999). The storms passed Bermuda with a distance of several 100 km and weakened closest to the island. During a Hurricane Fabian (September 2003), enhanced fluxes of particles were detected at the OFP site due to the resuspension and southward transport of slope material from the Bermuda Rise [Conte, 2005; Weber *et al.*, 2006]. Material, resuspended from the Bermuda pedestal consists of calcareous sediments. Because of the great distance from the storms, a lack of enhanced contribution of carbonate to the BATS-IOW sediment trap material, and the lack of enhanced fluxes during the time of the storms, a lateral input of particles to the trap due to these hurricanes can be neglected. Despite that, lateral influx of suspended clays and other lithogenic particles from continental shelf and slopes of the ocean margins can have an affect on the lithogenic composition of sediment trap material and the signal of continental, or to be more precise, North African source regions.

## 5.4 Conclusions and summary

The analysis of a one year record of sediment trap material from 3200 m depth in the Sargasso Sea supports results of earlier scientific studies in this region concerning the contribution of biogenic and lithogenic material to the particle flux and their seasonal variability. Particle fluxes are variable within the Sargasso Sea and are generally elevated during in February–March with smaller maximum fluxes sometimes observed during wintertime, e.g. in December–January [Conte *et al.*, 2001]. The occurrence of flux maxima in October/November 1998 and January/February 1999 at BATS-IOW is an expression of the high interannual variability of seasonal flux patterns in this region. Those interannual differences can be caused by the occurrence of temporal and spatial mesoscale features like eddies, which influence the nutrient flux, the biological production and the export of particles [Steinberg *et al.*, 2001; Conte *et al.*, 2001, 2003]. The reversing of currents at different depth levels have obviously a strong impact on particle fluxes due to the transport of different water masses over the trap position during 1998–1999. Lithogenic and biogenic fluxes are affected by these flow conditions. The general southward flow of water masses is interrupted by northward currents lasting for several days to weeks, which transport material from the south, where the bloom was already terminated.

The investigated BATS-IOW samples contain remarkable amounts of barite in contrast to sediment trap samples of Kiel 276. The flux of this authigenic mineral is strongly coupled to the flux of important biogenic components like opal, POC and PON. Although, barite follows the seasonal cycle of biogenic particle production, its formation is known to be linked to microenvironments due to the decay of biogenic components. Further research should address the question of the link between export production and barite flux.

The chemical and mineralogical composition of BATS-IOW sediment trap samples points to a North African origin of the lithogenic particles. TOMS aerosol indices show maximum dust occurrence over the study sites present in summer months, which is typical feature of dust transport over the North Atlantic during summer. Illite-to-kaolinite ratios, the presence of palygorskite and Si/Al and Fe/Al ratios resemble clay mineral assemblages found in North Africa. The mixture of

sources and different air masses during long-range transport of dust leads to virtually uniform dust compositions arriving in North America [Trapp *et al.*, 2010]. Elemental ratios and clay mineral assemblages in the BATS-IOW sediment trap indicates a mixture of different North African sources as well, whereby modifications of the original aerosol composition during transport processes in the water column must be taken into account. Although elemental ratios and the mineralogical composition of sediment trap material point to North African sources, lateral advected material via the Gulf Stream can not be excluded.

## 6 General conclusions and future perspectives

The present work investigated the mass flux and composition of the lithogenic fraction of sediment trap material at two different mooring sites (BATS-IOW and Kiel276) in the subtropical North Atlantic particularly with regard to eolian dust input and sources of dust. Therefore the sediment trap data were compared with chemical and mineralogical composition of North African dust and soil sources, based on referenced data, and with satellite and modeled aerosol products. The present study has demonstrated that a strong link between dust input and lithogenic flux at depth can be observed:

- The lithogenic particle flux is largely controlled by the input of dust at the sampling site Kiel276. Satellite aerosol optical depth (AOD) data, which are supported by modeled GOCART AODs show the occurrence, relative amount and distribution of mineral aerosols over the mooring site. Dust events and the general occurrence of dust over the sampling site Kiel276 is seasonal (mostly in winter) and also variable in strength and frequency on interannual time scales. The AOD patterns are very similar compared to observed lithogenic flux patterns. Both are positively correlated with each other. This observation explains the difference between average total particle flux and average lithogenic particle flux (see Chapter 4, *Brust et al.* [2011]).
- The lithogenic flux responds to the atmospheric aerosol signal (AOD) with a time lag, which means that dust reaches the sediment trap at 2000 m after about one and a half months (see Chapter 4, *Brust et al.* [2011]).
- Clay mineral assemblages hint to different source areas of dust from North Africa at the eastern sampling site (Kiel276). Specific North African dust sources vary rather interannually than within seasonal time scale. Year to year variability is expressed by mixtures of North African source areas with dominant sources in Mauritania and northwestern parts of Northwest Africa

(sampling years 2002–2004) and central Sahara (Algeria–Mali; sampling year 2004–2005) (see Chapter 3, *Brust and Waniek* [2010]).

Eolian iron inputs play an important role for nitrogen fixers living in the tropical to subtropical North Atlantic Ocean [*Mills et al.*, 2004], and hence influence primary production. Lithogenic and biogenic sediment trap fluxes at Kiel 276 along with satellite chlorophyll-a and aerosol data were investigated to assess a possible effect of dust input and delivery of nutrients like iron on primary production:

- Dust outbreaks from North Africa reach the sampling site Kiel 276 mostly in the winter and early spring months. During this time, nutrients are generally elevated due to winter mixing and entrainment of nutrients from below into the euphotic zone. Total flux as well as biogenic flux and chlorophyll-a concentration are highly variable during the late winter/early spring bloom from year to year defined by the availability of nutrients as a result of the strength of winter mixing. A biological response to nutrient input by atmospheric dust is therefore only visible during summer dust events, when the mixed layer depth is shallow and nutrients are depleted (see Chapter 4, *Brust et al.* [2011]).
- Based on the eolian iron flux and applying the Redfield ratio according to *Kuss and Kremling* [1999b] the theoretical additional carbon fixation per season would yield a 17% enhanced primary production in this region (see Chapter 3, [*Brust and Waniek*, 2010]).
- Dust inputs during summer are rare at the sampling site in the subtropical Northeast Atlantic. Only the summer months in 2004 are characterized by multiple dust outbreaks, which reached the sampling site. The ocean surface biology might be able respond within one week on nutrient delivery due to dust inputs. An enhanced flux of biogenic particle flux was observed in August 2004 in 2000 m water depth. This was interpreted as an enhanced biological production in ocean surface waters followed by dust and nutrient delivery to ocean surface during summer dust event (see Chapter 4, *Brust et al.* [2011]).

- Enhanced biogenic flux is related to dust input derived from satellite and modeled aerosol data. Satellite chlorophyll-a concentrations of ocean surface waters do not show a relation to aerosol occurrence or a response to nutrient input via dust due to the presence of deep a chlorophyll maximum at Kiel 276 positioned in the northeastern subtropical Atlantic Ocean [see Chapter 4, *Brust et al.*, 2011].

For the sampling site BATS-IOW located in the western subtropical North Atlantic Ocean following can be stated:

- Even the western part of the subtropical Atlantic (BATS-IOW) is reached by mineral dust from North Africa. North African dust sources at this site are palygorskite-bearing soils of the northwestern part of North Africa in 1998–1999, whereas North American soil dust seems to be negligible (see Chapter 5, *Brust et al.* [in prep.]).
- Sediment trap material at BATS-IOW contains notably amounts of barite. The present barite shows seasonal patterns similar to the flux of major biogenic phases as opal, POC and PON (see Chapter 5, *Brust et al.* [in prep.]).

The obtained results indicate the need for further research to support observations at both study sites and to clarify open questions. For example, in contrast to the BATS-IOW site barite at Kiel 276 was absent or present in negligible amounts. Comparisons between western and eastern NAST regions provided evidence for an enhanced export ratio at BATS compared to the eastern site close to the Canary Islands (ESTOC, *Helmke et al.* [2010]). A more effective export of biogenic matter and especially POC could result in the presence of microenvironments favorable for barite formation at BATS-IOW. The lack of barite at Kiel 276 might be due to lower export ratios at this site. A profound comparison of biogeochemical parameters between BATS and Kiel 276 within simultaneous time intervals will give more clarity. Such a comparison is also aspired regarding the lithogenic dust input at both sampling sites. BATS-IOW is situated farer to the west. Dust traveling over the Atlantic reaches the Caribbean area within a week [*Carlson and Prospero*, 1972], whereas grain size of dust particles decreases during long-range transport

[*Glaccum and Prospero*, 1980]. The grain size distributions of lithogenic particles at Kiel 276 are slightly coarser (median:  $1.8 \mu\text{m}$ ) than at BATS-IOW samples (median:  $1.4 \mu\text{m}$ , *Brust et al.*, unpublished). Grain-size decrease and mixing with anthropogenic dust components leads to chemical alteration of minerals and also influences the solubility of elements as iron associated with mineral dust [e.g. *Baker and Croot*, 2010]. This might in turn influence biogeochemistry at BATS as well. No effect of fertilization by North African mineral dust deposition in the Sargasso Sea has been observed yet [*Jickells et al.*, 1998] and the present study at BATS gives also no hint to a possible effect. Nevertheless, to comprise BATS-IOW and Kiel 276, analysis of samples from parallel sediment trap deployments will support the understanding of dust transport across the Atlantic Ocean and the temporal variability of dust delivery from North African sources. An investigation of concurrent sediment trap time series at BATS and Kiel 276 has not been done yet and might be subject to future research.

Although satellite aerosol optical depth data show that the presence of dust over the sampling sites and lithogenic fluxes are well correlated with AOD signals, the question for deposition rates, which mainly control the lithogenic particles in these open ocean regions, remain. At least, the lithogenic flux in open ocean regions can be used as an estimate for aerosol deposition to the oceans. Thereby factors controlling the particle transport in the ocean such as displacements by currents, which also affect trap efficiency, and biological processes (e.g. aggregation, disaggregation), must be taken into account. Future investigations at both study sites should involve modeled dust deposition rates and measured dust deposition rates from nearby islands. Involving atmospheric dust deposition rates will also help to decipher the contribution of possible lateral sources at both study sites.

Further on, the question for the relative homogeneity in lithogenic/clay mineral composition within sediment trap time series, though lithogenic flux follows rapidly aerosol deposition with a 1.5 months time lag, is still open. The present study has shown that the lithogenic particle flux is primarily determined by the aeolian input and secondly affected by biologically mediated downward transport of lithogenic particles. SEM-EDX samples of suspended particulate matter (SPM)



of the ocean surface and the ocean water column could help to understand the lithogenic particle transport and the distribution or variability of mineral species within the ocean. Such samples will reflect lithogenic mineral distributions within the ocean on time scales shorter than the temporal resolution of individual sediment trap samples, but could successfully supplement sediment trap data. For this reason the lithogenic composition of sediment trap samples should additionally be compared with simultaneous mineral composition of aerosol samples. For example, aerosol samples were taken with cascade impactors over the subtropical Northeast Atlantic during ship cruises in September 2010 and April/May 2011 and overlap sediment trap sampling at Kiel276. These data will provide a better insight into dust composition variability and sources between seasons.

Concerning the dust deposition – biological response effect, the effect seen in summer 2004 at Kiel276 is an exceptional observation, albeit this event is supported by a similar observation in August 2004 south of the Canary Islands. *Ramos et al.* [2005] reported a strong bloom of diazotrophic cyanobacteria triggered by iron input into ocean surface waters due to a dust event. However, the single enhanced biogenic particle flux, which followed dust deposition and possible fertilization at Kiel276 is not significant. Longer sediment trap time series, together with available synchronous satellite data are necessary to capture more summer dust events and prove the dust deposition – biological response effect at Kiel276.

Decadal variabilities of dust transport over the Atlantic ocean are characterized by the North Atlantic Oscillation (NAO; *Moulin et al.* [1997]). Sediment-trap time series investigated within this work are too short for reproducing those variations. In terms of NAO variability, climate change, anthropogenic induced desertification and possible increase of dust in Earth's atmosphere, long-term sediment trap studies and lithogenic flux measurements will show whether an increase of dust is measurable in the deep ocean and the interannual atmospheric dust variability is detectable in the deep ocean.

## References

- Acker, J. G., and G. Leptoukh (2007), Online Analysis Enhances Use of NASA Earth Science Data, *Eos*, *88*(2), 14–17.
- Andreae, M. O., C. D. Jones, and P. M. Cox (2005), Strong present-day aerosol cooling implies a hot future, *Nature*, *435*, 1187–1190.
- Arimoto, R., R. A. Duce, D. L. Savoie, and J. M. Prospero (1992), Trace elements in aerosol particles from Bermuda and Barbados: Concentrations, sources and relationships to aerosol sulfate, *Journal of Atmospheric Chemistry*, *14*(1), 439–457.
- Arimoto, R., R. A. Duce, B. J. Ray, W. G. Ellis, Jr., J. D. Cullen, and J. T. Merrill (1995), Trace elements in the atmosphere over the North Atlantic, *Journal of Marine Research*, *100*(D1), 1199–1213.
- Armstrong, R. A., C. Lee, J. I. Hedges, S. Honjo, and S. G. Wakeham (2002), A new, mechanistic model for organic carbon fluxes in the ocean based on the quantitative association of POC with ballast minerals, *Deep-Sea Research II*, *49*(1–3), 219–236.
- Armstrong, R. A., M. L. Peterson, C. Lee, and S. G. Wakeham (2009), Settling velocity spectra and the ballast ratio hypothesis, *Deep-Sea Research II*, *56*(18), 1470–1478.
- Asper, V. L., W. G. Deuser, G. A. Knauer, and S. E. Lohrenz (1992), Rapid coupling of sinking particle fluxes between surface and deep ocean waters, *Nature*, *357*, 670–672.
- Avila, A., I. Queralt, and J. Martin-Vide (1996), African dust over northeastern Spain: Mineralogy and source regions, in *The Impact of Desert Dust Across the Mediterranean*, edited by S. Guerzoni and R. Chester, pp. 201–205, Dordrecht: Kluwer Academic Publishers.
- Avila, A., I. Queralt-Mitjans, and M. Alarcón (1997), Mineralogical composition of African dust delivered by red rains over northeastern Spain, *Journal of Geophysical Research*, *102*(D18), 21,977–21,996.
- Baker, A. R., and P. L. Croot (2010), Atmospheric and marine controls on aerosol iron solubility in seawater, *Marine Chemistry*, *120*(1–4), 4–13.
- Baker, A. R., T. D. Jickells, K. F. Biswas, K. Weston, and M. French (2006), Nutrients in atmospheric aerosol particles along the Atlantic Meridional Transect, *Deep-Sea Research II*, *53*(14–16), 1706–1719.
- Bauerfeind, E., T. Leipe, and R. O. Ramseier (2005), Sedimentation at the permanently ice covered Greenland continental shelf (75°N/13°W). Significance of biogenic and lithogenic particles in particulate matter flux, *Journal of Marine Systems*, *56*, 151–166.
- Bergametti, G., L. Gomes, G. Coudé-Gaussen, P. Rognon, and M. N. L. Coustumer (1989a), African dust observed over Canary Islands: Source-regions identification and transport pattern for some summer situations, *Journal of Geophysical Research*, *94*(1), 4855–14,864.

- Bergametti, G., L. Gomes, and E. Remoudaki (1989b), Present transport and deposition patterns of African dust to the North Western Mediterranean, in *Palaeoclimatology and palaeometeorology: modern and past patterns of global atmospheric transport*, edited by M. Leinen and M. Sarnthein, pp. 227–252, Dordrecht: Kluwer Academic.
- Bettis III, E. A., D. R. Muhs, H. M. Roberts, and A. G. Wintle (2003), Last Glacial loess in the conterminous USA, *Quaternary Science Reviews*, 22(18-19), 1907–1946.
- Bishop, J. K. B. (1988), The barite-opal-organic carbon association in oceanic particulate matter, *Nature*, 332, 341–343.
- Bishop, J. K. B., R. E. Davis, and J. T. Sherman (2002), Robotic observations of dust storm enhancements of carbon biomass in the North Pacific, *Science*, 298, 817–820.
- Blain, S., F. Carlotti, U. Christaki, A. Corbiere, I. Durand, F. Ebersbach, J. L. Fuda, N. Garcia, L. Gerringa, B. Griffiths, C. Guigue, B. Queguiner, C. Guillerm, S. Jacquet, C. Jeandel, P. Laan, D. Lefevre, C. L. Monaco, A. Malits, J. Mosseri, I. Obernosterer, Y. H. Park, L. K. Armand, M. Picheral, P. Pondaven, T. A. Remenyi, V. Sandroni, G. Sarthou, N. Savoye, L. Scouarnec, M. Souhaut, D. Thuiller, K. Timmermans, S. Belviso, T. W. Trull, J. Uitz, P. van Beek, M. Veldhuis, D. Vincent, E. Viollier, L. Vong, T. Wagener, B. Bombled, L. Bopp, A. R. Bowie, C. Brunet, and C. Brussaard (2007), Effect of natural iron fertilization on carbon sequestration in the Southern Ocean, *Nature*, 446, 1070–1074.
- Blanco, A., F. De Tomasi, E. Filippo, D. Manno, M. R. Perrone, A. Serra, A. M. Tafuro, and A. Tepore (2003), Characterization of African dust over southern Italy, *Atmospheric Chemistry and Physics*, 3, 2147–2159.
- Bonelli, P., G. M. Braga Marcazzan, and E. Cereda (1996), Elemental composition and air trajectories of African dust transported in northern Italy, in *The Impact of Desert Dust Across the Mediterranean*, edited by S. Guerzoni and R. Chester, pp. 276–238, Kluwer Academic Publishers.
- Bory, A., F. Dulac, C. Moulin, I. Chiapello, P. P. Newton, W. Guelle, C. E. Lambert, and G. Bergametti (2002), Atmospheric and oceanic dust fluxes in the northeastern tropical Atlantic Ocean: how close a coupling?, *Annales Geophysicae*, 20, 2067–2076.
- Bory, A. J.-M., and P. P. Newton (2000), Transport of airborne lithogenic material down through the water column in two contrasting regions of eastern subtropical North Atlantic Ocean, *Global Biogeochemical Cycles*, 14(1), 297–315.
- Bout-Roumazeilles, V., N. Combourieu Nebout, O. Peyron, E. Cortijo, A. Landais, and V. Masson-Delmotte (2007), Connection between South Mediterranean climate and North African atmospheric circulation during the last 50,000 yr BP North Atlantic cold events, *Quaternary Science Reviews*, 26(25-28), 3197–3215.
- Bristow, C. S., K. A. Hudson-Edwards, and A. Chappell (2010), Fertilizing the Amazon and equatorial Atlantic with West African dust, *Geophysical Research Letters*, 37(L14807), doi:10.1029/2010GL043486.
- Brust, J., and J. J. Waniek (2010), Atmospheric dust contribution to deep-sea particle fluxes in the subtropical Northeast Atlantic, *Deep-Sea Research I*, 57(8), 988–998.

- Brust, J., D. E. Schulz-Bull, T. Leipe, V. Chavagnac, and J. J. Waniek (2011), Descending particles: from the atmosphere to the deep ocean - A time series study in the subtropical NE Atlantic, *Geophysical Research Letters*, *38*(L06603), doi:10.1029/2010GL045399.
- Buat-Ménard, P., J. Davies, E. Remoudaki, J. C. Miquel, G. Bergametti, C. E. Lambert, U. Ezat, C. Q. J. L. Rosa, and S. W. Fowler (1989), Non-steady-state biological removal of atmospheric particles from Mediterranean surface waters, *Nature*, *340*, 131–134.
- Bücher, A., J. Dubief, and C. Lucas (1983), Retombées estivales de poussières sahariennes sur l'Europe (Summer falls of Sahara dust in Europe), *Revue de Géologie Dynamique et de Géographie Physique*, *24*, 153–165.
- Buck, C. S., W. M. Landing, J. A. Resing, and C. I. Measures (2010), The solubility and deposition of aerosol Fe and other trace elements in the North Atlantic Ocean: Observations from the A16N CLIVAR/CO<sub>2</sub> repeat hydrography section, *Marine Chemistry*, *120*(1–4), 57–70.
- Buesseler, K. O., A. N. Antia, M. Chen, S. W. Fowler, W. D. Gardner, O. Gustafsson, K. Harada, A. F. Michaels, M. R. van der Loeff, M. Sarin, D. K. Steinberg, and T. K. Trull (2007), An assessment of the use of sediment traps for estimating upper ocean particle fluxes, *Journal of Marine Research*, *65*, 345–416.
- Cachorro, V. E., R. Vergaz, A. M. de Frutos, J. M. Vilaplana, D. H. N. Laulainen, and C. Toledano (2006), Study of desert dust events over the southwestern Iberian Peninsula in year 2000: two case studies, *Annales Geophysicae*, *24*, 1493–1510.
- Caquineau, S., A. Gaudichet, L. Gomes, M.-C. Magonthier, and B. Chatenet (1998), Saharan dust: clay ratio as a relevant tracer to assess the origin of soil-derived aerosols, *Geophysical Research Letters*, *25*, 983–986.
- Caquineau, S., A. Gaudichet, L. Gomes, and M. Legrand (2002), Mineralogy of Saharan dust transported over northwestern tropical Atlantic Ocean in relation to source regions, *Journal of Geophysical Research*, *107*(D15), doi:10.1029/2000JD000247.
- Carlson, T., and J. Prospero (1972), The Large-Scale Movement of Daharan Air Outbreaks over the Northern Equatorial Atlantic, *Journal of Applied Meteorology*, *11*, 283–297.
- Castillo, S., T. Moreno, X. Querol, A. Alastuey, E. Cuevas, L. Herrmann, M. Mounkaila, and W. Gibbons (2008), Trace element variation in size-fractionated African desert dusts, *Journal of Arid Environments*, *72*(6), 1034–1045.
- Chamley, H. (1989), *Clay Sedimentology*, Springer-Verlag: 623p, Berlin, New York.
- Chavagnac, V., J. J. Waniek, D. Atkin, J. A. Milton, T. Leipe, D. R. H. Green, R. Bahlo, T. E. F. Hayes, and D. E. Schulz-Bull (2007), Anti-Atlas Moroccan Chain as the source of lithogenic-derived micronutrient fluxes to the deep Northeast Atlantic Ocean, *Geophysical Research Letters*, *34*(L21604), doi:10.1029/2007GL030985.
- Chavagnac, V., M. Lair, J. A. Milton, A. Lloyd, I. W. Croudace, M. R. Palmer, D. R. H. Green, and G. A. Cherkashev (2008), Tracing dust input to the Mid-Atlantic Ridge between 14°45'N and 36°14'N: geochemical and Sr isotope study, *Marine Geology*, *247*(3–4), 208–225.

- Chavez, F. P., and J. R. Toggweiler (1995), Physical estimates of global new production: the upwelling contribution, in *Upwelling in the Ocean: Modern Processes and Ancient Records*, edited by C. Summerhayes, K. C. Emeis, M. V. Angel, R. L. Smith, and B. Zeitzschel, pp. 313–320, John Wiley, New York.
- Chavez, F. P., M. Messié, and J. T. Pennington (2011), Marine Primary Production in Relation to Climate Variability and Change, *Annual Review of Marine Science*, *3*, 227–260.
- Chester, R., and L. R. Johnson (1971a), Atmospheric Dusts collected off the West African Coast, *Nature*, *229*, 105–107.
- Chester, R., and L. R. Johnson (1971b), Atmospheric dust collected off the Atlantic coast of North Africa and the Iberian peninsula, *Marine Geology*, *11*, 251–260.
- Chester, R., H. Elderfield, J. J. Griffin, L. R. Johnson, and R. C. Padgham (1972), Eolian dust along the eastern margins of the Atlantic ocean, *Marine Geology*, *13*, 91–105.
- Chiapello, I., G. Bergametti, B. Chatenet, P. Bousquet, F. Dulac, and E. S. Soares (1997), Origins of African dust transported over the North-Eastern Tropical Atlantic, *Journal of Geophysical Research*, *102*(D12), 13,701–13,709.
- Chiapello, I., J. M. Prospero, J. R. Herman, and N. Hsu (1999), Detection of mineral dust over the North Atlantic Ocean and Africa with the Nimbus 7 TOMS, *Journal of Geophysical Research*, *104*, 9277–9291.
- Chin, M., P. Ginoux, S. Kinne, O. Torres, B. N. Holben, B. N. Duncan, R. V. Martin, J. A. Logan, A. Higurashi, and T. Nakajima (2002), Tropospheric Aerosol Optical Thickness from the GOCART Model and Comparisons with Satellite and Sun Photometer Measurements, *Journal of Atmospheric Sciences*, *59*, 461–483.
- Conte, M. (2005), Will changing climate change the deep?, *Bermuda Biological Station Research Currents*, *Fall 2005*, pp. 6–7.
- Conte, M., N. Ralph, and E. Ross (2001), Seasonal and interannual variability in deep ocean particle fluxes at the Oceanic Flux Program (OFP)/Bermuda Atlantic Time Series (BATS) site in the western Sargasso Sea near Bermuda, *Deep-Sea Research II*, *48*, 1471–1505.
- Conte, M. H., T. D. Dickey, J. C. Weber, R. J. Johnson, and A. H. Knap (2003), Transient physical forcing of pulsed export of bioreactive material to the deep Sargasso Sea, *Deep-Sea Research I*, *50*(10–11), 1157–1187.
- Coudé-Gaussen, G., P. Rognon, G. Bergametti, L. Gomes, B. Strauss, J. M. Gros, and M. N. L. Coustumer (1987), Saharan dust on Fuerteventura Island (Canaries): Chemical and mineralogical characteristics, air mass trajectories, and probable sources, *Journal of Geophysical Research*, *92*(D8), 9753–9771.
- Croot, P. L., P. P. Streu, and A. R. Baker (2004), Short residence time for iron in surface seawater impacted by atmospheric dry deposition from Saharan dust events, *Geophysical Research Letters*, *31*(L23S08), doi:10.1029/2004GL020,153.
- D’Almeida, G. A. (1986), A model for Saharan dust transport, *Journal of Climate and Applied Meteorology*, *25*, 905–916.

- Davenport, R., S. Neuer, P. Helmke, J. Perez-Marrero, and O. Llinas (2002), Primary productivity in the northern Canary Islands region as inferred from SeaWiFS imagery, *Deep-Sea Research II*, 49(17), 3481–3496.
- de Baar, H. J. W., P. W. Boyd, K. H. Coale, M. R. Landry, A. Tsuda, P. Assmy, D. C. Bakker, Y. Bozec, R. T. Barber, M. A. Brzezinski, K. O. Buesseler, M. Boye, P. L. Croot, F. Gervais, M. Y. Gorbunov, P. J. Harrison, W. T. Hiscock, P. Laan, C. Lancelot, C. S. Law, M. Levasseur, A. Marchetti, F. J. Millero, J. Nishioka, Y. Nojiri, T. van Oijen, U. Riebesell, M. J. Rijkenberg, H. Saito, S. Takeda, K. R. Timmermans, M. J. Veldhuis, A. M. Waite, and C.-S. Wong (2005), Synthesis of iron fertilization experiments: From the Iron Age in the Age of Enlightenment, *Journal of Geophysical Research*, 110(C09S16), doi:10.1029/2004JC002601.
- De La Rocha, C. L., and U. Passow (2007), Factors influencing the sinking of POC and the efficiency of the biological carbon pump, *Deep-Sea Research II*, 54(5–7), 639–658.
- Dehairs, F., R. Chesselet, and J. Jedwab (1980), Discrete suspended particles of barite and the barium cycle in the open ocean, *Earth and Planetary Science Letters*, 49(2), 528–550.
- Desboeufs, K., E. Journet, J.-L. Rajot, S. Chevaillier, S. Triquet, P. Formenti, and A. Zakou (2010), Chemistry of rain events in West Africa: evidence of dust and biogenic influence in convective systems, *Atmospheric Chemistry and Physics*, 10, 9283–9293.
- Deuser, W. (1986), Seasonal and interannual variations in deep-water particle fluxes in the Sargasso Sea and their relation to surface hydrography, *Deep-Sea Research I*, 33(2), 225–246.
- Deuser, W. G., and E. H. Ross (1980), Seasonal change in the flux of organic carbon to the deep Sargasso Sea, *Nature*, 283, 364–365.
- Deuser, W. G., E. H. Ross, and R. F. Anderson (1981), Seasonality in the supply of sediment to the deep Sargasso Sea and implications for the rapid transfer of matter to the deep ocean, *Deep-Sea Research I*, 28(5), 495–505.
- Deuser, W. G., P. G. Brewer, T. D. Jickells, and R. F. Commeau (1983), Biological control of the removal of abiogenic particles from the surface ocean, *Science*, 219, 388–391.
- Deuser, W. G., F. E. Muller-Karger, R. H. Evans, O. B. Brown, W. E. Esaias, and G. C. Feldman (1990), Surface-ocean color and deep-ocean carbon flux: how close a connection?, *Deep-Sea Research I*, 37(8), 1331–1343.
- Duce, R. A., P. S. Liss, J. T. Merrill, E. L. Atlas, P. Buat-Menard, B. B. Hicks, J. M. Miller, J. M. Prospero, T. M. C. R. Arimoto, W. Ellis, J. N. Galloway, L. Hansen, T. D. Jickells, A. H. Knap, K. H. Reinhardt, B. Schneider, A. Soudine, J. J. Tokos, S. Tsunogai, R. Wollast, and M. Zhou (1991), The Atmospheric Input of Trace Species to the World Ocean, *Global Biogeochemical Cycles*, 5(3), 193–259.
- Dymond, J., and R. Collier (1996), Particulate barium fluxes and their relationships to biological productivity, *Deep-Sea Research II*, 43(4-6), 1283–1308.
- Dymond, J., R. Collier, J. McManus, S. Honjo, , and S. Manganini (1997), Can the aluminum and titanium contents of ocean sediments be used to determine the paleoproductivity of the oceans?, *Paleoceanography*, 12(4), 586–593.



- Dymond, J. E. S., and M. Lyle (1992), Barium in deep-sea sediment: A geochemical proxy for paleoproductivity, *Paleoceanography*, 7(2), 163–181.
- Erhardt, M., and W. Koeve (1999), Determination of particulate organic carbon and nitrogen, in *Methods of Seawater Analysis*, edited by e. a. Grasshoff, pp. 417–444, Wiley-VCH, New York.
- Falkowski, P. G., and M. J. Oliver (2007), Mix and match: how climate selects phytoplankton, *Nature Reviews Microbiology*, 5(10), 813–819.
- Fischer, G., G. Karakas, M. Blaas, V. Ratmeyer, N. Nowald, R. Schlitzer, P. Helmke, R. Davenport, B. Donner, S. Neuer, and G. Wefer (2007), Mineral ballast and particle settling rates in the coastal upwelling system off NW Africa and the South Atlantic, *International Journal of Earth Science*, pp. doi:10.1007/s00531-007-0234-7.
- Formenti, P., W. Elbert, W. Maenhaut, J. Haywood, and M. O. Andreae (2003), Chemical composition of mineral dust aerosol during the Saharan Dust Experiment (SHADE) airborne campaign in the Cape Verde region, September 2000, *Journal of Geophysical Research*, 108(D18, 8576), doi:10.1029/2002JD002648.
- Formenti, P., J. L. Rajot, K. Desboeufs, S. Caquineau, S. Chevaillier, S. Nava, A. Gaudichet, E. Journet, S. Triquet, S. Alfaro, M. Chiari, J. Haywood, H. Coe, and E. Highwood (2008), Regional variability of the composition of mineral dust from western africa: Results from the amma sop0/dabex and dodo field campaigns, *Journal of Geophysical Research*, 113(D00C13), doi:10.1029/2008JD009903.
- Formenti, P., L. Schuetz, Y. Balkanski, K. Desboeufs, M. Ebert, K. Kandler, A. Petzold, D. Scheuven, S. Weinbruch, and D. Zhang (2010), Recent progress in understanding physical and chemical properties of mineral dust, *Atmospheric Chemistry and Physics Discussions*, 10, 31,187–31,251, doi:10.5194/acpd-10-31,187-2010.
- François, R., S. Honjo, R. Krishfield, and S. Manganini (2002), Factors controlling the flux of organic carbon to the bathypelagic zone of the ocean, *Global Biogeochemical Cycles*, 16(GB1087), doi:10.1029/2001GB001722.
- Ganor, E. (1991), The composition of clay minerals transported to Israel as indicators of Saharan dust emission, *Atmospheric Environment A*, 25(12), 2657–2664.
- Ganor, E., and H. A. Foner (1996), The mineralogical and chemical properties and the behavior of Aeolian Saharan dust over Israel, in *Impact of Desert Dust Across the Mediterranean*, edited by S. Guerzoni and R. Chester, pp. 163–172, Kluwer Academic publisher, The Netherlands.
- Ganor, E., H. A. Foner, S. Brenner, E. Neeman, and N. Lavi (1991), The chemical composition of aerosols settling in israel following dust storms, *Atmospheric Environment. Part A. General Topics*, 25(12), 2665–2670.
- Gatz, D., and J. Prospero (1996), A large silicon-aluminum aerosol plume in central Illinois: North African desert dust?, *Atmospheric Environment*, 30(22), 3789–3799.
- Gillette, D., and K. Hanson (1989), Spatial and Temporal Variability of Dust Production Caused by Wind Erosion in the United States, *Journal of Geophysical Research*, 94(D2), 2197–2206.

- Ginoux, P., M. Chin, I. Tegen, J. M. Prospero, B. Holben, O. Dubovik, and S.-J. Lin (2001), Sources and distributions of dust aerosols simulated with the GOCART model, *Journal of Geophysical Research*, *106*(D17), 20,255–20,274.
- Ginoux, P., J. M. Prospero, O. Torres, and M. Chin (2004), Long-term simulation of global dust distribution with the gocart model: correlation with the north atlantic oscillation, *Environmental Modeling and Software*, *19*, 113–128.
- Glaccum, R. A., and J. M. Prospero (1980), Saharan aerosols over the tropical North Atlantic - Mineralogy, *Marine Geology*, *37*, 295–321.
- Goldberg, E. D., and G. O. S. Arrhenius (1958), Chemistry of pacific pelagic sediments, *Geochimica et Cosmochimica Acta*, *13*, 153–212.
- Goudie, A. S., and N. J. Middleton (2001), Saharan dust storms: nature and consequences, *Earth-Science Reviews*, *56*(1–4), 179–204.
- Gould, W. J. (1985), Physical Oceanography of the Azores Front, *Progress in Oceanography*, *14*, 167–190.
- Griffin, J. J., H. Windom, and E. D. Goldberg (1968), The distribution of clay minerals in the World Ocean, *Deep-Sea Research*, *15*, 433–459.
- Gruber, N., and J. L. Sarmiento (1997), Global patterns of marine nitrogen fixation and denitrification, *Global Biogeochemical Cycles*, *11*(2), 235–266.
- Guerzoni, S., E. Molinaroli, and R. Chester (1997), Saharan dust inputs to the western Mediterranean Sea: depositional patterns, geochemistry and sedimentological implications, *Deep-Sea Research II*, *44*(3–4), 631–654.
- Guieu, C., and A. Thomas (1996), Saharan aerosols: from the soil to the ocean, in *Impact of Desert Dust Across the Mediterranean*, edited by S. Guerzoni and R. Chester, pp. 207–216, Kluwer Academic publisher, The Netherlands.
- Gust, G., W. Bowles, S. Giordano, and M. Hüttel (1996), Particle accumulation in a cylindrical sediment trap under laminar and turbulent steady flow: An experimental approach, *Aquatic Sciences - Research Across Boundaries*, *58*(4), 297–326.
- Haidar, A. T., H. R. Thierstein, and W. G. Deuser (2000), Calcareous phytoplankton standing stocks, fluxes and accumulation in Holocene sediments off Bermuda (N. Atlantic), *Deep-Sea Research II*, *47*, 1907–1938.
- Harrison, S. P., K. E. Kohfeld, C. Roelandt, and T. Claquin (2001), The role of dust in climate changes today, at the last glacial maximum and in the future, *Earth-Science Reviews*, *54*(1–3), 43–80.
- Helmke, P., S. Neuer, M. W. Lomas, M. Conte, and T. Freudenthal (2010), Cross-basin differences in particulate organic carbon export and flux attenuation in the subtropical north atlantic gyre, *Deep-Sea Research I*, *57*(2), 213–227.
- Helsel, D. R., and R. M. Hirsch (2002), *Statistical methods in water resources*, U.S. Geological Survey. TWRI Book 4, (Chapter A3), 524 pp.



- Herman, J. R., P. K. Bhartia, O. Torres, C. S. C. Hs and, and E. Celarier (1997), Global distribution of UV-absorbing aerosols from Nimbus 7/TOMS data, *Journal of Geophysical Research*, *102*(D14), 16,911–16,922.
- Herwitz, S. R., D. R. Muhs, J. M. Prospero, S. Mahan, and B. Vaughn (1996), Origin of Bermuda’s clay-rich Quaternary paleosols and their paleoclimatic significance, *Journal of Geophysical Research*, *101*(D18), 23,389–23,400.
- Honjo, S., and K. W. Doherty (1988), Large aperture time-series sediment traps; design objectives, construction and application, *Deep-Sea Research I*, *35*(1), 133–149.
- Honjo, S., S. J. Manganini, and L. J. Poppe (1982), Sedimentation of lithogenic particles in the deep ocean, *Marine Geology*, *50*, 199–220.
- Honjo, S., J. Dymond, R. Collier, and S. J. Manganini (1995), Export production of particles to the interior of the equatorial Pacific Ocean during the 1992 Eqpac experiment, *Deep-Sea Research II*, *42*(2–3), 831–870.
- Honjo, S., R. Francois, S. Manganini, J. Dymond, and R. Collier (2000), Particle fluxes to the interior of the Southern Ocean in the Western Pacific sector along 170°W, *Deep-Sea Research II*, *47*(15–16), 3521–3548.
- Huang, S., and M. H. Conte (2009), Source/process apportionment of major and trace elements in sinking particles in the Sargasso sea, *Geochimica et Cosmochimica Acta*, *73*(1), 65–90.
- IPCC (2007), *Climate Change 2007: The Physical Science Basis-Contribution of Working Group I to the Fourth Assessment Report of the Intergovernmental Panel on Climate Change*, edited by S. Solomon et al., Cambridge Univ. Press, Cambridge, U. K.
- Ittekkot, V. (1993), The abiotically driven biological pump in the ocean and short-term fluctuations in atmospheric CO<sub>2</sub> contents, *Global and Planetary Change*, *8*(1–2), 17–25.
- Iversen, M. H., and H. Ploug (2010), Ballast minerals and the sinking carbon flux in the ocean: carbon-specific respiration rates and sinking velocity of marine snow aggregates, *Biogeosciences*, *7*, 2613–2624.
- Iversen, M. H., N. Nowald, H. Ploug, G. A. Jackson, and A. Fischer (2010), High resolution profiles of vertical particulate organic matter export off Cape Blanc, Mauritania: Degradation processes and ballasting effects, *Deep-Sea Research I*, *57*(6), 771–784.
- Jaenicke, R. (1980), Atmospheric aerosols and global climate, *Journal of Aerosol Science*, *11*, 577–588.
- Jickells, T., A. Knap, T. Church, J. Galloway, and J. Miller (1982), Acid rain on Bermuda, *Nature*, *297*, 55–57.
- Jickells, T. D., S. Dorling, W. G. Deuser, T. M. Church, R. Arimoto, and J. Prospero (1998), Air-Borne dust fluxes to a deep water sediment trap in the Sargasso Sea, *Global Biogeochemical Cycles*, *12*(2), 311–320.

- Jickells, T. D., Z. S. An, K. K. Andersen, A. R. Baker, G. Bergametti, N. Brooks, J. J. Cao, P. W. Boyd, R. A. Duce, K. A. Hunter, H. Kawahata, N. Kubilay, J. laRoche, P. S. Liss, N. Mahowald, J. M. Prospero, A. J. Ridgwell, I. Tegen, and R. Torres (2005), Global Iron Connections Between Desert Dust, Ocean Biogeochemistry, and Climate, *Science*, 308, 67–71.
- Johnson, L. R. (1979), Mineralogical dispersal patterns of North Atlantic deep-sea sediments with particular reference to eolian dust, *Marine Geology*, 29, 335–345.
- Jones, P. D., T. M. L. Wigley, and P. B. Wright (1986), Global temperature variations between 1861 and 1984, *Nature*, 322, 430–434.
- Jones, P. D., M. New, D. E. Parker, S. Martin, and I. G. Rigor (1999), Surface air temperature and its changes over the past 150 years, *Reviews of Geophysics*, 37(2), 173–199.
- Journet, E., K. Desboeufs, S. Caquineau, and J.-L. Colin (2008), Mineralogy as a critical factor of dust iron solubility, *Geophysical Research Letters*, 35(L07805), doi:10.1029/2007GL031,589.
- Karl, D. M., A. Michaels, B. Bergman, D. Capone, E. Carpenter, R. Letelier, F. Lipschultz, H. Paerl, D. Sigman, and L. Stal (2002), Dinitrogen fixation in the world’s oceans, *Biogeochemistry*, 57/58, 47–98.
- Käse, R., and G. Siedler (1982), Meandering of the subtropical front south-east of the Azores, *Nature*, 300, 245–246.
- Kaufman, Y., I. Koren, L. A. Remer, D. Tanré, P. Ginoux, and S. Fan (2005), Dust transport and deposition observed from the Terra-Moderate Resolution Imaging Spectroradiometer (MODIS) spacecraft over the Atlantic Ocean, *Journal of Geophysical Research*, 110(D10S12), doi:10.1029/2003JD004,436.
- Kaufman, Y. J., D. Tanré, and O. Boucher (2002), A satellite view of aerosols in the climate system, *Nature*, 419, 215–223.
- Keeling, C. D., R. B. Bacastow, A. E. Bainbridge, C. A. Ekdahl, P. R. Guenther, L. S. Waterman, and J. F. S. Chin (1976), Atmospheric carbon dioxide variations at Mauna Loa Observatory, Hawaii, *Tellus*, 28(6), 538–551.
- Klaas, C., and D. E. Archer (2002), Association of sinking organic matter with various types of mineral ballast in the deep sea: Implications for the rain ratio, *Global Biogeochemical Cycles*, 16(4), 1116, doi:1029/2001GB001,765.
- Klein, B., and G. Siedler (1989), On the origin of the Azores Current, *Journal of Geophysical Research*, 94(C5), 6159–6198.
- Kremling, K., U. Lentz, B. Zeitzschel, D. E. Schulz-Bull, and J. C. Duinker (1996), New type of time-series sediment trap for the reliable collection of inorganic and organic trace chemical substances, *Review of Scientific Instruments*, 67(12), 4360–4363.
- Kuss, J., and K. Kremling (1999a), Particulate trace element fluxes in the deep northeast Atlantic Ocean, *Deep-Sea Research I*, 46(1), 149–169.

- Kuss, J., and K. Kremling (1999b), Spatial variability of particle associated trace elements in near-surface waters of the North Atlantic (30°N/60°W to 60°N/2°W), derived by large volume sampling, *Marine Chemistry*, 68(1–2), 71–86.
- Kuss, J., J. J. Waniek, K. Kremling, and D. E. Schulz-Bull (2010), Seasonality of particle-associated trace element fluxes in the deep northeast Atlantic Ocean, *Deep-Sea Research I*, 57(6), 785–796, doi:10.1016/j.dsr.2010.04.002.
- Lamborg, C. H., K. O. Buesseler, J. Valdes, C. H. Bertrand, R. Bidigare, S. Manganini, S. Pike, D. Steinberg, T. Trull, and S. Wilson (2008), The flux of bio- and lithogenic material associated with sinking particles in the mesopelagic "twilight zone" of the northwest and North Central Pacific Ocean, *Deep-Sea Research II*, 55(14–15), 1540–1563.
- Lange, H. (1982), Distribution of Chlorite and kaolinite in eastern Atlantic sediments off North Africa, *Sedimentology*, 29, 427–431.
- Leipe, T., B. Knoppers, E. Marone, and R. Camargo (1999), Suspended matter transport in coral reef waters of the Abrolhos Bank, Brazil, *Geo-Marine Letters*, 19, 186–195.
- Lewis, C. V. W., C. S. Davis, and G. Gawarkiewicz (1994), Wind forced biological-physical interactions on an isolated offshore bank, *Deep-Sea Research II*, 41(1), 51–73.
- Longhurst, A. (1998), *Ecological Geography of the Sea*, Academic Press, New York.
- Lundgreen, U., J. J. Waniek, D. E. Schulz-Bull, and J. Duinker (1997), Azide as a tool to evaluate sediment trap behaviour, *German Journal of Hydrography*, 49(1), 57–69.
- Mahaffey, C., R. G. Williams, G. A. Wolff, N. Mahowald, W. Anderson, and M. Woodward (2003), Biogeochemical signatures of nitrogen fixation in the eastern north atlantic, *Geophysical Research Letters*, 30(6), 1300, doi:10.1029/2002GL016,542.
- Martin, J. H. (1990), Glacial-interglacial CO<sub>2</sub> Change: The Iron Hypothesis, *Paleoceanography*, 5(1), 1–13.
- Martin, R. V., D. J. Jacob, R. M. Yantosca, M. Chin, and P. Ginoux (2003), Global and regional decreases in tropospheric oxidants from photochemical effects of aerosols, *Journal of Geophysical Research*, 108(4097), doi:10.1029/2002JD002,622.
- McClain, C. R., and J. Firestone (1993), An Investigation of Ekman Upwelling in the North Atlantic, *Journal of Geophysical Research*, 98(C7), 12,327–12,339.
- McGillicuddy, D. J., A. R. Robinson, D. A. Siegel, H. W. Jannasch, R. Johnson, T. D. Dickey, J. McNeil, A. F. Michaels, and A. H. Knap (1998), Influence of mesoscale eddies on new production in the Sargasso Sea, *Nature*, 394(6690), 263–266.
- Michaels, A. F., and A. H. Knap (1996), Overview of the U.S. JGOFS Bermuda Atlantic Time-series Study and the Hydrostation S program, *Deep-Sea Research II*, 43(2–3), 157–198.
- Migon, C., V. Sandroni, J.-C. Marty, B. Gasser, and J.-C. Miquel (2002), Transfer of atmospheric matter through the euphotic layer in the northwestern Mediterranean: seasonal pattern and driving forces, *Deep-Sea Research II*, 49(11), 2125–2141.

- Mills, M. M., C. Ridame, M. Davey, J. L. Roche, and R. J. Geider (2004), Iron and phosphorus co-limit nitrogen fixation in the eastern tropical North Atlantic, *Nature*, *429*, 292–294.
- Molinaroli, E. (1996), Mineralogical characterization of Saharan dust with a view to its final destination in Mediterranean sediments, in *Impact of Desert Dust Across the Mediterranean*, edited by S. Guerzoni and R. Chester, pp. 153–162, Kluwer Academic publisher, The Netherlands.
- Moore, D., and J. R. Reynolds (1997), *X-Ray Diffraction and the Identification and Analysis of Clay Minerals*, 2nd edition ed., Oxford University Press, Oxford, New York.
- Moreno, T., X. Querol, S. Castillo, A. Alastuey, E. Cuevas, L. Herrmann, M. Mounkaila, J. Elvira, and W. Gibbons (2006), Geochemical variations in aeolian mineral particles from the Sahara-Sahel Dust Corridor, *Chemosphere*, *65*(2), 261–270.
- Moulin, C., C. E. Lambert, F. Dulac, and U. Dayan (1997), Control of atmospheric export of dust from North Africa by the North Atlantic Oscillation, *Nature*, *387*(6634), 691–694.
- Muhs, D., E. Bettis III, J. Been, and J. McGeehin (2001), Impact of climate and parent material on chemical weathering in loess-derived soils of the Mississippi River Valley, *Soil Science Society of America Journal*, *65*, 1761–1777.
- Muhs, D. R., and E. A. Bettis III (2000), Geochemical variations in Peoria Loess of western Iowa indicate Last Glacial paleowinds of midcontinental North America, *Quaternary Research*, *53*, 49–61.
- Muhs, D. R., C. A. Bush, and K. C. Stewart (1990), Geochemical evidence of Saharan dust parent material for soils developed on Quaternary limestones of Caribbean and Western Atlantic Islands, *Quaternary Research*, *33*, 157–177.
- Neftel, A., E. Moor, H. Oeschger, and B. Stauffer (1985), Evidence from polar ice cores for the increase in atmospheric CO<sub>2</sub> in the past two centuries, *Nature*, *315*(6014), 45–47.
- Neuer, S., V. Ratmeyer, R. Davenport, G. Fischer, and G. Wefer (1997), Deep water particle flux in the Canary Island region: seasonal trends in relation to long-term satellite derived pigment data and lateral sources, *Deep-Sea Research I*, *44*(8), 1451–1466.
- Neuer, S., T. Freudenthal, R. Davenport, O. Llinás, and M.-J. Rueda (2002), Seasonality of surface water properties and particle flux along a productivity gradient off NW Africa, *Deep-Sea Research II*, *49*(17), 3561–3576.
- Neuer, S., M. E. Torres-Padrón, M. D. Gelado-Caballero, M. J. Rueda, J. Hernández-Brito, R. Davenport, and G. Wefer (2004), Dust deposition pulses to the eastern subtropical North Atlantic gyre: Does ocean’s biogeochemistry respond?, *Global Biogeochemical Cycles*, *18*(GB4020), doi:10.1029/2004GB002,228.
- Ohde, T., and H. Siegel (2010), Biological response to coastal upwelling and dust deposition in the area off Northwest Africa, *Continental Shelf Research*, *30*(9), 1108–1119.
- Okin, G., N. Mahowald, O. Chadwick, and P. Artaxo (2004), Impact of desert dust on the biogeochemistry of phosphorus in terrestrial ecosystems, *Global Biogeochemical Cycles*, *18*(GB2005), doi:10.1029/2003GB002,145.

- Okin, G. S., and H. J. E. Gillette, D. A. and (2006), Multi-scale controls on and consequences of aeolian processes in landscape change in arid and semi-arid environments, *Journal of Arid Environments*, 65, 253–275.
- Oschlies, A. (2008), Eddies and upper-ocean nutrient supply, in *Ocean Modeling in an Eddying Regime*, AGU, *Geophysical Monograph Series*, vol. 177, edited by M. Hecht and H. Hasumi, pp. 115–130, Washington DC, USA.
- Paquet, H., G. Coudé-Gaussen, and P. Rognon (1984), Etude minéralogique de poussières sahariennes le long d’un itinéraire entre 19° et 35° de latitude nord, *Revue Géologie Dynamique et Géographie Physique*, 25, 257–265.
- Passow, U. (2004), Switching perspectives: Do mineral fluxes determine particulate organic carbon fluxes or vice versa?, *Geochemistry, Geophysics, Geosystems*, 5(4), Q04,002, doi:10.1029/2003GC000,670.
- Passow, U., and C. L. De La Rocha (2006), Accumulation of mineral ballast on organic aggregates, *Global Biogeochemical Cycles*, 20(GB1013), doi:10.1029/2005GB002,579.
- Paytan, A., and E. M. Griffith (2007), Marine barite: Recorder of variations in ocean export productivity, *Deep-Sea Research II*, 54, 687–705.
- Perry, K. D., T. A. Cahill, R. A. Eldred, D. D. Dutcher, and T. E. Gill (1997), Long-range transport of North African dust to the eastern United States, *Journal of Geophysical Research*, 102(D10), 11,225–11,238.
- Péwé, T. L. (1981), Desert Dust: An Overview, in *Desert Dust: Origin, Characteristics, and Effect on Man*, vol. 186, edited by T. L. Péwé, pp. 1–10, Boulder, Geological Society of America Special Paper.
- Phillips, H., and T. Joyce (2007), Bermuda’s Tale of Two Time Series: Hydrostation S and BATS, *Journal of Physical Oceanography*, 37, 554–571.
- Ploug, H., M. H. Iversen, and G. Fischer (2008), Ballast, sinking velocity, and apparent diffusivity within marine snow and zooplankton fecal pellets: Implications for substrate turnover by attached bacteria, *Limnology and Oceanography*, 53(5), 1878–1886.
- Prospero, J., and T. N. Carlson (1972), Vertical and areal distribution of Saharan dust over the western Equatorial North Atlantic Ocean, *Journal of Geophysical Research*, 77(27), 5255–5265.
- Prospero, J. M. (1981), Eolian transport to the World Ocean, in *The Oceanic Lithosphere, The Sea*, vol. 7, edited by C. Emiliani, pp. 801–874, Wiley Interscience, N.Y.
- Pye, K., and R. Johnson (1988), Stratigraphy, geochemistry, and thermoluminescence ages of Lower Mississippi Valley loess, *Earth Surface Processes and Landforms*, 13, 103–124.
- Ramaswamy, V., R. R. Nair, S. Manganini, B. Haake, and V. Ittekkot (1991), Lithogenic fluxes to the deep Arabian Sea measured by sediment traps, *Deep-Sea Research*, 38(2), 169–184.

- Ramos, A., A. Martel, G. Codd, E. Soler, J. Coca, A. Redondo, L. Morrison, J. Metcalf, A. Ojeda, S. Suárez, and M. Petit (2005), Bloom of the marine diazotrophic cyanobacterium *Trichodesmium erythraeum* in the Northwest African Upwelling, *Marine Ecology Progress Series*, 301, 303–305.
- Ratmeyer, V., G. Fischer, and G. Wefer (1999a), Lithogenic particle fluxes and grain size distributions in the deep ocean off northwest Africa: Implications for seasonal changes of aeolian dust input and downward transport, *Deep-Sea Research I*, 46, 1289–1337.
- Ratmeyer, V., W. Balzer, G. Bergametti, I. Chiapello, G. Fischer, and U. Wyputta (1999b), Seasonal impact of mineral dust on deep-ocean particle flux in the eastern subtropical Atlantic Ocean, *Marine Geology*, 159, 241–252.
- Rea, D. K. (1994), The paleoclimatic record provided by eolian deposition in the deep sea: The geological history of wind, *Reviews of Geophysics*, 32, 159–195.
- Rea, D. K., M. Leinen, and T. R. Janecek (1985), Geologic approach to the long-term history of atmospheric circulation, *Science*, 227, 721–725.
- Reiff, J., G. S. Forbes, F. T. M. Spieksma, and J. J. Reynders (1986), African Dust Reaching Northwestern Europe: A Case Study to Verify Trajectory Calculations, *American Meteorological Society*, 25(11), 1543–1567.
- Remer, L. A., Y. J. Kaufman, D. Tanré, S. Mattoo, D. A. Chu, J. V. Martins, R.-R. Li, C. Ichoku, R. C. Levy, R. G. Kleidman, T. F. Eck, E. Vermote, and B. N. Holben (2005), The MODIS Aerosol Algorithm, Products, and Validation, *Journal of Atmospheric Sciences*, 62(4), 947–973.
- Roberts, G. C., M. O. Andreae, W. Maenhaut, and M.-T. Fernández-Jiménez (2001), Composition and sources of aerosol in a central african rain forest during the dry season, *Journal of Geophysical Research*, 106, 14,423–14,434.
- Rogerson, M., E. J. Rohling, P. P. E. Weaver, and J. W. Murray (2004), The Azores Front since the Last Glacial Maximum, *Earth and Planetary Science Letters*, 222(3–4), 779–789.
- Rutten, A., G. J. de Lange, P. Ziveri, J. Thomson, P. J. M. van Santvoort, S. Colley, and C. Corselli (2000), Recent terrestrial and carbonate fluxes in the pelagic eastern Mediterranean; a comparison between sediment trap and surface sediment, *Palaeogeography, Palaeoclimatology, Palaeoecology*, 158, 197–213.
- Sanders, R., P. J. Morris, A. J. Poulton, M. C. Stinchcombe, A. Charalampopoulou, M. I. Lucas, and S. J. Thomalla (2010), Does a ballast effect occur in the surface ocean?, *Geophysical Research Letters*, 37(L08602), doi:10.1029/2010GL042,574.
- Schepanski, K., I. Tegen, and A. Macke (2009), Saharan dust transport and deposition towards the tropical northern Atlantic, *Atmospheric Chemistry and Physics*, 9, 1173–1189.
- Schiebel, R., J. J. Waniek, and A. Zeltner (2002), Impact of the Azores Front on the distribution of planktic Foraminifers, Gastropods and Coccolithophorids, *Deep-Sea Research II*, 49(19), 4035–4050.



- Scholten, J. C., J. Fietzke, S. Vogler, M. M. Rutgers Van Der Loeff, A. Mangini, W. Koeve, J. Waniek, P. Stoffers, A. Antia, and J. Kuss (2001), Trapping efficiencies of sediment traps from the deep Eastern North Atlantic: the 230Th calibration, *Deep-Sea Research II*, 48(10), 2383–2408.
- Schütz, L. (1989), Atmospheric mineral dust - properties and source markers, in *Palaeoclimatology and palaeometeorology: modern and past patterns of global atmospheric transport*, edited by M. Leinen and M. Sarnthein, pp. 359–383, Dordrecht: Kluwer Academic.
- Siedler, G., L. Armi, and T. J. Müller (2005), Meddies and decadal changes at the Azores Front from 1980 to 2000, *Deep-Sea Research II*, 52(3-4), 583–604.
- Siegel, D. A., and R. A. Armstrong (2002), Corrigendum to "Trajectories of sinking particles in the Sargasso Sea: modeling of statistical funnels above deep-ocean sediment traps" [*Deep-Sea Research I* 44, 1519-1541], *Deep-Sea Research I*, 49(6), 1115–1116.
- Siegel, D. A., and W. G. Deuser (1997), Trajectories of sinking particles in the Sargasso Sea: modeling of statistical funnels above deep-ocean sediment traps, *Deep-Sea Research I*, 44(9–10), 1519–1541.
- Siegel, D. A., T. C. Granata, A. F. Michaels, and T. Dickey (1990), Mesoscale Eddy Diffusion, Particle Sinking, and the Interpretation of Sediment Trap Data, *Journal of Geophysical Research*, 95(C4), 5305–5311.
- Siegenthaler, U., T. F. Stocker, E. Monnin, D. Lüthi, J. Schwander, B. Stauffer, D. Raynaud, J.-M. Barnola, H. Fischer, V. Masson-Delmotte, and J. Jouzel (2005), Stable Carbon Cycle - Climate Relationship During the Late Pleistocene, *Science*, 310(5752), 1313–1317.
- Sigman, D. M., and E. A. Boyle (2000), Glacial/interglacial variations in atmospheric carbon dioxide, *Nature*, 407, 859–869.
- Signorini, S. R., R. G. Murtugudde, C. R. McClain, J. R. Christian, J. Picaut, and A. J. Busalacchi (1999), Biological and physical signatures in the tropical and subtropical Atlantic, *Journal of Geophysical Research*, 104(C8), 18,367–18,382.
- Sirocko, F., and H. Lange (1991), Clay-mineral accumulation rates in the Arabian Sea during the late Quaternary, *Marine Geology*, 97, 105–119.
- Steinberg, D. K., C. A. Carlson, N. R. Bates, R. J. Johnson, A. F. Michaels, and A. H. Knap (2001), Overview of the US JGOFS Bermuda Atlantic Time-series Study (BATS): a decade-scale look at ocean biology and biogeochemistry, *Deep-Sea Research II*, 48(8–9), 1405–1447.
- Storz, D., H. Schulz, J. J. Waniek, D. E. Schulz-Bull, and M. Kucera (2009), Seasonal and interannual variability of the planktic foraminiferal flux in the vicinity of the Azores Current, *Deep-Sea Research I*, 56(1), 107–124.
- Stramma, L., and G. Siedler (1988), Seasonal Changes in the North Atlantic Subtropical Gyre, *Journal of Geophysical Research*, 93(C7), 8111–8118.
- Swap, R., M. Garstang, S. Greco, R. Talbot, and P. Kallberg (1992), Saharan dust in the amazon basin, *Tellus B*, 44(2), 133–149.



- Sy, A. (1988), Investigation of large-scale circulation patterns in the central North Atlantic: the North Atlantic Current, the Azores Current, and the Mediterranean Water plume in the area of the Mid-Atlantic Ridge, *Deep-Sea Research*, 35(3), 383–413.
- Talley, L. D. (1982), Eighteen degree water variability, *Journal of Marine Research*, 40, 757–775.
- Taylor, S. R., and S. M. McLennan (1985), *The Continental Crust: Its Composition and Evolution*, Blackwell, Oxford.
- Tegen, I., P. Hollrigl, M. Chin, I. Fung, D. Jacob, and J. Penner (1997), Contribution of different aerosol species to the global aerosol extinction optical thickness: Estimates from model results, *Journal of Geophysical Research*, 102, 23,895–23,915.
- Thiry, M. (2000), Palaeoclimatic interpretation of clay minerals in marine deposits: an outlook from the continental origin, *Earth–Science Reviews*, 49(1-4), 201–221.
- Thoning, K. W., P. P. Tans, and W. D. Komhyr (1989), Atmospheric Carbon Dioxide at Mauna Loa Observatory 2. Analysis of the NOAA GMCC Data, 1974-1985, *Journal of Geophysical Research*, 94(D6), 8549–8565.
- Tomadin, L., R. Lenaz, V. Landuzzi, A. Mazzucolletti, and R. Vannucci (1994), Wind-blown dust over the Central Mediterranean, *Oceanologica Acta*, 7(1), 13–23.
- Torres-Padrón, M. E., M. D. Gelado-Caballero, C. Collado-Sánchez, V. F. Siruela-Matos, P. J. Cardona-Castellano, and J. J. Hernández-Brito (2002), Variability of dust inputs to the CANIGO zone, *Deep-Sea Research II*, 49(17), 3455–3464.
- Trapp, J. M., F. J. Millero, and J. M. Prospero (2010), Temporal variability of the elemental composition of African dust measured in trade wind aerosols at Barbados and Miami, *Marine Chemistry*, 120(1–4), 71–82.
- Turekian, K. K., and K. H. Wedepohl (1961), Distribution of the elements in some major units of the Earth’s crust, *Geological Society of America Bulletin*, 72, 175–192.
- Waniek, J., W. Koeve, and R. Prien (2000), Trajectories of sinking particles and the catchment areas above sediment traps in the northeast Atlantic, *Journal of Marine Research*, 58(6), 983–1006.
- Waniek, J. J., D. E. Schulz-Bull, T. Blanz, R. Prien, A. Oschlies, and T. Müller (2005a), Inter-annual variability of deep water particle flux in relation to production and lateral sources in the northeast Atlantic, *Deep-Sea Research I*, 52, 33–50.
- Waniek, J. J., D. E. Schulz-Bull, J. Kuss, and T. Blanz (2005b), Long-time series of deep water particle flux in three biogeochemical provinces of the northeast Atlantic, *Journal of Marine Systems*, 56, 391–415.
- Weber, J., M. H. Conte, S. Huang, T. Dickey, and J. Acker (2006), Advection of detrital carbonate sediment to the deep ocean by passage of Hurricane Fabian over Bermuda, *EOS Transactions of the American Geophysical Union*, 87(36), Ocean Sciences Meeting Supplement.
- Wedepohl, H. K. (1995), The composition of the continental crust, *Geochimica et Cosmochimica Acta*, 59(7), 1217–1232.

- Westphal, D. L., O. B. Toon, and T. B. Carlson (1987), A two-dimensional numerical investigation of the dynamics and microphysics of saharan dust storms, *Journal of Geophysical Research*, *92*(D3), 3027–3049.
- Windom, H. L. (1976), Lithogenous Material in Marine Sediments, in *Chemical Oceanography*, Vol. 5, 2nd ed., edited by J. Riley and R. Chester, pp. 103–135, Academic Press, London.
- Zhang, J., and J. S. Reid (2006), MODIS aerosol product analysis for data assimilation: Assessment of over-ocean level 2 aerosol optical thickness retrievals, *Journal of Geophysical Research*, *111*(D22207), doi:10.1029/2005JD006898.

## List of Figures

1.1	Scheme of major connections between desert dust, ocean biogeochemistry and climate according to <i>Jickells et al.</i> [2005]. . . . .	3
1.2	Annual cycle of total particle flux and clay flux in 2000 m depth at Kiel 276 (33°N, 22°W) in $\text{mg m}^{-2} \text{d}^{-1}$ (redrawn from <i>Waniek et al.</i> [2005b]). . . . .	6
2.1	Location of the sampling sites in the subtropical North Atlantic. . .	10
2.2	Simplified sketch of a funnel-type sediment trap according to <i>Kremling et al.</i> [1996]. . . . .	12
3.1	Map showing the position of the study site Kiel 276 and displaying major sea surface currents of the subtropical Northeast Atlantic and main wind fields over North Africa and the north eastern Atlantic. .	17
3.2	Total particle flux, flux of main lithogenic particle groups and clay mineral fluxes of investigated time series. . . . .	24
3.3	Grain size distributions retrieved from SEM-EDX analysis of investigated sediment trap series. . . . .	26
3.4	Grain size distributions of lithogenic particle groups of the whole data set (samples of all sample years are involved) and for single years of sampling (series 22, series 23 and series 24). . . . .	28
3.5	Ternary diagram (after <i>Caquineau et al.</i> [2002]) displaying illite/kaolinite ratios (I/K) of investigated samples (a) and I/K ratios plotted against the palygorskite content (% from clay mineral species) of the investigated samples with relevant end-members redrawn from <i>Bout-Roumazeilles et al.</i> [2007] (b). . . . .	30
3.6	Comparison of the flux of biogenic particles (involves opal, carbonates, barite, organic particles) and flux of iron and phosphate (a). Relation between P and biogenic particle flux, Fe and biogenic particle flux and Fe and POC flux showcased for series 22 (b). . . . .	35
3.7	Relationship between content of lithogenic fraction referred to mass flux and lithogenic flux. . . . .	37

4.1	Position of the sampling site in the subtropical NE Atlantic and catchment area of the 2000 m sediment trap at Kiel 276 (a). Lithogenic particle flux versus GOCART dust aerosol optical thickness (b) and moving averages (3 points) for lithogenic flux time series and GOCART AOD time series (c). . . . .	42
4.2	Scenarios of dust deposition during winter and summer and its possible effects on primary production (a). Area averaged data of 8-day mean SeaWiFS chlorophyll-a values shown together with biogenic particle flux from the 2000 m sediment trap (b). . . . .	46
5.1	Position of the sediment trap sample site BATS-IOW southeast of Bermuda and within the North Atlantic. . . . .	56
5.2	Comparison between double measurements, showing the reproducibility of the determination of the chemical composition (element oxides in %) of three samples. . . . .	58
5.3	Currents in 1090 m, 2170 m and 3570 m depth levels (in $\text{cm s}^{-1}$ ) measured between 1998 and 1999 at the BATS-IOW site. . . . .	59
5.4	Total particle flux at the BATS-IOW site from 5 <sup>th</sup> September 1998 to 30 <sup>th</sup> August 1999 (in $\text{mg m}^{-2} \text{d}^{-1}$ ). . . . .	61
5.5	Flux of POC and PON, and flux of barite shown together with chlorophyll-a concentrations in the upper water column (SeaWiFS data, area averaged). . . . .	62
5.6	Relationships between barite, POC, PON and opal. . . . .	63
5.7	Scatter plot of Si/Al versus Fe/Al mass ratios of literature data and BATS-IOW sediment trap data. . . . .	66
5.8	Proportion of main lithogenic particle groups within the lithogenic fraction and proportion of clay minerals within the clay fraction. . .	70
5.9	Contribution of palygorskite to clay mineral flux and TOMS aerosol index. . . . .	71
5.10	Illite/Kaolinite ratios (I/K) plotted against the palygorskite content (% of the lithogenic fraction) present in BATS-IOW sediment trap samples. . . . .	73

## List of Tables

2.1	Different ways of determining the lithogenic fraction of sediment trap material. . . . .	13
3.1	Results of the repeated measurements of one sample (series 23/9) given in $\text{mg m}^{-2}\text{d}^{-1}$ . . . . .	22
4.1	Pearson ( $r$ ) and Spearman's rank ( $\rho$ ) correlation coefficients between lithogenic flux at 2000 m water depth and MODIS AOD and GO-CART AOD <sub>dust</sub> values given in monthly (n=37) and half-monthly (n=74) resolution. . . . .	43
5.1	List of references which provide chemical data of soil and aerosol samples with North African provenance. . . . .	68

## List of Abbreviations

<b>AC</b>	Azores Current
<b>AERONET</b>	AERosol RObotic NETwork
<b>AI</b>	Aerosol Index
<b>AOD</b>	Aerosol optical depth
<b>BATS</b>	Bermuda Atlantic Time-series Study
<b>Chl-a</b>	Chlorophyll-a
<b>DFG</b>	Deutsche Forschungsgemeinschaft
<b>EDX</b>	Energy dispersive X-ray spectroscopy
<b>ESTOC</b>	European Station for Time-series in the Ocean
<b>GEOS DAS</b>	Goddard Earth Observing System Data Assimilation System
<b>Giovanni</b>	Goddard Earth Sciences Data and Information Services Center Interactive Online Visualization AND aNalysis Infrastructure
<b>GOCART</b>	Goddard Chemistry Aerosol Radiation and Transport model
<b>HNLC</b>	High Nutrient Low Chlorophyll
<b>IOW</b>	Institut für Ostseeforschung
<b>JGOFS</b>	Joint Global Ocean Flux Study
<b>MODIS</b>	Moderate Resolution Imaging Spectroradiometer
<b>NAST</b>	North Atlantic Subtropical Gyral Province
<b>NAO</b>	North Atlantic Oscillation
<b>OFE</b>	Ocean fertilization experiment
<b>OFFP</b>	Oceanic Flux Program
<b>POC</b>	Particulate organic carbon
<b>PON</b>	Particulate organic nitrogen
<b>REE</b>	Rare earth elements
<b>SAL</b>	Saharan air layer
<b>SEM</b>	Scanning electron microscope
<b>SPM</b>	Suspended particulate matter
<b>SeaWiFS</b>	SEA-viewing Wide Field of-view Sensor
<b>TOMS</b>	Total Ozone Mapping Spectrometer
<b>XRD</b>	X-ray diffraction

## Specific contribution to the manuscripts

The contributions of the authors to the manuscripts are indicated in the following:

Brust, J., and J. J. Waniek (2010), Atmospheric dust contribution to deep-sea particle fluxes in the subtropical Northeast Atlantic, *Deep Sea Research I*, 57(8), 988-998.

**Specific contribution:** J. J. W. provided sediment trap material and SEM-EDX data for the work mentioned above. J. B. carried out SEM-EDX analysis, data evaluation and interpretation. Concept and first edition of manuscript: J.B., revision of manuscript: J. J. W.. J. J. W. is the project holder.

Brust, J., Schulz-Bull, D.E., Leipe, T., Chavagnac, V. and Waniek, J.J. (2011), Descending particles: from the atmosphere to the deep ocean - A time series study in the subtropical NE Atlantic, *Geophysical Research Letters*, 38(L06603), doi:10.1029/2010GL045399.

**Specific contribution:** J. B. prepared the concept of the paper and did most of the writing. J. B. and T. L. carried out SEM-EDX analysis and data interpretation. J. J. W. is the project holder and initiated the work. D. E. S.-B., T. L., V. C., and J. J. W. made contributions to the discussion.

Brust, J. et al. (Manuscript), Barite and North African dust in 3200 m deep sediment trap material southeast of Bermuda, to be submitted to *Deep-Sea Research I*.

**Specific contribution:** Sample analysis and interpretation has been carried out by J. Brust, as well as concept development and manuscript writing. Samples and mass flux data were kindly provided by D. E. Schulz-Bull and J. J. Waniek.



## Acknowledgements

I am grateful to my supervisor Dr. habil. Joanna J. Waniek and would like to thank her for giving me the opportunity to do this PhD thesis, and to take part in scientific cruises and scientific conferences. Likewise I would like to thank all of my thesis committee members, Dr. habil. Joanna J. Waniek, Prof. Dr. Detlef E. Schulz-Bull, Dr. Thomas Leipe and Dr. Valérie Chavagnac from Toulouse in France for fruitful scientific discussions and always having an open ear for me, no matter what distance we had to overcome.

I thank Dr. Slobodan Nickovic of the World Meteorological Organization for inviting me to the WMO SDS–WAS/GESAMP workshop held in Malta this year.

For their scientific and practical support in many different ways during my PhD thesis I would like to thank Bernd Schneider, Ralf Prien, Thomas Ohde, Rainer Bahlo, Hildegard Kubsch, Ines Hand, Birte Fründt, Andrea Bauer, Andreia Rebotim, Zhen Xia, Christina Augustin and Ruth Anderson. As a whole, I would like to thank all of my colleagues from the IOW for sharing good times at the institute.

At this point I would also like to thank captain and crew of RV 'Poseidon' for their technical support during cruises.

Thanks to my office mates Andrea Bauer and Birte Fründt for their company and making the office time easier and last but not least, for helping in such things like 'MATLAB'.

I also appreciated lunch times with Iris Stottmeister and would like to thank her for helpful scientific discussions and her friendship. Similarly, I would also like to say thanks you to my flat-mate Ruth Anderson, who supported 'easy living' at home. I am grateful to my friends for their encouragement, understanding and indulgence.

My final thanks goes to my family and especially to Conny, Jürgen, Rike and Irene for their support and giving me hope and love during the past years.

## Eidesstattliche Erklärung

Ich versichere hiermit an Eides statt, dass ich die vorliegende Arbeit selbstständig angefertigt und ohne fremde Hilfe verfasst habe, keine außer den von mir angegebenen Hilfsmitteln und Quellen dazu verwendet habe und die den benutzten Werken inhaltlich und wörtlich entnommenen Stellen als solche kenntlich gemacht habe.

Rostock, den 29. Juni 2011

Juliane Brust